A COMPARISON OF POWER SYSTEMS FOR AUTONOMOUS UNDERWATER VEHICLES

by

GARY E. SCHUBAK
B.A.Sc. University of British Columbia, 1989

A Thesis Submitted in Partial Fulfillment of the
Requirements for the Degree Of

MASTER OF APPLIED SCIENCE

in the Department of
Mechanical Engineering

We accept this thesis as conforming
to the required standard

[redacted]

Dr. D. S. Scott, Supervisor, Dept. of Mechanical Engineering

[redacted]

Dr. H.-H. Rogner, Member, Dept. of Mechanical Engineering

[redacted]

Dr. A. K. S. Bhat, Member, Dept. of Electrical Engineering

[redacted]

Dr. S. Dost, Graduate Advisor, Dept. of Mechanical Engineering

[redacted]

Dr. J. Collins , External Examiner, Royal Roads Military College

Supervisor: Dr. David S. Scott

ABSTRACT

Autonomous underwater vehicles (AUV's) can provide operational advantages in comparison to other subsea work systems. One of the principal barriers to the market development of AUV's has been the limited submerged endurance capability of lead-acid batteries. Recently, advanced battery systems, closed-cycle dynamic converters and H_2-O_2 fuel cells have become available for subsea applications. These power systems can provide greater submerged endurance than can lead-acid batteries and consequently improve market opportunities for AUV's.

This thesis presents a techno-economic comparison of power systems for AUV applications. The power system technologies included within this study are the lead-acid battery, sodium-sulfur battery, solid polymer fuel cell and closed cycle diesel engine. A *generic* AUV is considered, which is common to all power systems and consistent throughout the analysis. The AUV application is described in terms of a parametric mission and life cycle. Power systems are evaluated by two criteria: 1) maximum submerged endurance and 2) life cycle cost. This thesis seeks *categories* of AUV applications for which each power system is preferred in terms of techno-economic performance.

The results show that the SPFC can provide measures of submerged endurance greater than all other power systems examined. This result is particularly strong for missions characterized by: 1) great depth, for which the high specific energy of liquid hydrogen storage is advantageous, and 2) high degree of part load operation, for which the SPFC benefits by its high part load efficiency. Consequently, despite its high present cost, the SPFC system has a market niche for long duration AUV missions, for which no other power system is technically feasible.

This thesis considers *cost projections* for the power system technologies, allowing each to benefit from the economies of scale. The results show that each

power system exhibits a characteristic domain of preference in terms of prescribed techno-economic criteria. The lead-acid battery is preferred in terms of life cycle cost for those AUV applications for which it is technically feasible. Nevertheless, it is restricted to extremely short mission durations by its inherent low energy density. The sodium-sulfur battery can provide roughly 2.5 times the submerged endurance capability of the lead-acid battery, and is preferred for short mission durations coupled with high peak power requirements. Beyond the performance envelope of advanced battery systems, and within its own domain of mission feasibility, the closed cycle diesel engine is typically preferred in terms of life cycle cost. Nevertheless, the ability of the solid polymer fuel cell to compete with the diesel engine in terms of cost in this domain increases with increasing mission duration and mission frequency. For high values of both, the solid polymer fuel cell can exhibit lower life cycle cost than the closed cycle diesel engine.

Examiners:

[redacted]

Dr. D. S. Scott, Supervisor (Dept. of Mechanical Engineering)

[redacted]

Dr. H.-H. Rogner, Member (Dept. of Mechanical Engineering)

[redacted]

Dr. A. K. S. Bhat, Outside Member (Dept. of Electrical Engineering)

[redacted]

Dr. S. Dost, Graduate Advisor (Dept. of Mechanical Engineering)

[redacted]

Dr. J. Collins, External Examiner (Royal Roads Military College)

Table of Contents

List of Tables

List of Figures

Nomenclature

ROV	Remotely operated vehicle
AUV	Autonomous underwater vehicle
LCC	Life cycle cost
$	Canadian dollars expressed at 1992 prices and exchange rates
SPFC	Solid polymer fuel cell
CCDE	Closed cycle diesel engine
GH_2	Compressed hydrogen storage in composite pressure vessels at 310 bar (4500 psia)
LH_2	Liquid hydrogen storage in cryogenic dewars
LOX	Liquid oxygen storage in cryogenic dewars
E_{rev}	Reversible open circuit voltage
G	Gibbs Free Energy
H	Enthalpy
S	Entropy
Q	Heat
F	Faraday's constant (96,487 coulombs)
k	Ratio of specific heats $\left(\frac{C_p}{C_v}\right)$

r_v	Compression ratio for diesel engine
r_c	Cut-off ratio of expansion stroke for diesel cycle
lhv	Lower heating value
hhv	Higher heating value
DOD	Depth-of-discharge of battery
Wh	Watt-hours
Ah	Amp-hours
η	Efficiency
dc	Direct current
ac	Alternating current
ρ	Density (kg/m^3)
γ	Specific weight (N/m^3)

Acknowledgments

I would like to thank my colleagues at IES *Vic*. I feel privileged to be a part of this group, and I am grateful for the assistance and friendship I have received here. I reserve special thanks for David Sanborn Scott for his guidance and support over the past two years.

I would also like to thank those who have supported me financially throughout this program: NSERC, the University of Victoria, and IES *Vic*. I give special acknowledgment to the SPIRIT Subsea Systems Corporation for funding the initial power system study which eventually evolved into a thesis. I also appreciate the contribution made by Mike Muirhead during the early stages of this study.

Last, I am grateful to my family and friends for their encouragement and understanding.

Chapter 1

Introduction

1.1 Motivation

Earth's oceans cover roughly 70% of the planet surface. They contain a rich diversity of ecological systems that are pivotal to the natural processes of the earth. Furthermore, the oceans represent a relatively untapped resource base for materials, food and energy. As world population continues to increase, and land-based resources continue to be depleted, humankind will likely turn to the oceans as a future resource base. Indeed, this process has already begun, with offshore oil practices well through two decades of operation [1].

But even today, the oceans are not well understood. Less than 3% of the deep ocean has been properly charted, and our understanding of the subsea resource potential is even more sparse [2]. The continued evolution of subsea work systems is critical for humankind's extension into the sea.

The dominant underwater work system today is still the diver. The human can provide levels of performance and dexterity superior to any remote system. But divers face physiological limitations, which restrict their access into the deep ocean. Hyperbaric diving practices are limited to depths of approximately 300 metres and less [3].

The submersible isolates the human from the harsh subsea environment. Small, manned submersibles have recently been developed, which can extend the human reach to significant depths. One such vessel is the manned research

submersible *Shinkai 6500* [4]. This submersible can take three human operators to a depth of 6500 metres, allowing access to almost 97% of the ocean floor. It is currently the deepest diving submersible of its kind in the world. Applications of the *Shinkai 6500* include the survey of subsea resources and investigation of earthquake mechanisms off the coast of Japan.

Manned submersibles have the advantage of putting the human operator directly at the work site. But they have the disadvantage of being inherently large displacement vehicles, a requirement necessitated by the human payload onboard. Consequently, the surface support vessel, for launch and recovery of manned submersibles, is typically very large and associated with high operating costs. For instance, the support vessel *Yokosuka* for the *Shinkai 6500* is over 100 metres in length, with a total crew of fifty-seven members [4]. A second, and no less significant, disadvantage of the manned submersible has been its limited submerged endurance capability.

Remotely operated vehicles (ROV's) address the limitations of manned submersibles. ROV's are unmanned, receiving power and information from the surface support vessel through an umbilical cable [5]. This arrangement allows for virtually unlimited submerged endurance, restricted only by the availability of fuel at the surface. Furthermore, because ROV's are unmanned, they can be very small displacement vehicles. This can allow for smaller support vessel requirements and lower associated operating costs, in comparison with manned submersibles.

In today's offshore oil industry, ROV's are used for pipeline surveillance, diving support, drilling support and platform inspection [1]. Scientific applications for ROV's have also increased since the early 1980's, and today include ocean floor mapping, environmental monitoring, mineral exploration and the study of sea life [6].

The limiting feature of the ROV is the umbilical cable [7]. Operational experience suggests the continuing incidence of umbilical snagging and damage

seriously reduces the operational effectiveness of this subsea work system [1]. Risk of cable damage is particularly high when conducting operations along steep cliff walls [6]. Furthermore, because of its reliance on the surface support vessel, the ROV is a weather-dependent system.

The *autonomous underwater vehicle* (AUV) provides operational advantages in comparison with both the manned submersible and the ROV. Because it is unmanned, the AUV can achieve small displacements. Furthermore, it has its own onboard power system and mission control, and is therefore free from the constraining umbilical cable. One of the principal barriers to the market development of the AUV has been the lack of a high energy density, atmosphere independent power system. Low energy density lead-acid batteries, which have dominated subsea power, cannot provide endurance suitable for the developing AUV applications. In past development efforts, energy storage has been labeled as a major obstacle [8].

Recently, advanced battery systems, H_2-O_2 fuel cells, and closed-cycle dynamic converters have become available for submersible applications. These power systems can offer greater submerged endurance than can lead-acid batteries. The issue of power facing the AUV developer today is more promising than it has been in the past. But it is also more complex. Today, AUV developers must plan to meet unseen markets, and choose among power system technologies which are not yet fully developed for commercialization. An understanding of where these technologies are evolving, in terms of both technical and economic performance, is required.

1.2 Objective

This thesis presents a techno-economic comparison of power systems for autonomous underwater vehicle applications. The power systems considered are chosen to represent the categories of emerging technologies in subsea applications, and include:

- Lead-acid battery
- Sodium-sulfur (Na-S) battery
- Solid polymer fuel cell (SPFC)
- Closed cycle diesel engine (CCDE)

The concept of *service* is critical to this comparison. People demand energy services, not necessarily energy or energy conversion technologies [9]. Consequently, a useful comparison of power systems must be cast in terms of the service provided. The service that an AUV provides may be to survey Victoria Harbour once a month for ten years, or it may be to weld a pipeline joint eight hours a day, every day for six months. This study recognizes the wide variety of possible AUV applications, and anticipates that different power systems will be preferred for different services.

The objective of this thesis is to identify the categories of AUV services for which each power system is preferred.

This thesis limits the scope of the study to the power system alone. In order to eliminate considerations of the AUV and its required support vessel from the comparison, the vehicle is specified to be consistent throughout the analysis and common for all power systems. The AUV is generic in nature, obeying rules of statics, hydrostatics and hydrodynamics. The vehicle displacement and the vehicle subsystems considered are selected to best represent the current concept of the autonomous underwater vehicle. The generic AUV considered in this study is detailed in Chapter 2.

Each power system is *put inside* the vehicle and evaluated in terms of its techno-economic performance. Two criteria for comparison are used in this analysis:

- **Maximum submerged endurance:** Submerged endurance has historically been a limiting feature of the AUV. Indeed, the limited submerged endurance capability of the lead-acid battery has been one of the principal barriers to the market development of the AUV. The maximum submerged endurance gives a measure of the services that can be accommodated by each power system.

- **Life cycle cost (LCC):** As advanced power systems become commercially available for AUV's, an understanding of their associated costs becomes more important. Life cycle costing is a method of calculating the total cost of ownership over the life span of an asset [14]. It includes the initial capital cost, all subsequent operation and maintenance costs, as well as the disposal value and any other quantifiable benefits and costs.

With these two metrics for comparison, the categories of service for which each power system is preferred can be identified.

Contributions of Thesis

Available literature comparing power systems for AUV applications is not abundant. And of that which exists, power system cost is rarely examined. This may not be surprising when one considers the lack of parity in the present state of development and associated production costs of the candidate subsea power systems. For example, a cost comparison between the lead-acid battery and the solid polymer fuel cell in **today's** market environment has a very predictable result. The test bench levels of production associated with the fuel cell today simply make it too expensive for most commercial applications.

But in addition to knowing the present cost situation, the AUV community requires an understanding of where these costs are evolving. This thesis addresses this issue. Cost projections for the lead-acid battery and the CCDE are relatively easy to make, since the components of these power systems are already commercially available and optimized in terms of production price. But for the

Na-S battery and the SPFC, production levels are still on the test bench. Cost projections for these systems assume *large scale production* levels, the specifics of which are discussed in the relevant chapters. The time horizon for these projections is unclear, as it depends largely on the success of these technologies to compete for land-based transportation markets. Nevertheless, the projections used in this study give some measure of the *cost potential* of the power systems.

Another contribution of this thesis to the present body of literature comparing power systems for AUV's is its treatment of the concept of *service*. This work considers the AUV service in greater generality than previous studies, allowing a wider assortment of scenarios to be treated. Rather than searching for one power system which is preferred for all AUV applications, this thesis reveals *domains of preference* for each power system. A review of pertinent literature will help to put this point into perspective.

Sedor [10] and Kumm [11] compare directly the attributes of candidate power systems, such as efficiency, specific energy, capital cost and reliability. Each attribute is evaluated by a *quality index*, ranging on a scale from 0 to 10. This quality index is then multiplied by a *weighting factor*, which is some measure of the power system attribute's (say efficiency's) significance to the AUV mission. The product of quality index and weighting factor is a measure of *merit*. Summing these products for all the power system attributes considered quantifies the merit of the entire power system for the AUV application. The power system with the largest figure of merit is the preferred power system.

This comparison methodology recognizes that AUV services are unique from other power system applications. But it *replaces* the concept of service with the previously described weighting scheme. In so doing, it says that all AUV services are the same and can be represented by the same set of weighting factors. Furthermore, this technique requires perfect judgement from the examiner to assign the appropriate weighting factors in characterizing the service. Also, the results are not put in context with the service provided. Issues of interest to

the AUV community, such as submerged endurance and power system cost, are not addressed.

Lee [12] compares power systems for the DARPA (Defense Advanced Research Projects Agency) prototype vehicle. Considering the same two cubic meter power system module for all power systems, he uses the maximum onboard energy storage capacity of each as a metric for comparison. This comparison is cast in terms of the service technology, not in terms of the service provided. Onboard energy storage alone is not an adequate measure of power system performance. One must consider the required mission profile and the associated energy conversion efficiencies of each power system. Furthermore, because the concept of service is not treated in this study, it can be of interest only to those within the DARPA program, who seek to maximize onboard energy storage for their vehicle.

Brighenti [13] comes closest to the concept of service, as it is treated in this thesis. He defines a parametric representation of an AUV mission, characterized by depth, speed and range. Furthermore, he defines the AUV in the proper perspective, as a neutrally buoyant vehicle consisting of a vehicle shell, payload, propulsion system and power system. The comparison technique is to determine the required vehicle displacement for a prescribed set of mission variables, using different power systems.

The treatment of service used in this thesis expands upon the work of Brighenti. In addition to vehicle transit, this study incorporates the performance of high power on-station work tasks (such as welding) into the mission definition. This allows the examination of a wider variety of AUV missions, and emphasizes the importance of power system part load efficiency when examining technical performance. Furthermore, this thesis adds the repetition of missions in time into the service definition. This is required for the proper assessment of power system cost.

1.3 Methodology

1.3.1 The Service

The comparison methodology is driven by the service requirement. This thesis considers the AUV service to be a specific mission, which is repeated over time. The service is characterized in generality, so that a wide variety of AUV scenarios may be examined.

The *generic* AUV mission is illustrated in Figure 1.1. It is comprised of two repeating modes of operation:

- Transit at constant speed.
- Performance of on-station work, requiring constant power.

The percentage of total mission time spent on-station is defined to be the *time ratio*. The mission depth is effectively the maximum depth encountered. The five variables (depth, speed, on-station power, time ratio and total mission duration) define the set of possible AUV missions considered by this thesis.

Categories of missions are examined in this thesis. Each is a two-dimensional subset of the total set of possible AUV missions. Each is characterized by judiciously assigning three mission constants, and allowing the remaining two mission variables to vary over a suitable range of values. In order to *bookend* the categories of AUV missions, two opposite extremes are considered:

- **Example 1 - Survey Mission:** This mission is purely transit in nature. Since there is no performance of on-station work, the time ratio is set to zero. A transit speed of 5 m/s (10 knots) is considered. Power requirements are dominated by the propulsion system, and are characterized by a low steady-state demand. The subset of possible survey missions is defined by the variables **depth** and mission duration.
- **Example 2 - Work Mission:** This mission is purely for the performance of on-station work. Since there is no requirement for vehicle transit, the

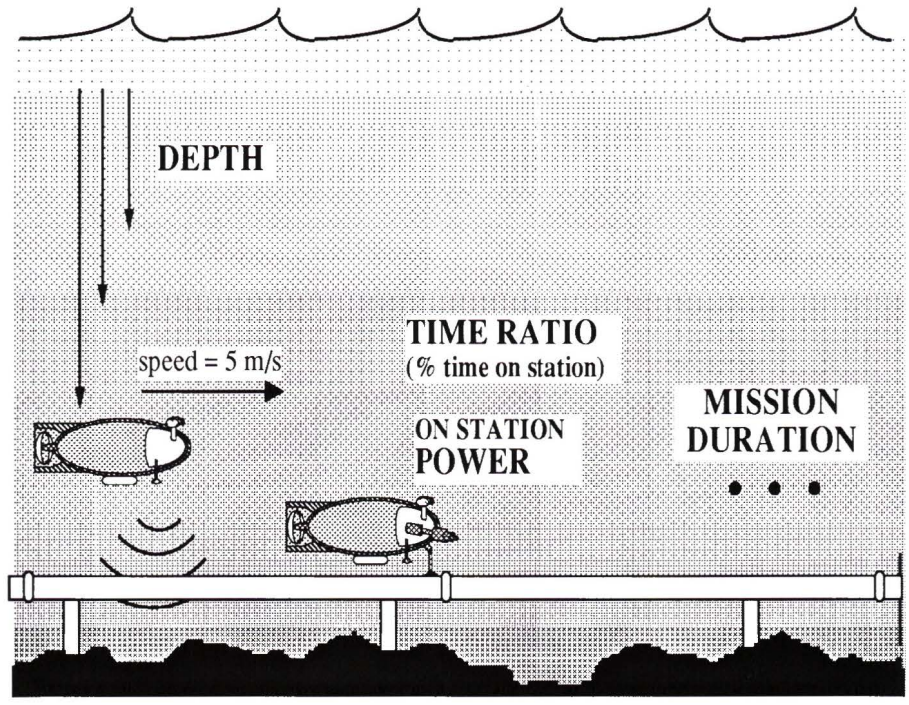

Figure 1.1: The generic AUV mission.

time ratio is set to 1. This mission profile is characterized by a **high** steady-state power demand. Depth is fixed at 300 metres, coinciding with the typical depth of the Continental Shelf. The subset of work missions is defined by the variables **on-station power** and mission duration.

A third mission example combines the features of these two extremes:

- **Example 3 - Combined Mission:** This mission example combines low power transit with high power work operations. Again, vehicle speed is a constant 5 m/s and depth is fixed at 300 metres. On-station power is 50 kW, corresponding to a welding operation. The subset of combined missions is defined by the variables **time ratio** and mission duration.

Autonomous underwater vehicles are likely to be mission-specific, performing a particular function over their entire useful life. The complete service

definition consists of a prescribed mission and **life cycle**. The life cycle defines the utilization of the AUV over time. It is characterized by a mission frequency, expressed in missions per year, and a service lifetime. In this thesis, the service lifetime is considered to be ten years, corresponding with the assumed useful lifetime for a typical AUV.

1.3.2 Performance Envelopes

A specific AUV mission is completely defined by the assignment of all five mission variables. This study identifies the subset of possible AUV missions for which each power system is technically feasible. These subsets are referred to as *Performance Envelopes.*

Performance envelopes are examined for each of the three AUV mission categories previously discussed. Practically, they are determined by calculating the maximum submerged endurance of each power system, over a suitable variation of the independent mission variable. For the survey mission, performance envelopes are the feasible combinations of mission depth and mission duration. For the work mission, they are the feasible combinations of on-station power and mission duration. And for the combined mission, performance envelopes examine maximum submerged endurance versus time ratio.

Figure 1.2 illustrates the simulation technique for constructing power system performance envelopes. The calculation procedure is divided into four distinct steps:

1. Define the mission. Mission duration is a variable which is to be maximized for each power system.

2. Determine the power requirements of the mission. Also, determine the mass and volume constraints imposed on the power system by the vehicle configuration. The AUV must be neutrally buoyant, as discussed in Chapter 2.

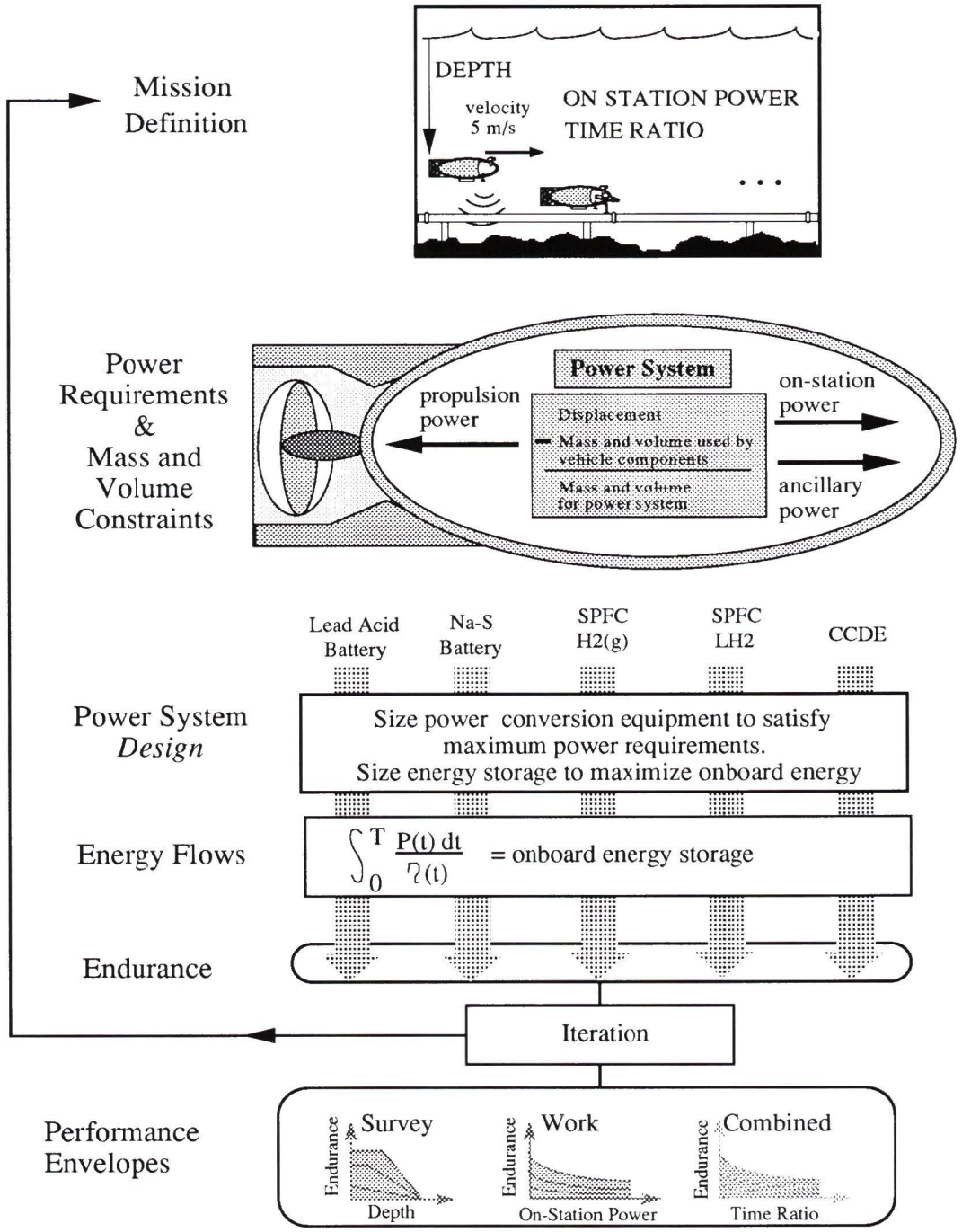

Figure 1.2: Simulation technique for constructing power system performance envelopes.

3. *Design* the power system. Size power conversion equipment to satisfy the peak power requirement. Maximize onboard energy storage subject to the constraint of neutral buoyancy.

4. Determine the maximum submerged endurance by time step simulation of energy flows. In mathematical form, this can be expressed:

$$\int_0^T \frac{P(t)\,dt}{\eta(t)} = \text{onboard energy storage} \tag{1.1}$$

where P(t) is the instantaneous power requirement, η(t) is the corresponding instantaneous energy conversion efficiency, and T is the mission duration.

A comparison of performance envelopes illuminates the missions for which each power system is feasible. It reveals mission profiles for which one power system may be uniquely appropriate, allowing AUV services available to no other system. Furthermore, performance envelopes give a relative measure of the AUV markets that can be gained by each power system technology.

1.3.3 Domains of Least Cost

Life cycle costing is a method for calculating the total cost of ownership [14]. This thesis uses life cycle cost (LCC) as the metric for comparing power systems which provide a common service. The LCC of each power system is calculated over its domain of feasible missions. *Domains of Least Cost* indicate the subset of possible AUV missions for which each power system is preferred by this criteria.

Figure 1.3 illustrates the simulation technique used for constructing domains of least cost. The calculation procedure is divided into four steps:

1. Define the service. The complete service definition requires the assignment of all mission and life cycle parameters.

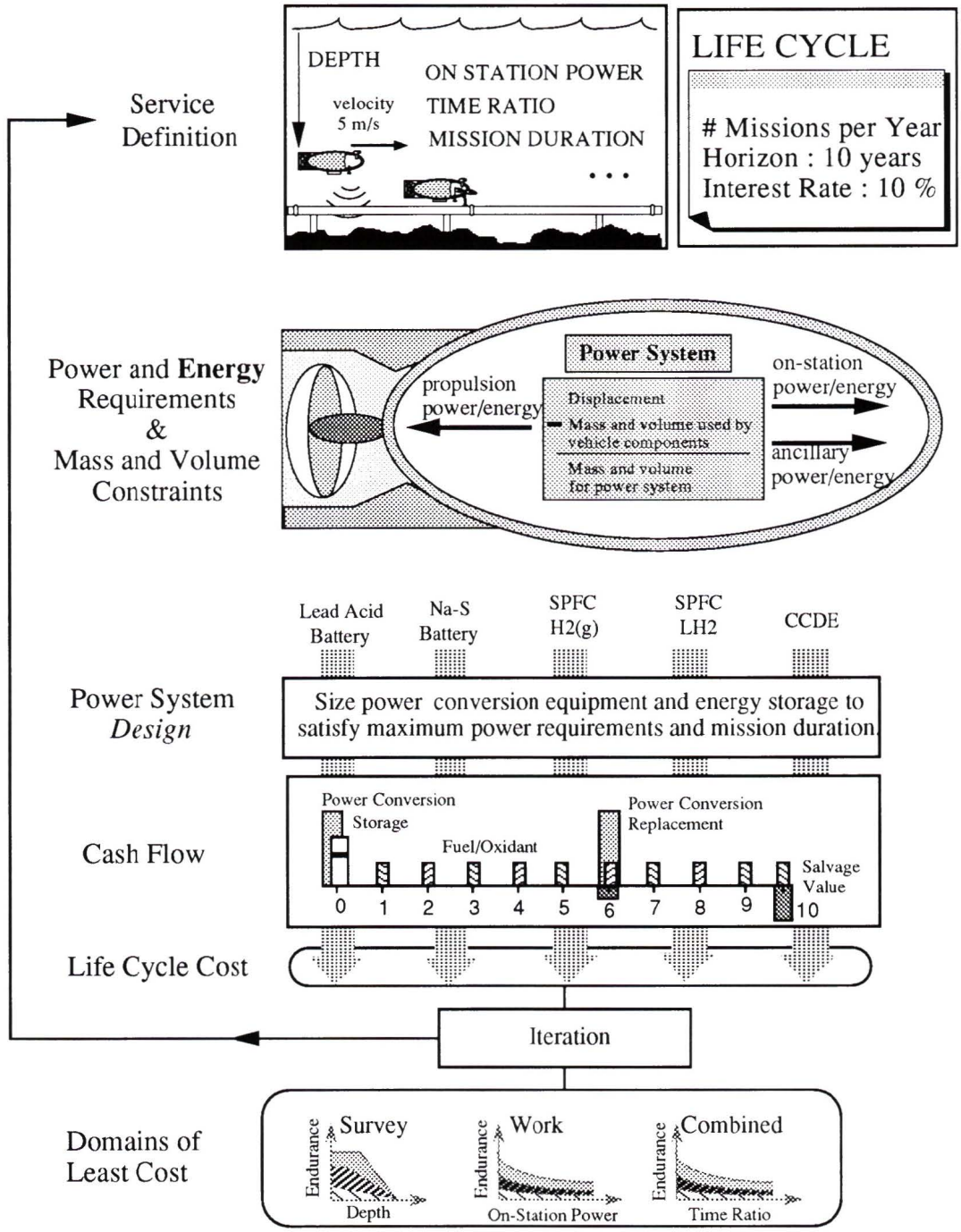

Figure 1.3: Simulation technique for constructing domains of least cost.

2. Determine the power **and energy** requirements associated with the mission. Also, determine the mass and volume constraints imposed by the vehicle configuration.

3. Size the power system components to satisfy the mission requirements. Power conversion equipment is sized to satisfy the maximum power. Energy storage tanks (and batteries) are sized to provide the required mission duration. The power system *design* must not violate vehicle neutral buoyancy.

4. Calculate the life cycle cost of the power system. All relevant costs associated with the power system are tracked over the AUV life cycle, as shown by the cash flow in Figure 1.3. To represent the time-value of money, an interest rate of 10% is assumed. All costs are converted to their present value and normalized per hour of service provided.

The cash flow in Figure 1.3 includes the following cost components for each power system:

- **Capital cost:** Capital cost is considered for power conversion equipment (i.e. fuel cell stack, engine) and energy storage equipment (i.e. fuel tanks, batteries) The lifetimes of these technologies are considered within the techno-economic modelling. Salvage value is depreciated using a double-declining balance depreciation model. Possible repurchasing of capital equipment is also considered within the cash flow.

- **Operating cost:** Operating cost is considered for the delivery of fuel and oxidant (or electricity for the case of the battery). No additional cost or benefit is associated with the waste products (such as CO_2 or battery disposal).

Maintenance costs are not included within the cash flow on the basis that their inclusion would not significantly alter the *relative* cost of power systems. Taxes

and profits are also not included within the cash flow. All costs are expressed in Canadian dollars at 1992 prices and exchange rates.

Execution of the comparison methodology requires modelling the service and the service technologies. The service model has been discussed in this section. Chapter 2 defines the generic AUV which is to be used throughout the analysis. Chapter 3 discusses storage batteries for AUV applications, and concludes with techno-economic models for the lead-acid and sodium-sulfur batteries. Chapters 4 and 5 address the solid polymer fuel cell and the closed cycle diesel engine, respectively. Finally, Chapter 6 presents the techno-economic comparison of power systems for three distinct categories of AUV applications.

Chapter 2

The Autonomous Underwater Vehicle (AUV)

This thesis compares power systems for autonomous underwater vehicle (AUV) applications. It is **not** an optimization study of the AUV work *system* for providing subsea services. The complete service technology includes the AUV (and all of the relevant subsystems onboard) as well as its surface support requirements. Optimization of this work system to provide a given service involves careful design decisions regarding *all* of the component technologies. This thesis focusses on the power system. A *generic* AUV is considered, which is common for all power systems and consistent throughout the analysis. Consequently, the influence of the AUV and its surface support requirements are eliminated from the power system comparison.

The generic AUV, as illustrated in Figure 2.1, is comprised of the following five components:

- Vehicle shell
- Propulsion system
- Payload
- Buoyancy system
- Power system

The power system provides power and energy to each of the vehicle subsystems. Furthermore, these components must fit within the configuration of the hull in a neutrally buoyant fashion[1], thus imposing mass and volume constraints upon the power system. Because the vehicle is fixed in the analysis, the requirements and constraints imposed by the mission profile and vehicle configuration are common to all power systems.

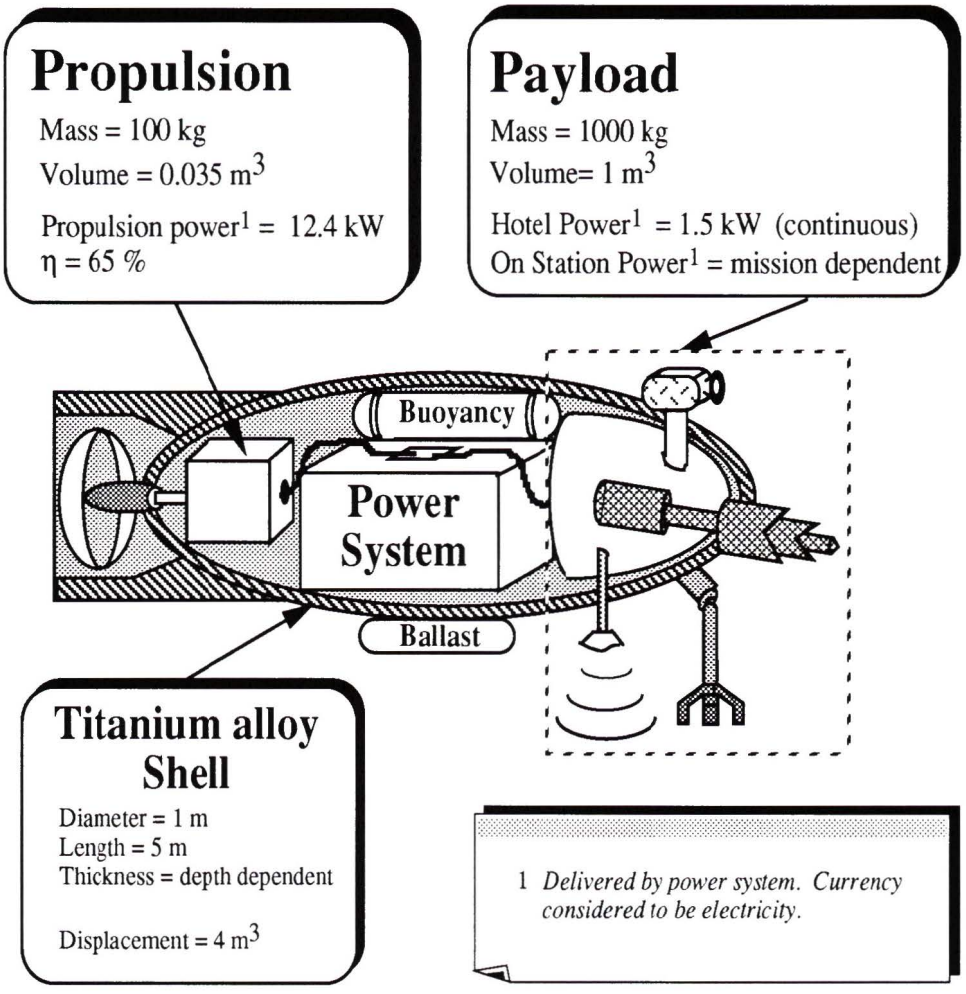

Figure 2.1: The generic autonomous underwater vehicle.

[1]For neutral buoyancy, the sum of the component masses must equal the mass of water displaced by the vehicle shell. No consideration is given to the shapes of these component technologies in fitting them inside the vehicle shell.

2.1 Vehicle Shell

AUV's are inherently small displacement vehicles, benefitting from easy deployment and reduced surface support vessel requirements. Two examples of current AUV development programs illustrate this point. The ARCS (Autonomous Remote Controlled Submersible) vehicle, made by Lavalin Ocean Systems, has a displacement of 1.5 m^3 [2]. It is modular and can be separated into four sections for transportation by light aircraft. The DARPA vehicle has a displacement of 10 m^3 [12], perhaps representing the upper limit to AUV size [13]. This thesis considers a vehicle displacement of 4 m^3, lying between these two extremes.

In further similarity to the ARCS and DARPA vehicles, the generic AUV considered in this study has a slender shape, with a length-to-diameter ratio of 5. This shape allows for efficient hydrodynamic properties, beneficial for missions of long transit range.

The vehicle shell resists the ambient pressure of the surrounding water, maintaining atmospheric pressure inside. Consequently, the required shell thickness (and mass) increases with depth. Because underwater vehicles must be neutrally buoyant in the water, the vehicle shell mass can play an important role in power system analysis. Guerrier [8] discusses the importance of minimizing shell mass in order to maximize onboard storage of payload and energy. He suggests that considerable improvements in energy storage can be achieved by using composite materials rather than steel for the vehicle pressure vessel. This thesis considers a vehicle shell made from titanium alloy (6% Al, 4% V), as used in the manned research submersible *Shinkai 6500* [4].

Pressure vessel mass is the sum of the contributions by a cylindrical shell, two hemispherical heads, penetrations, flanges, and ancillary structural details. As an approximation to the pressure vessel mass, this thesis uses membrane theory to determine the required pressure vessel thickness for a given vehicle depth. Membrane theory considers all pressure vessel stresses to be carried

in either tension or compression [15]. The effect of bending stresses, which would be encountered at the hemispherical ends of the vehicle shell, are not considered. Furthermore, there is a potential for shell buckling and consequently shell stiffeners would likely be required. Nevertheless, membrane theory offers a suitable approximation to the response of required shell thickness to depth.

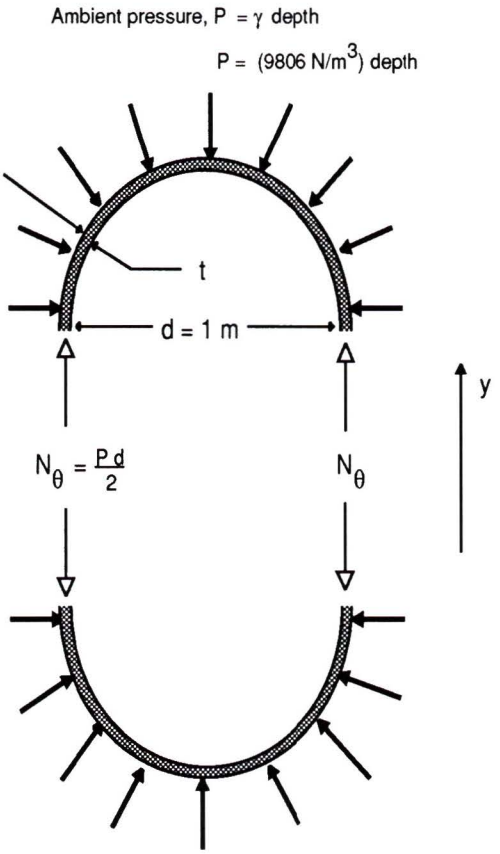

Figure 2.2: Stresses in the vehicle pressure vessel.

Figure 2.2 shows the freebody diagram of a cylindrical pressure vessel under external pressure, P. A balance of forces in the y-direction suggests that the maximum compression stress in the shell is given by:

$$\sigma_\theta = \frac{N_\theta}{t} = \frac{P\,d}{2\,t} \tag{2.1}$$

where P is the ambient pressure, d is the diameter of the vessel and t is the

shell thickness.

The required shell thickness is calculated by assuming a yield criterion where the maximum compression stress in the shell is equated to the yield stress of the material.

$$t = \frac{P\,d}{2\,\sigma_y} \tag{2.2}$$

where σ_y is the yield stress of the shell material (250 MPa). From this, the mass and internal volume occupied by the vehicle shell is calculated (the density of the titanium-alloy shell material is 4.46 kg/l).

2.2 Propulsion System

This thesis assumes an electric propulsion system similar to that used in the *Shinkai 6500* [4]. It consists of a single screw propeller, reduction gear, ac induction motor and power conditioning unit, as shown in Figure 2.3. Each component of the propulsion system is assumed to operate at its optimal efficiency: 75% for the propeller [16] and 95% for the gear reducer, induction motor and inverter, respectively [17, 18]. The net efficiency of the propulsion system is 65%.

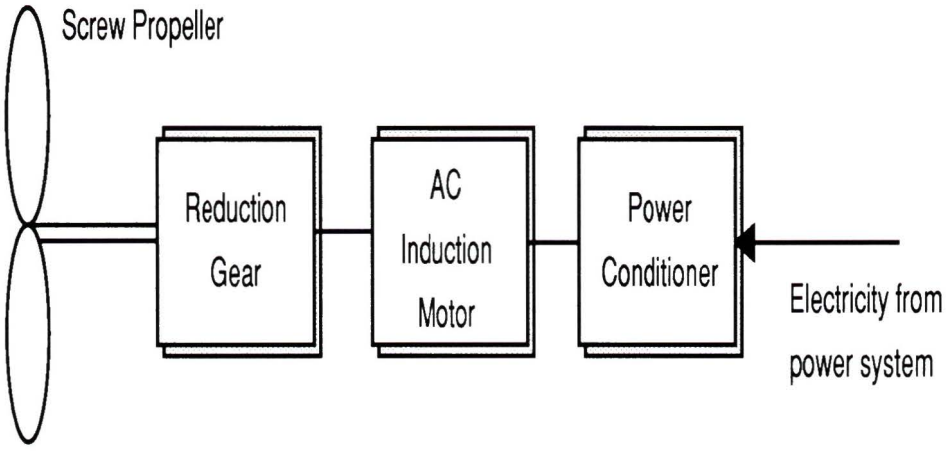

Figure 2.3: Electric propulsion system.

The propulsion power required at the propeller is calculated by the formula [13]:

$$P_{propeller} = \frac{1}{2} \rho C_D V^{2/3} v^3 \tag{2.3}$$

where ρ is the seawater density (1.024 kg/l), C_D is the volumetric drag coefficient ($C_D = 0.05$ for a vehicle with $\frac{L}{D} = 5$ [13]), V is the vehicle volume (4 m^3), and v is the speed (5 m/s). The required electric power from the power system for propulsion is then:

$$P_{propulsion} = \frac{P_{propeller}}{\eta_{propulsion\ system}} = 12.4\,kW \tag{2.4}$$

The mass and volume of each propulsion system component is proportional to its maximum power requirement. Using specific power and power density data presented in [17, 18], propulsion system mass and volume are assumed to be 100 kg and 35 l, respectively.

2.3 Payload

The payload is divided into two subcomponents: 1) the hotel load and 2) the working load. The hotel load consists of the control system, communication system, navigation system and sonar. These subsystems have a constant power requirement over the course of the AUV mission. This thesis assumes a hotel load of 1.5 kW [13]. The working load may include lights, cameras, robotic manipulators, tools, etc., all for the purpose of performing some on-station task. The working or on-station power is treated as a variable in the analysis. The size of the payload is assumed to be 1000 kg, neutrally buoyant, for all AUV scenarios considered [13].

2.4 Buoyancy System

As the name suggests, the buoyancy system controls the buoyancy of the vehicle. There are two types of buoyancy systems for underwater vehicles [19]:

- Buoyancy foam is used to balance vehicle buoyancy. Movement in the vertical plane is achieved by using the thrusters.
- A ballast tank is used to control the vehicle buoyancy. Flooding the tank with water causes the vehicle to descend, pumping the water out causes the vehicle to ascend. Ballast weights may also be used to control vehicle motion in the vertical plane.

This analysis considers the second of these two options. This is the technique used in the manned research submersible *Shinkai 6500* [4]. Using buoyancy control, the *Shinkai 6500* can descend to a depth of 6500 metres in 2.5 hours, and ascend to the surface in the same amount of time. Thus, propulsion power is not required for these two periods of transit. Compressor power is required, however, for discharging the buoyancy tank.

The sole purpose of the buoyancy systems in this analysis is to satisfy the neutral buoyancy requirement of the vehicle, and to complete the mass and volume constraints on the power system. The buoyancy system is seen to be either a lead ballast weight outside the pressure hull (to add vehicle mass), or an air tank inside the vehicle shell (to add vehicle volume). Pumping power requirements for buoyancy control are not considered.

2.5 Power System

The power system must provide power to all vehicle subsystems over the course of the mission. Power requirements are the sum of the contributions made by the propulsion system, hotel load, and the working payload. In a practical submersible, this power may be provided in a number of forms: shaft power,

hydraulic power, and electricity (ac and dc). Electricity is generally the most useful energy currency, and is the most flexible for conversion into other currencies [20]. Therefore, this thesis considers the energy currency delivered by the power system to be electricity. No distinction is made between ac and dc electricity, since their power conditioning requirements are largely the same (in terms of mass, volume, efficiency and cost criteria).

Furthermore, each power system is constrained in size by the requirement for vehicle neutral buoyancy. This may be a mass constraint or a volume constraint, depending on the vehicle hull configuration and the density of energy storage. Consideration of neutral buoyancy is critical to the proper assessment of power system performance for AUV applications.

The power system technologies considered in this thesis are the lead-acid battery, sodium-sulfur (Na-S) battery, solid polymer fuel cell (SPFC) and the closed-cycle diesel engine (CCDE). The following three chapters discuss each of these technologies, and present techno-economic models for comparison purposes.

Chapter 3

Storage Battery

For decades, the lead-acid battery has dominated autonomous subsea power. But its low energy density has been a long-standing barrier to many underwater vehicle applications. Nevertheless, reliability and low cost will ensure that the lead-acid battery remains a subsea workhorse for many years to come. This thesis considers the lead-acid battery in the analysis to provide a baseline for comparison. But more than this, we anticipate that there will be domains of service for which this system will be preferred in terms of life cycle cost.

Other battery systems have been developed for the subsea environment. The silver-zinc battery is one such example, which can provide energy density and power output greater than the lead-acid battery. The silver-zinc battery has extensive experience in marine applications. It is used as the principal power plant for the submerged research vessels *Shinkai 2000* [21] and *Shinkai 6500* [4]. The burdens of this technology are its low cycle life and high initial capital cost. Consequently the silver-zinc battery has been confined largely to military applications. Cousins of the silver-zinc battery, the silver-cadmium battery [22] and the silver-iron battery [23], offer improved lifetime characteristics. But the high cost of silver makes this family of secondary batteries inherently expensive.

Primary lithium batteries have also been proposed for submersibles [24]. The lithium/thionyl-chloride (Li-$SOCl_2$) primary battery exhibits the highest energy density of any available battery and for this reason can provide very

compelling measures of submerged endurance. But the extreme volatility of the reacting materials make safety an issue of concern for this technology [25]. Furthermore, the Li-$SOCl_2$ battery is primary; it is not rechargeable. Consequently, it will be confined to submersible applications for which repeatability is of little consequence [26].

Extensive electric vehicle research has provided the emergence of a new family of *advanced secondary batteries.* Perhaps the most developed of these is the sodium-sulfur (Na-S) battery. The Na-S battery, made by Powerplex Technologies Inc. of Canada, is to be integrated with the ETX-II powertrain and installed in a Ford Aerostar for test and development [27, 28]. The same battery was recently tested by Daimler-Benz, BMW and Volkswagen and found to exhibit superior performance to all other batteries tested [29]. And Chloride Silent Power, another significant manufacturer of the Na-S battery, currently operates a pilot plant near Manchester, where they investigate the optimization of large scale production techniques [30].

Of the emerging advanced secondary battery systems, the Na-S battery appears to be the most developed, the most promising, and the most poised to enter the expanding electric vehicle market. Furthermore, it has previously been proposed for submersible applications [25]. This thesis chooses the Na-S battery to represent this emerging family of battery systems and includes it within the techno-economic comparison presented.

3.1 Sodium-Sulfur Cell

A simplified cross-section of a sodium-sulfur cell is shown in Figure 3.1. The cell consists of a solid ceramic electrolyte of beta alumina and liquid electrodes of sodium (Na) and sulfur (S). Operating temperatures between 570 K and 620 K are required to ensure the reactants are molten and the ceramic electrolyte is adequately conductive [31]. The ceramic electrolyte allows Na^+ ions to pass

through, but does not allow molecules of sodium and sulfur to mix. The sodium anode is contained in a steel can. Should the ceramic divider break, sodium is metered out through a small hole in the bottom to safely react with sulfur in the formation of polysulfides.

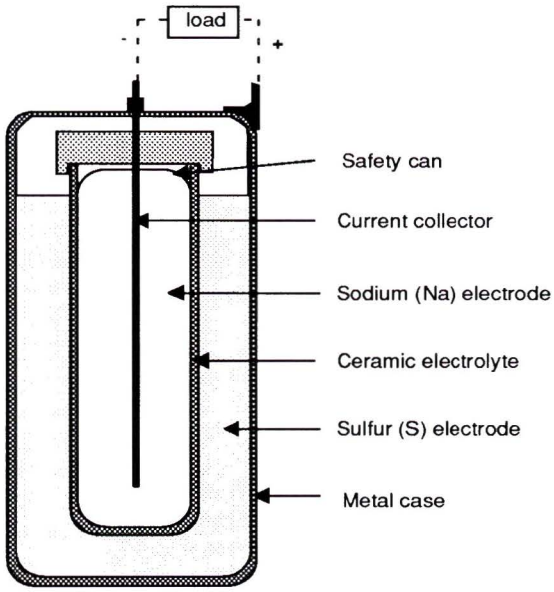

Figure 3.1: Simplified cross-section of sodium-sulfur cell.

During discharge, sodium is oxidized at the sodium/solid electrolyte interface, releasing electrons to the external circuit. The Na^+ ions migrate through the electrolyte to the cathode where they react with sulfur. The *initial* reaction product is sodium pentasulfide (Na_2S_5).

$$2\,Na \;+\; 5\,S \;\rightarrow\; Na_2S_5 \tag{3.1}$$

Na_2S_5 is immiscible in sulfur, and a two-phase mixture, consisting of sulfur and sodium pentasulfide, forms at the cathode. This reaction process is maintained so long as free sulfur is available for reaction, lasting for approximately 60% of the discharge capacity. Throughout this discharge condition, the open circuit voltage remains constant at 2.08 volts. After all of the sulfur has been consumed, further discharge progressively converts the Na_2S_5 in a single phase to Na_2S_3.

When this conversion is complete, the cell is effectively completely discharged. During this polysulfide conversion process, the open circuit voltage of the cell falls linearly from 2.08 volts to 1.76 volts [32].

Recharging the cell is achieved by applying a voltage (in excess of open circuit because of irreversibilities) of reverse polarity to the electrodes. Charging efficiencies for the sodium-sulfur cell are high, typically in the order of 90% [32]. As opposed to its lead-acid counterpart, the sodium-sulfur cell exhibits virtually no memory effect[1] [31].

Another advantage of the sodium-sulfur cell is that it exhibits a Faradaic (amp-hour) efficiency of 100%. That is to say, all of the electrons donated to the cell during charging are eventually converted into energy output in the form of electric current. This is due to the absence of side reactions which detract electrons from useful electric energy storage. Consequently, the cell's state-of-charge can be easily determined by simply recording the amp-hours (or coulombs) into and out of the cell. Determining the state-of-charge can be a difficult assignment with some other battery systems. Furthermore, the virtual absence of self-discharge means that the Na-S battery can exhibit extremely long shelf life [31].

The discharge voltage characteristics of the Na-S cell are illustrated in Figure 3.2 [31]. As previously mentioned, output voltage is a function of state-of-charge, since the electrochemical reaction changes as the products are formed. Nevertheless, the cell's inherently low internal resistance is independent of state-of-charge, and therefore good voltage regulation is maintained throughout cell discharge.

Cell voltage is also a function of discharge rate. Cell output voltage decreases with increasing current due to polarization within the cell. Three types of polarization are commonly identified in electrochemical systems:

[1] Memory effect or hysteresis is the reduction in capacity that a cell undergoes when it is cycled in shallow discharges [32].

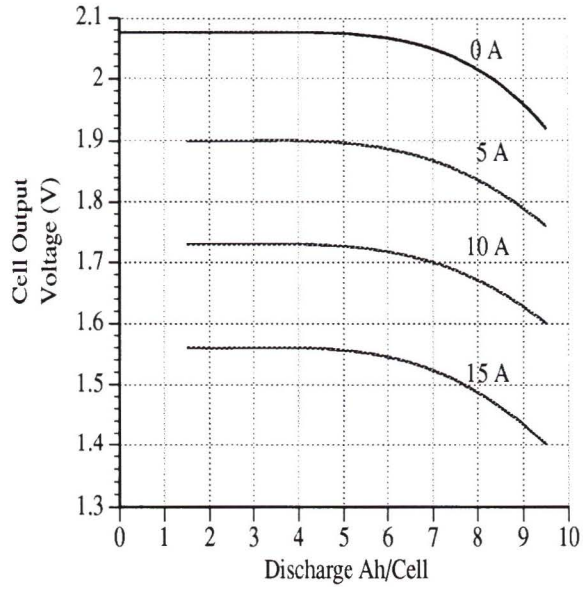

Figure 3.2: Discharge voltage characteristics of sodium-sulfur cell [31]. Cell output voltage decreases with decreasing state-of-charge and with increasing output current.

- **Activization Polarization:** Activization polarization is the potential required to drive the reduction and oxidation processes at the electrodes. This overpotential may be reduced by the addition of a suitable electrocatalyst.

- **Ohmic Polarization:** Ohmic polarization includes losses due to resistance in the electrolyte, electrodes and terminal connections of the cell.

- **Concentration Polarization:** Concentration polarization is caused by mass transport limitations of the reacting species.

The *maximum* work output of the cell is given by the change in Gibbs Free Energy for the electrochemical reaction:

$$\Delta G = n F E_{rev} \tag{3.2}$$

where n is the number of electrons involved in the reaction, F is Faraday's constant (96,487 coulombs) and E_{rev} is the reversible open-circuit voltage for

the electrochemical reaction. Because of polarization effects, the *actual* work output of the cell is less than the maximum.

The energy conversion efficiency of the cell can be expressed:

$$\eta = \eta_{charge}\,\eta_F\,\frac{E_{cell}}{E_{rev}} \tag{3.3}$$

where η_{charge} is the charging efficiency, η_F is the Faradaic efficiency, and $\frac{E_{cell}}{E_{rev}}$ is defined to be the voltage efficiency. The voltage efficiency is dependent on the discharge conditions of the cell, decreasing with increasing discharge rate.

Two conclusions can be made from the above discussion on sodium-sulfur cell electrochemistry:

- The energy conversion efficiency of the cell decreases with increasing discharge current.
- The maximum power output of the cell decreases with decreasing state-of-charge.

3.2 Sodium-Sulfur Battery

The sodium-sulfur battery consists of many cells connected in series and parallel to provide the voltage and current requirements of the service. Care must be taken to ensure that the battery output characteristics are compatible with its companion technologies. For instance, in electric vehicle applications, upper and lower limits are imposed on the peak battery voltage by the inverter and ac motor, respectively [28].

Battery lifetime is governed by the failure rate of the cells. Cells fail abruptly in two modes [33]:

- Cracking of the solid ceramic electrolyte

- Failure of the seals between negative (sodium) and positive (sulfur) compartments.

Failed cells are sensed and shorted out of the battery string. Consequently, battery energy capacity decreases with increased number of charge/recharge cycles, as individual cell failures compound.

The cells are mechanically arranged within a carriage, which slides into a vacuum enclosure for thermal insulation. A thermal management system maintains battery operating temperature between 570 K and 620 K. During operation, I^2R losses are sufficient to maintain required operating temperatures. But during idle times, a heater may be required. Thermal losses are small (approximately 200 W for a 50 kWh electric vehicle battery) and a typical Na-S battery can stand off-charge for up to 48 hours [31]. Cold start takes about 24 hours [30].

Maximum battery power can be maintained for several minutes. The time limit is imposed by the large amount of waste heat produced and the fast temperature rise of the battery. *Sustained* battery power is determined by the rate of waste heat removal.

Ancillary equipment required for proper battery operation reduces the energy density of the battery, as compared to the cell alone. The ratio of cell weight to battery weight is approximately 50% [28]. Nevertheless, the sodium-sulfur battery *system* can provide specific energy in the order of 100 Wh/kg, approximately three times higher then the lead-acid battery.

Other attractive features of the Na-S battery for electric vehicle applications are:

- Stable discharge characteristics
- Practically no maintenance required
- State-of-charge easy to measure
- Extremely long shelf life

3.3 Techno-Economic Models

Techno-economic models for the lead-acid battery and sodium-sulfur battery are illustrated in Figure 3.3. Modelling data presented is specific for the following two battery systems:

- **Na-S battery, manufactured by Chloride Silent Power Ltd.:** One third size electric vehicle battery, 300 amp-hours, 64 volts. Includes battery charger and thermal management system.
- **3ET205 tubular lead-acid battery, manufactured by Chloride Silent Power Ltd.:** This battery is currently receiving some consideration for the General Motors G-Van.

These two batteries were evaluated by Argonne Analysis and Diagnostic Lab for electric vehicle applications under simulated conditions [34]. Standardized tests were developed to characterize battery performance:

- **Available energy versus constant power discharge rate (Ragone plot):** Specific energies are measured using constant power discharge to 100% depth-of-discharge (DOD) or 0% state-of-charge.
- **Available peak power versus depth-of-discharge (DOD):** Specific peak power is derived from driving profile discharge data and is plotted as a function of DOD, based on the available energy for the average power discharge rate.

The results of these tests are used to model the technical performance of the Na-S battery and lead-acid battery, as shown in Figure 3.3. The relationship of energy capacity with discharge power is used to track the state-of-charge of the battery over the course of the AUV mission. The instantaneous depth-of-discharge (DOD) of the battery can be expressed in mathematical form by:

$$DOD(t) = \int_0^t \frac{P(t)\,dt}{Wh(t)} \tag{3.4}$$

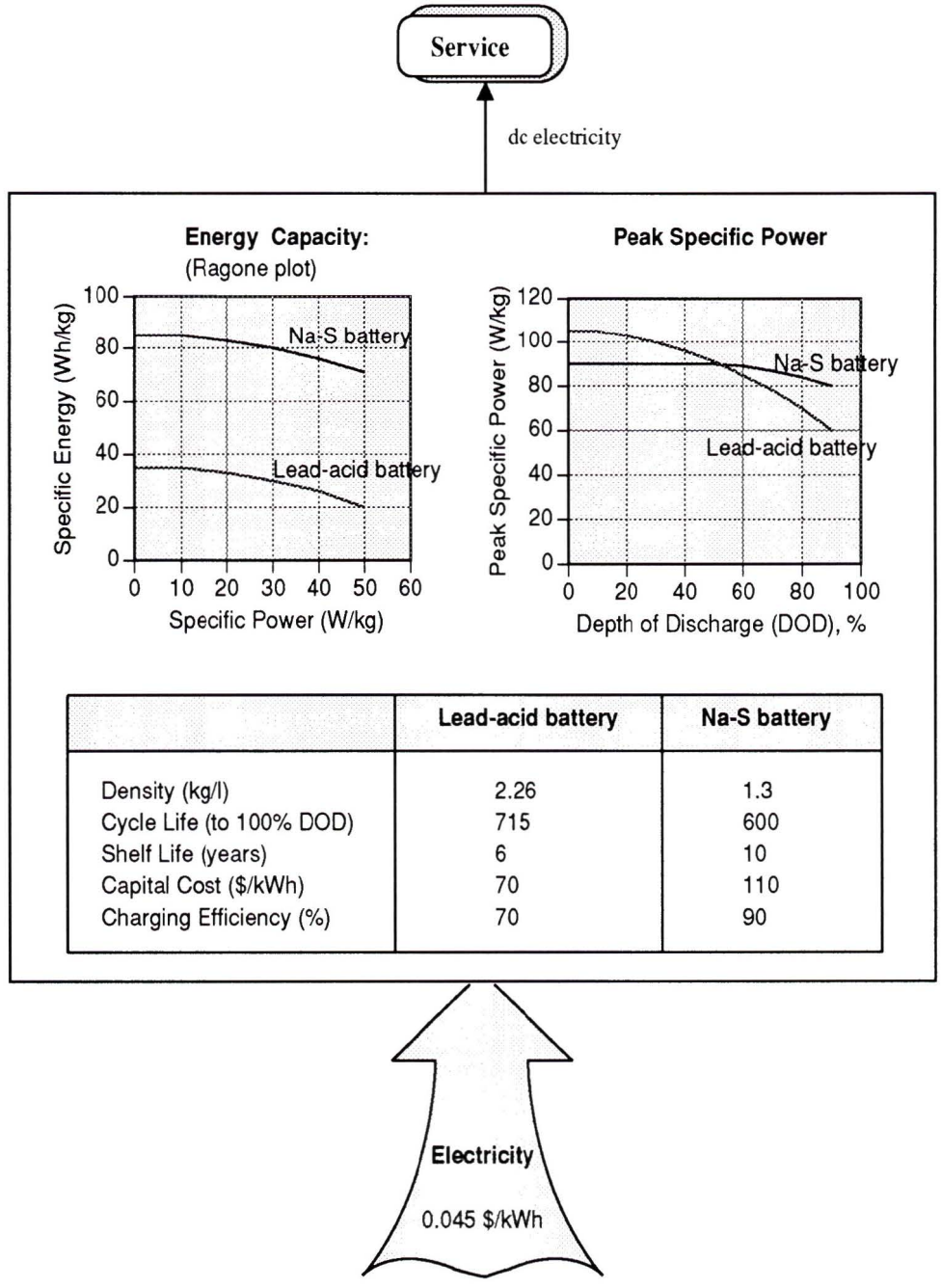

	Lead-acid battery	Na-S battery
Density (kg/l)	2.26	1.3
Cycle Life (to 100% DOD)	715	600
Shelf Life (years)	6	10
Capital Cost ($/kWh)	70	110
Charging Efficiency (%)	70	90

Figure 3.3: Techno-economic models for the lead-acid battery and sodium-sulfur battery.

where P(t) is the instantaneous power requirement, and Wh(t) is the energy capacity of the battery associated with this discharge power level (as determined from the Ragone plot). The simulation technique used in this thesis assumes the batteries to be discharged to 100% DOD.

Burke [35] examines the Chloride 3ET205 lead-acid battery for electric vehicle applications. He presents the battery discharge profile when simulated over a standard federal urban driving cycle, and shows that the *actual* energy capacity of the battery under these discharge conditions is *less* than that predicted by the constant power Ragone plot. Nevertheless, the Ragone plot is a suitable model of battery discharge characteristics for this thesis, since the AUV mission considered is comprised almost entirely of constant power discharges.

Battery lifetime characteristics are required for the calculation of life cycle cost. Two parameters are used for this purpose:

- **Cycle life:** Cycle life is the number of charge/discharge cycles that can be accommodated by the battery before it reaches 80% of its initial capacity. This thesis uses results of life-cycle testing performed by the Argonne Analysis and Diagnostic Lab for the same two batteries under consideration [34]. The tests were conducted with 100% capacity discharges, using a standard federal urban driving cycle. Deep discharges are considered to evaluate a worst-case condition. In the reported test, 715 cycles were measured for the lead-acid battery. The cycle life of the Na-S battery was *projected* to be 600 cycles. (The battery lifetime ended prematurely at 225 cycles because of fabrication-related failure of cell seals.)

- **Shelf life:** Shelf life is a measure of how long a battery can be stored when not in use. It becomes an important modelling parameter for AUV services demanding a very low mission frequency. In such cases, the shelf life imposes an upper limit to the battery lifetime. The shelf life of lead-acid traction batteries is given by Linden [32] to be 6 years. A shelf life

of ten years is assumed for the Na-S battery.

The calculation of battery life cycle cost includes the capital cost of the battery and charger, as well as operating (electricity) costs. The following assumptions are used:

- The capital cost of the sodium-sulfur battery assumes large scale, optimized production. Chloride Silent Power Ltd. [36] have calculated the required factory cost and the required selling price for such a scenario. They consider producing 69 kWh electric vehicle batteries at a scale of 6600 batteries per year. This thesis uses the factory cost, since the selling price includes license fees, royalties, return on investment and taxes which are *not* included in the cash flow. The reported production cost is 110 $/kWh.

- The capital cost of the lead-acid battery is taken to be 70 $/kWh [37].

- Electricity cost is assumed to be 0.045 $/kWh throughout this thesis.

Chapter 4

Solid Polymer Fuel Cell (SPFC)

The operation of a fuel cell is fundamentally the same as that of a battery. Similar to a battery, a fuel cell converts the chemical energy of reactants directly into dc electricity by means of an electrochemical reaction. However, unlike a battery, the reactants and products associated with the reaction are stored outside the fuel cell. This leads to significant operational advantages of fuel cell systems with respect to batteries [38]:

- Fuel cells will produce current so long as a fuel and oxidant are supplied. The performance is not dependent on the *state-of-charge* (or the degree to which the storage tanks are full), as is the case for battery systems.
- The components of the fuel cell do not enter into the reaction and therefore fuel cells can exhibit very long lifetimes.
- Fuel cells do not require lengthy recharging as do batteries. Refueling can be quickly accomplished by replacing or refilling reactant storage tanks.

Fuel cells were first developed to exploit the properties of hydrogen for space exploration [39]. Hydrogen has the highest specific energy (heating value) of any conventional fuel. Furthermore, when combined with oxygen in a fuel cell, water and heat are the only products. This feature may be advantageous for closed system operation, as in space.

Transfer of fuel cell technology to commercial applications has been inhibited by two principle barriers:

- **High capital cost of stack:** Presently, the capital cost of the solid polymer fuel cell stack is in the order of 6,000 $/kW. Developers claim that improvements in hardware, reductions in platinum requirements, and the benefits of mass production can reduce capital cost by an order of magnitude. [40]

- **Onboard storage of hydrogen and oxygen:** Storage as a compressed gas in steel pressure vessels adds considerable mass and volume to the power system. Storage of hydrogen as a cryogenic liquid can offer energy storage densities more comparable to gasoline. On a per unit of energy basis, liquid hydrogen storage occupies about twice the mass and four times the volume as gasoline (including the storage tank) [41]. The main barrier to widespread use of liquid hydrogen as a fuel for vehicles has been and continues to be the high cost of hydrogen liquefaction.

Recently, major advances in fuel cell technology has made its bid for commercial transportation applications more viable. These advances include large increases in power density and reductions in intrinsic cost [42].

A number of fuel cell systems have been developed. They can be distinguished by the electrolyte used and the temperature of operation, as shown in Table 4.1 [43]. Of these systems, only the alkaline and solid polymer fuel cells are particularly well suited for transportation applications. Both have the advantage of low-temperature operation, leading to quicker start-up times and lower levels of system complexity than systems operating at elevated temperatures.

Both the alkaline fuel cell and the solid polymer fuel cell have successful operational experience in submarines. In the 1970's, the U.S. Navy developed the *Deep Submergence Rescue Vehicle* (DSRV), and Lockheed developed *Deep Quest*, both using the alkaline fuel cell with H_2-O_2 [38]. More recently, the Fed-

Table 4.1: Types of fuel cells categorized by electrolyte and operating temperature.

Type	Electrolyte	Operating Temperature, K
Alkaline	Potassium hydroxide	320-360
Proton exchange membrane	Solid polymer	320-400
Phosphoric acid	Orthophosphoric acid	460-480
Molten carbonate	Li-K carbonate mixture	900-920
Solid oxide	Stabilized zirconia	1170-1270

eral German Navy has installed a 48 kW alkaline fuel cell stack in its type 205 submarine, greatly increasing submerged endurance. The first of the class is expected to be commissioned in 1995 [2]. In July of 1989, Perry Offshore/Energy Systems (recently renamed Energy Partners) successfully tested the solid polymer fuel cell (made by Ballard Power System in North Vancouver) for use in its two-person observation submersible *PC-1401*. The SPFC system, using compressed hydrogen and oxygen storage, can provide three times the energy as the previously used lead-acid battery while occupying only half of the space [44].

Although both systems have proven to be suitable for underwater vehicle applications, recent studies have favoured the solid polymer fuel cell over the alkaline system [12, 45, 46]. The primary reason given for this preference is that the solid polymer membrane allows for a more robust stack design, whereas the alkaline system requires the use of a corrosive electrolyte and the associated electrolyte management system. This thesis follows current research trends and considers the solid polymer fuel cell as the representative fuel cell technology.

This chapter is divided into three sections. The first section discusses the electrochemical principles of the solid polymer fuel cell. The second considers the operational principles of the solid polymer fuel cell *system*. Last, the techno-economic model used in the comparison of Chapter 6 is presented.

4.1 Solid Polymer Fuel Cell Electrochemistry

The membrane/electrode assembly for the solid polymer fuel cell is shown schematically in Figure 4.1. The electrolyte is a solid polymer ion-conducting membrane. The electrolyte is sandwiched between two electrodes of porous carbon paper, which allow the passage of reactant gases to the reaction sites. To facilitate anode and cathode reactions, an electrocatalyst (typically platinum) is placed between each electrode and the electrolyte.

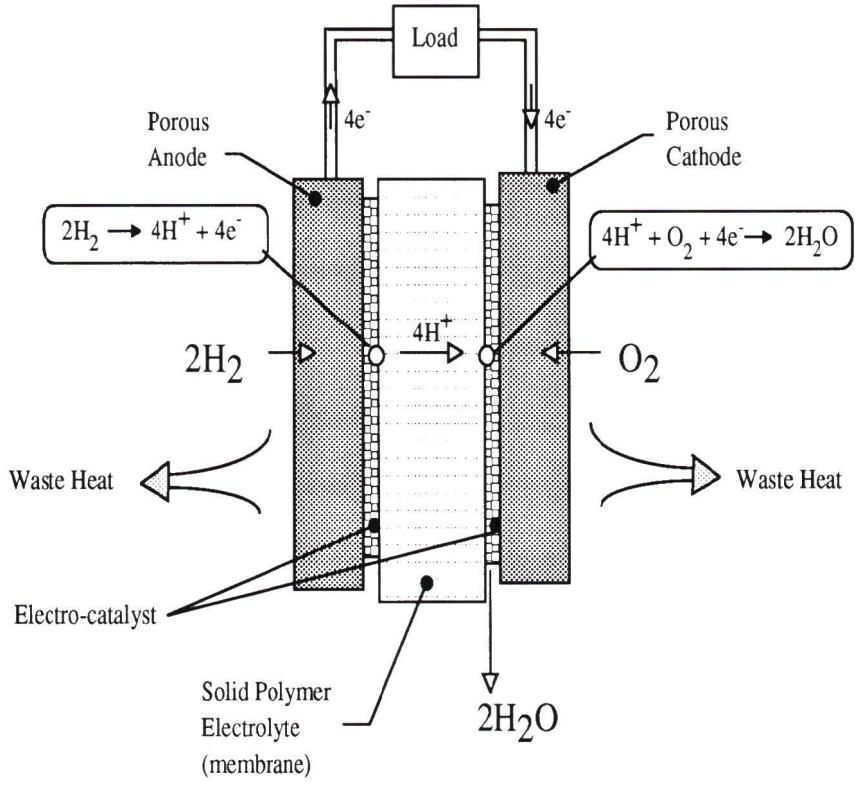

Figure 4.1: The solid polymer fuel cell.

At the anode, H_2 is catalytically dissociated according to the reaction

$$2H_2 \rightarrow 4H^+ + 4e^- \tag{4.1}$$

Electrons are donated to the external circuit. Hydrogen ions (H^+) pass through the solid polymer electrolyte. At the cathode, they combine catalytically with

oxygen and electrons from the external circuit to form water, according to the reaction

$$4H^+ + O_2 + 4e^- \rightarrow 2H_2O \tag{4.2}$$

The polymer electrolyte is a thin plastic-like membrane made of perfluorosulfonic acids. H^+ ions are transferred in combination with water molecules within the electrolyte molecular structure as H_3O^+ [48]. To maintain protonic conductivity, the membrane must contain sufficient water. The electrochemical processes of the cell result in dehydration of the polymer membrane, and a subsequent loss in protonic conductivity and membrane life. For this reason, the water content of the electrolyte must be maintained throughout cell operation [42]. This is usually accomplished by humidifying the H_2 inlet gas stream using water produced at the cathode [49, 45].

Ideally, the fuel cell operates at the reversible open circuit voltage for the electrochemical reaction[1]. In practice, when current is drawn from the fuel cell, the actual cell voltage, E_{cell}, decreases from the open circuit voltage by an amount which increases with increasing cell output (i.e. current density). This voltage drop is due to polarization, of which there are three main types: activation polarization, ohmic polarization and concentration polarization. The relative effects of each are shown schematically in Figure 4.2. Ideally, for low currents, the cell potential would be close to the reversible open circuit voltage. In practice, the catalyst does not work perfectly and activation losses of 0.2 to 0.3 V result. At higher currents, ohmic losses due to resistances in the electrolyte, electrodes and terminal connections in the cell contribute another 0.1 to 0.3 V of potential drop. At sufficiently high current densities, the reactant gases can no longer be supplied to the reaction sites in sufficient concentration to sustain the electrochemical reaction, and the voltage drops quickly to zero [42].

The maximum fuel cell work output is given by the change in Gibbs Free

[1]The open circuit voltage of the electrochemical reaction depends on the states of the reactants and product. For reactants and product at their standard states (298 K, 1 atmosphere), $E_{rev} = 1.23$ V.

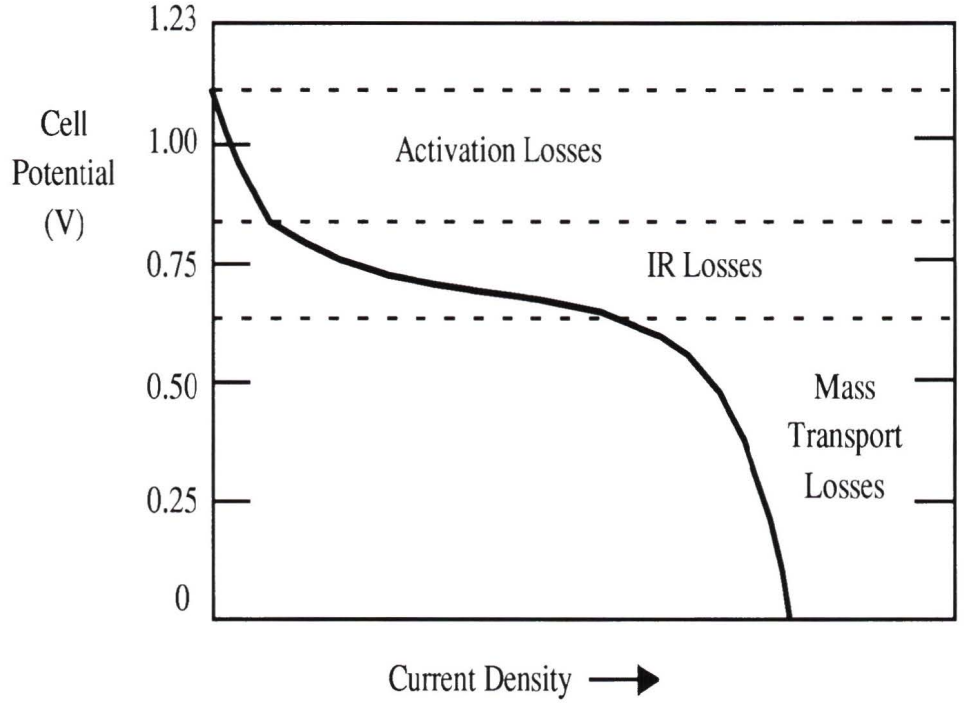

Figure 4.2: Conceptual representation of the voltage vs. current density relationship for the H_2-O_2 fuel cell [42]. The figure illustrates the major contributions to voltage loss: 1) Activation Polarization due to imperfect catalysis, 2) Ohmic Polarization due to resistive losses in the cell, and 3) Concentration Polarization due to mass transport limitations of the reacting species.

Energy of the electrochemical reaction:

$$\Delta G = n F E_{rev} \tag{4.3}$$

where n is the number of electrons involved in the reaction, F is Faraday's constant (96,487 C), and E_{rev} is the reversible open circuit voltage. E_{rev} depends on the states of the reactants and product, and varies with the operating conditions of the fuel cell. Convention is to take H_2 and O_2 at 1 atmosphere and 298 K, and product water as a liquid at 298 K [48]. The resulting open circuit voltage is 1.23 V.

The *maximum* fuel cell efficiency is given by the ratio of Gibbs Free Energy to the change in enthalpy for the electrochemical reaction. Consistency requires the use of the *higher heating value*, which considers product water in liquid

state. The maximum fuel cell efficiency is then:

$$\eta_{max} = \frac{\Delta G}{\Delta H_{hhv}} = 83\% \tag{4.4}$$

In practice, the fuel cell operates well below the open circuit voltage because of losses due to polarization. The actual fuel cell efficiency is given by:

$$\eta = \eta_{max} \frac{E_{cell}}{E_{rev}} \tag{4.5}$$

where $\frac{E_{cell}}{E_{rev}}$ is commonly referred to as the voltage efficiency. Fuel cell efficiency decreases with increasing load, as losses due to polarization compound.

This discussion points out two important features of the fuel cell technology:

- Energy conversion is *direct*. That is to say, it does not involve an intermediate conversion step into heat. For this reason, the energy conversion efficiency is not restricted by the Carnot expression of the 2^{nd} Law, and therefore not restricted by present material limitations which curtail the high temperatures required for high efficiency heat engines. Consequently, fuel cells can exhibit much higher energy conversion efficiencies than can heat engines.

- Fuel cells exhibit very good part load efficiency (as opposed to heat engines which typically exhibit poor part load efficiency). This is advantageous for many transportation applications because a substantial portion of the duty cycle is at part load.

4.2 Solid Polymer Fuel Cell System

A solid polymer fuel cell system for application in AUV's has been developed by Treadwell Corporation, in conjunction with the Naval Research Laboratory, Washington D.C. [49, 50]. The system is shown schematically in Figure 4.3. It can be divided into three principal components: 1) the fuel cell stack, 2) its related ancillary equipment, and 3) the onboard storage of reactants and products. These three components are discussed.

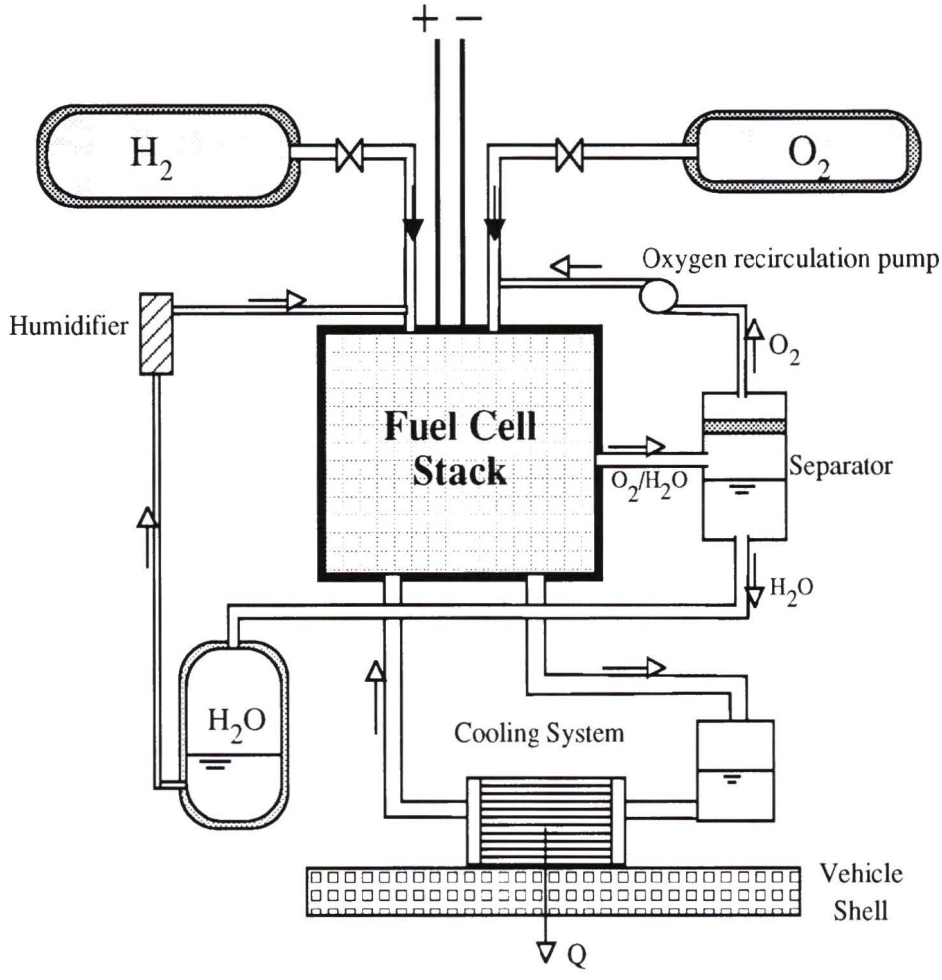

Figure 4.3: Schematic illustration of the solid polymer fuel cell system.

4.2.1 Fuel Cell Stack

A complete fuel cell consists of a membrane electrode assembly (as discussed in section 4.1), along with conductive plates in contact with the back of each porous electrode. The plates provide electrical contact to the external circuit. They also contain flow channels through which reactant gases are brought to the back of the electrodes and product water is removed. [51]

A fuel cell *stack* consists of a number of cells placed in series. The cells are arranged in bipolar configuration such that current is exchanged between conducting plates of adjacent cells [42]. The stack voltage is simply the sum of the individual cell voltages. Stack output power is then related to the cross-sectional area of the cells by the polarization relationship (cell voltage vs. current density) described in the previous section. A practical power plant may be comprised of several stacks, connected in series or parallel, to provide the required voltage and current [45].

4.2.2 Ancillary Equipment

Ancillary equipment required for fuel cell stack operation includes subsystems for the delivery of reactant gases, and for the removal of product water and heat. Furthermore, a humidification system is required to maintain the water content (and consequent protonic conductivity) of the polymer membrane electrolyte.

Hydrogen is delivered to the fuel cell anode at regulated pressure. Maintenance of the water content in the polymer membrane electrolyte is achieved by humidifying the H_2 inlet stream using water produced at the cathode [45, 48, 49]. Carey [49] shows that fuel cell operation using dry hydrogen results in performance well below that predicted from computer models, and that the use of humidified hydrogen brings this performance much closer to design expectations.

Oxygen is delivered to the cathode at regulated pressure, in quantities excess

of stoichiometric. Some of the O_2 is consumed in the reaction. The excess O_2 is used to carry the product water away from the cathode. This is required to prevent H_2O molecules from blocking reactant gases at the electrode reaction sites, thereby decreasing cell output voltage. The resulting mixture of O_2 and H_2O is fed to the separator/reservoir, where water is condensed out for onboard storage. The excess O_2 is recycled back to the inlet stream at the appropriate pressure by the oxygen recirculation pump [45, 49].

Heat produced by irreversibilities is removed from the stack by cooling water, which flows through plates positioned every two cells in the stack [44]. For manned submersibles, this waste heat may be utilized for space heating, thus raising system efficiency. However, for autonomous underwater vehicles, this heat is simply expelled overboard. Waste heat in the cooling loop is transferred to the vehicle shell, where it can be removed by convective heat transfer to the surrounding water.

A microcomputer controller handles the system start up and shut down, oxygen recirculation, sensor monitoring and fault detection [49].

4.2.3 Reactant/Product Storage

Effective storage of reactants and products is crucial to maximizing the onboard energy storage of an AUV. This section discusses various techniques of H_2 and O_2 storage for AUV applications, and highlights the relative merits and disadvantages of each system.

Hydrogen Storage

Table 4.2 compares the mass and volume of various hydrogen storage techniques. The numbers presented include the contribution of the storage vessel. Tank sizes considered are typical for electric vehicle applications.

Hydrogen storage as a compressed gas has been employed successfully in submersible applications (*Deep Quest* and *Perry PC-1401*). The disadvantage

is the large mass and volume required for the pressure vessel. Indeed, this characteristic has been one of the principle barriers to the penetration of hydrogen systems into commercial applications. Table 4.2 shows that even using modern composite materials and high storage pressures, compressed hydrogen storage is relatively bulky in comparison with other hydrogen storage techniques. Nevertheless, this technique benefits by its simplicity.

Table 4.2: Comparison of hydrogen storage techniques.

	Percent mass hydrogen kg_{H_2}/kg_{total}	Partial hydrogen density kg_{H_2}/m^3_{total}	Reference
H_2(g) @ 310 bar, composite tank	3.8%	15.4	[52]
Cryogenic Liquid hydrogen	14.5%	36.2	[53]
Metal hydride ($FeTiH_{1.95}$)	1.1%	96	[53]
Methanol	9.0%	98	[53]
Lithium hydride (LiH)	22.4%	120	[54]

The storage of hydrogen as a cryogenic liquid can provide energy densities far greater than those obtainable by compressed gases. Considerable experience in liquid hydrogen storage has been gained in space applications and in terrestrial vehicle development projects. The principal barrier to the commercial application of this technology has been and continues to be the high cost of producing liquid hydrogen.

Storage and refueling techniques for liquid hydrogen fueled vehicles are well discussed in [41, 53]. Cryogenic liquid hydrogen is stored at a temperature of 20 K with a maximum operating pressure of about 4.5 bar (65 psi). The storage vessel (commonly referred to as a dewar) consists of two shells of aluminum alloy, separated by a vacuum. Further insulation is provided by multiple layers of aluminized foil separated by spacers. In addition to this, the vessel is completely surrounded by vapour cooled radiation shields, representing temperature levels of approximately 60 and 90 K, respectively. Current levels of hydrogen

evaporation loss are less than 1.8% per day [53].

Metal hydride storage techniques have been considered as a possible solution to the problems associated with compressed gas and liquid hydrogen storage. As can be seen from Table 4.2, metal hydrides can achieve very high volumetric packing densities. This is their principal advantage. The disadvantage of metal hydride storage systems is the low weight percent of hydrogen stored. As a result, these systems are heavy as compared to other hydrogen storage techniques. This characteristic of metal hydride storage is particularly unattractive for submersibles, which require neutral buoyancy.

Many suggest that hydrogen could be stored in liquid fuels, such as alcohols and hydrocarbons, the most notable of these being methanol. The advantage of methanol is that it can be stored in a simple lightweight tank. But there are considerable disadvantages to this hydrogen storage method. Utilization of methanol in a SPFC requires onboard reforming to produce hydrogen. The process involves steam reforming of the methanol to produce hydrogen and carbon monoxide.

$$CH_3OH \rightarrow CO + 2H_2 \tag{4.6}$$

The SPFC electrodes are poisoned by CO, and therefore the steam reforming process is followed by a water gas shift reaction, using steam to remove the CO and produce further H_2.

$$CO + H_2O \rightarrow CO_2 + H_2 \tag{4.7}$$

A disadvantage associated with methanol reforming, particularly for subsea applications, is that CO_2 must be stored onboard or expelled overboard at some parasitic power loss. Furthermore, development work at Los Alamos [42] has shown that reformers can not yet meet requirements of rapid start-up and quick transient response. Commercial reformers often take an hour or more to start up, and many minutes to change output significantly.

Dunn [54] has suggested that a particularly attractive means for storing H_2 is in chemical hydrides, such as lithium hydride (LiH). Lithium hydride is a

powder which yields hydrogen by reaction with water.

$$LiH + H_2O \rightarrow LiOH + H_2 \tag{4.8}$$

As can be seen from Table 4.2, this system can offer significant advantages in terms of storage mass and volume. Hollandsworth [55] compares various hydrogen storage systems for underwater vehicle applications, and concludes that lithium hydride can provide the greatest energy capacity of all systems considered (including liquid hydrogen). Nevertheless, considerable development work is still required to increase the rate of hydrogen evolution to levels suitable for vehicle applications. Secondly, LiH is not rechargeable, and for this reason could be considered unsuitable for commercial AUV operations[2].

This thesis considers the following two techniques for hydrogen storage:

- Compressed gas at 310 bar (4500 psi) using composite pressure vessels (GH_2).
- Cryogenic liquid hydrogen storage (LH_2).

Oxygen Storage

For subsea fuel cell applications, onboard oxidant storage is necessary. For stoichiometric reaction in a SPFC, 8 kg of O_2 are required for every kg of H_2, which illustrates the significance of effective oxygen storage.

The choice of oxidant for an underwater power plant is limited by current technology to compressed or liquid oxygen, or concentrated hydrogen peroxide (H_2O_2). An aqueous solution of H_2O_2 at 50% concentration dissociates into steam and oxygen at a temperature of 373 K and a pressure of 1 atmosphere. Hydrogen peroxide can be stored in fabric-reinforced plastic bags outside of

[2]Safety considerations associated with using lithium as a *hydrogen carrier* have not been addressed by this study.

the pressure hull, offering advantages in terms of volume [56]. Despite this, concentrated H_2O_2 is a dangerous chemical, and safety concerns have precluded its use in recent times. Liquid oxygen storage is the lightest system with the lowest operating costs, and represents the current trend in underwater power system technology [57]. This thesis considers liquid oxygen.

Storage of Reaction Products

Cryogenic liquid oxygen and hydrogen contain impurities[3]. Depending on the purity of the reactants and the duration of operation, these impurities may accumulate at the electrodes, blocking access of the reactants and reducing output. In this event, the electrodes will require periodic purging of impurities, which are then stored onboard in evacuated tanks [56]. For short mission durations characteristic of small autonomous underwater vehicles, electrode purging can be done after the mission is completed [50].

Product water may be discharge overboard or stored onboard the vehicle. This thesis considers a closed system, since product discharge results in compressor power losses and complexities associated with vehicle buoyancy.

4.3 Techno-Economic Model

The techno-economic model for the solid polymer fuel cell system is shown in Figure 4.4. The system model is divided into three components: 1) reactants of the electrochemical reaction, namely hydrogen and oxygen, 2) onboard storage of reactants and products, and 3) the solid polymer fuel cell stack and its related ancillary equipment which converts the stored chemical energy directly into dc electricity. The sources and assumptions used in quantifying the parameters shown in Figure 4.4 are discussed.

[3]The impurities in liquid hydrogen are very low. Typical concentrations of most impurities are in the parts per million range [58].

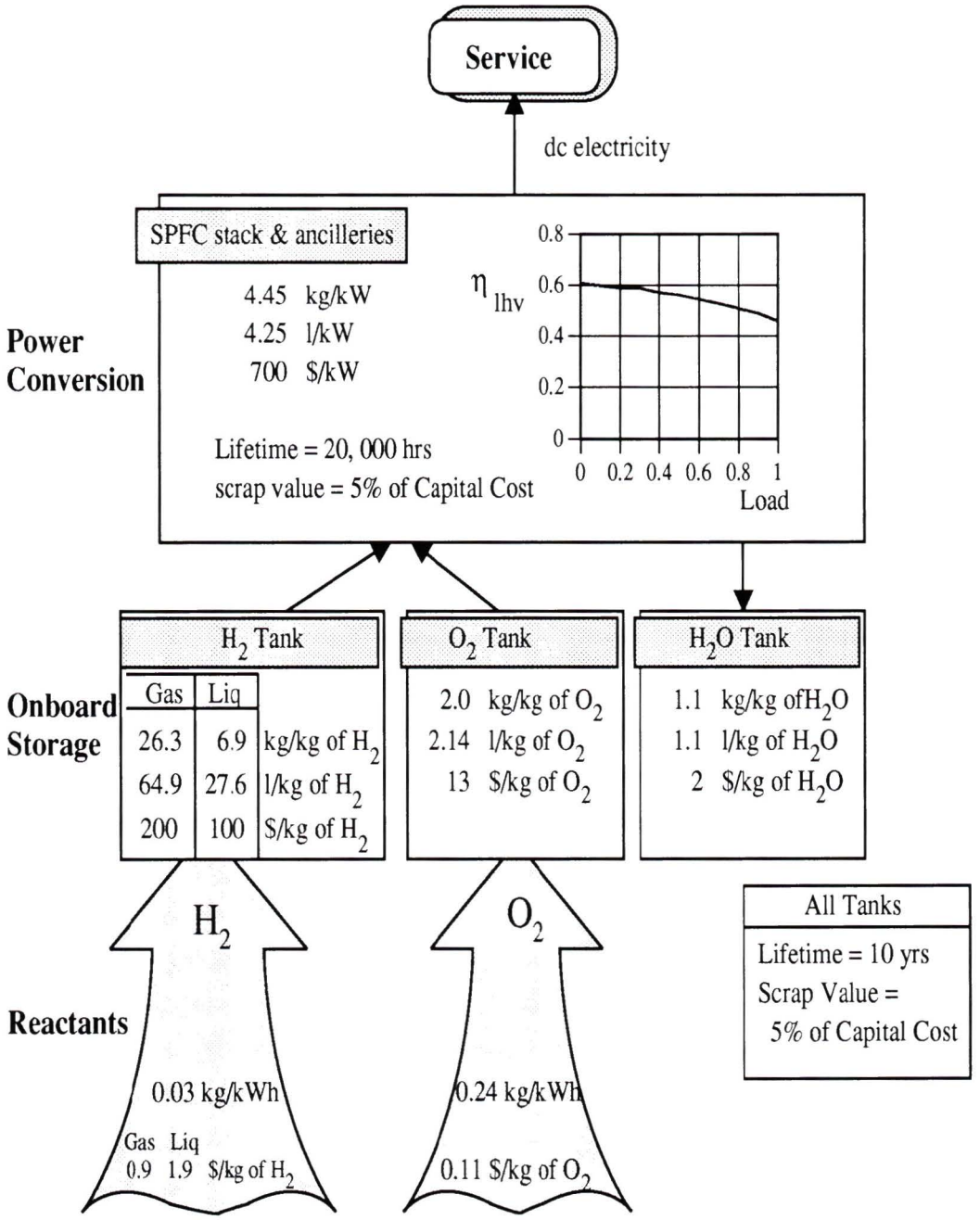

Figure 4.4: Techno-economic model for the solid polymer fuel cell system.

Reactants

- Energy stored is expressed in terms of the *lower heating value* of hydrogen. This is done to be consistent with the representation of the CCDE, presented in the following chapter.

$$lhv_{H_2} = 33.33\, kWh/kg_{H_2} \tag{4.9}$$

- Stoichiometric reaction between the H_2 and O_2 is assumed. That is to say, effectively all excess O_2 required for product water removal is recycled to the fuel cell cathode. Thus, for every kg of H_2 consumed, 8 kg of O_2 are required and 9 kg of H_2O are produced.

- Liquid oxygen delivery cost is taken to be 0.11 $\$/kg_{O_2}$ [12].

- Hydrogen delivery cost is comprised of production cost, compression or liquefaction cost and distribution cost. Table 4.3 shows the cost breakdown for the hydrogen delivery chain. Production levels of 200 tonnes per day are assumed. These production rates are far in excess of those presently encountered; the largest hydrogen liquefaction plant in North America today produces only 66 tonnes per day [58]. Nevertheless, 200 tonnes per day was selected to allow the hydrogen delivery cost to benefit from the economies of scale.

- This thesis considers hydrogen production by steam methane reforming. Assuming a production rate of 200 tonnes per day and a natural gas cost of 2.2 \$/GJ, Scheihing [60] reports a hydrogen production cost of 6.3 \$/GJ.

- The cost for hydrogen compression is taken to be 0.6 \$/GJ, as reported by Plass [61].

- This thesis considers conventional liquefaction techniques at production levels of 200 tonnes per day. Syed [62] reports the cost for such a liquefaction scheme to be 8.8 \$/GJ. Further reductions in hydrogen liquefaction

cost may be achieved by using magnetic refrigeration techniques [59]. This possibility is not considered in this thesis.

- The cost for compressed and liquid hydrogen distribution is taken to be 0.6 \$/GJ, as reported by Plass [61].

Table 4.3: Breakdown of hydrogen delivery costs, assuming production levels of 200 tonnes per day. Hydrogen production is by steam methane reforming. Conventional hydrogen liquefaction processes are considered.

Cost (\$/GJ)	Compressed Hydrogen Gas at 310 bar	Cryogenic Liquid Hydrogen	Reference
Production	6.3	6.3	[60]
Compression	0.6	-	[61]
Liquefaction	-	8.8	[62]
Distribution	0.6	0.6	[61]
Total H_2 Delivery	7.5	15.7	

Onboard Storage

- Mass and volume for compressed and liquid hydrogen storage tanks are obtained from data presented in Table 4.2. The data presented is for tank sizes representative of automobile applications.

- Capital cost of composite pressure vessels for compressed hydrogen storage (at 310 bar) is assumed to be 200 \$/kg$_{H_2}$. Manufacturer's price is divided by two to reflect OEM (original equipment manufacturing) cost [63].

- Capital cost of a 100 litre liquid hydrogen dewar (including fuel delivery and boil off control) is given by DeLuchi [64] to be \$700. Using the density of liquid hydrogen (0.071 kg/l), this translates into 100 \$/kg$_{H_2}$.

- Hydrogen evaporation losses are taken to be zero.

- Mass, volume and capital cost of liquid oxygen dewars is taken from manufacturer's specifications [65]. Manufacturer's price is divided by two to reflect OEM cost. This thesis assumes the capital cost of liquid oxygen dewars to be 13 $\$/kg_{O_2}$.

- Water storage tank is assumed to contribute an additional 10% to the mass and volume of water stored. Capital cost of the product water storage tank is assumed to be 2 $\$/kg_{water}$.

- All storage tanks are assigned a lifetime of ten years. At the end of their useful life, storage tanks are salvaged for 5% of their initial capital cost.

SPFC Stack and Related Ancillary Equipment

- Specific power and power density for the solid polymer fuel cell are assumed to be 4.45 kg/kW and 4.25 l/kW respectively, as presented in [66]. This includes the solid polymer fuel cell stack and all related ancillary equipment. It is assumed that maximum power density is drawn at 0.6 volts per cell.

- Fuel cell stack efficiency is taken from polarization data presented for the Ballard solid polymer fuel cell stack [51]. Parasitic power requirement for ancillary equipment is taken to be 5% of gross stack output [44]. The net fuel cell efficiency is shown in Figure 4.4 as a function of the load, and is expressed in terms of the *lower heating value* of hydrogen.

- Today, the capital cost of the solid polymer fuel cell stack is in the order of 6,000 \$/kW, which is much too high for most commercial applications. Significant reasons for this high cost are test-bench levels of production and immature manufacturing techniques. This thesis assumes a fuel cell capital cost that *could be* obtained today with optimized, large scale production. This is approximated by the total cost of materials used in the

fuel cell stack, using current day technology. Los Alamos Laboratories [67] reports this to be about 600 $/kW for the solid polymer fuel cell system. Further reductions in material costs may be achieved through further reductions in platinum loadings and increased power density. Ballard Power Systems projects capital costs for the solid polymer fuel cell stack as low as 250 $/kW [40]. Such possibilities are not considered in this thesis.

- Capital cost for ancillary equipment is estimated at 100 $/kW. This includes the H_2-O_2 delivery system, condenser, humidifier and cooling system.

- Endurance tests of the SPFC membrane-electrode assembly have exceeded 5,000 hours [66]. Potential lifetimes of the SPFC exceed 57,000 hours with projections to 100,000 hours [44]. This thesis considers a fuel cell lifetime of 20,000 hours of continuous operation. An upper limit of twenty years is assigned to the fuel cell's useful lifetime. For periods of time beyond this, the fuel cell technology will likely be obsolete. At the end of its useful life, a scrap value of 5% of the initial capital cost is applied.

Chapter 5

Closed Cycle Diesel Engine (CCDE)

The concept of operating a diesel engine underwater on a synthetic atmosphere of oxygen and recycled exhaust gases is not new. In fact, the concept was first proposed, and the first patent was issued, in 1901 [68]. Significant research into the development of underwater engines began during the Second World War. At that time, the German Navy was focussing on efforts to increase the submerged endurance and speed of their military submarines, which to that point relied entirely on lead-acid batteries for submerged propulsion power. Several prototype systems were built, although no operational submarines were commissioned. The introduction of the nuclear powered submarine in the late 1950's resulted in the eventual cancellation of all research on underwater diesel engines. In recent years, the development of commercial markets for submarines (for which nuclear power plants are not cost effective) has brought renewed interest in the diesel engine. Over the past fifteen years, the closed cycle diesel engine (CCDE) has been the subject of research projects in Britain, Japan, Italy, Sweden and Germany.

The main advantage of the closed cycle diesel engine is that it is based on a standard, highly developed and relatively inexpensive engine [69]. The technical challenges associated with the CCDE technology fall primarily in two categories:

- **Engine operation on a simulated air environment:** Onboard storage of air requires too much vehicle volume, and the combustion of diesel fuel with pure oxygen results in a flame temperature too high for today's engine materials. Thus, a simulated air environment is required. This is typically a mixture of oxygen and recycled exhaust gases, with the possible addition of some moderating medium such as nitrogen or argon.

- **Treatment and handling of exhaust products:** Water vapour is simply condensed out of the exhaust gas stream and stored onboard as a liquid. Surplus carbon dioxide presents a more demanding requirement. Proposed solutions recommend either to discharge the surplus CO_2 to the ambient environment, or to store it onboard the vehicle.

The first half of this chapter discusses the evolution of the diesel engine for subsea applications, to provide an appreciation of its technical potential. The second half presents the techno-economic model used in the comparison of Chapter 6. The techno-economic model was constructed for the system which best represents the closed cycle diesel engine in its most mature state of development.

5.1 Evolution of the CCDE

The evolution of the CCDE is well discussed in [69]. Many techniques have been developed for the provision of a simulated air environment and for the treatment and handling of exhaust products. CCDE development has progressed towards systems which can: 1) offer performance and efficiency comparable to air breathing engines independent of depth, and 2) minimize the mass, volume and parasitic power required for the treatment and storage of exhaust products. This section does not discuss all or even most of the systems developed, but rather addresses those systems which represent significant improvements in the technology evolution.

5.1.1 Recycle Diesel Engine

The recycle diesel engine is the precursor to the closed cycle diesel engine. A schematic diagram of this system is shown in Figure 5.1. The water vapour in the exhaust products is condensed out and stored onboard as liquid water. Product water may also be discharged overboard at the expense of parasitic power losses for compression. A portion of the exhaust gas (composed primarily of CO_2 and excess O_2) is recirculated to the engine inlet where it is combined with oxygen to form a synthetic atmosphere for combustion with diesel fuel. The surplus exhaust gas is discharged overboard, after being compressed to a pressure greater than that of the ambient environment.

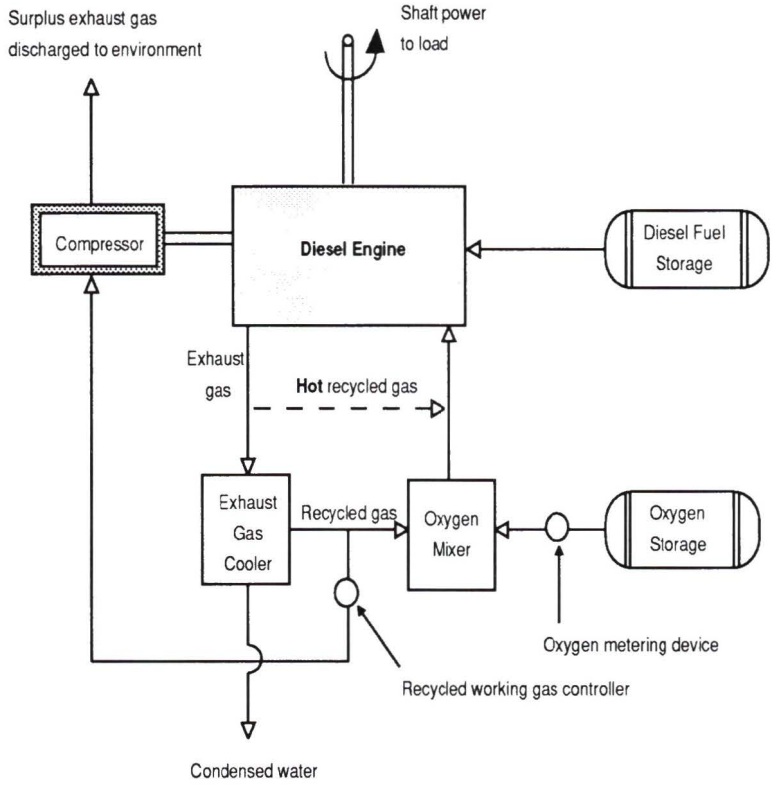

Figure 5.1: Schematic diagram of the recycle diesel engine system.

There are several drawbacks associated with using CO_2 as a diluent for the simulated air mixture. Recirculation of CO_2 will lead to reduced system

efficiency. The ideal thermal efficiency of the diesel cycle is given by:

$$\eta = 1 - \left(\frac{1}{r_v}\right)^{k-1} \left(\frac{r_c^k - 1}{k\,(r_c - 1)}\right) \tag{5.1}$$

where r_v is the compression ratio of the engine, r_c is the cutoff ratio of the power stroke for the engine, and k is the ratio of specific heats of the working fluid ($\frac{C_p}{C_v}$), otherwise known as the gas index. The working fluid for the recycle diesel engine is comprised of O_2 and CO_2. Carbon dioxide is a triatomic gas with a low ratio of specific heats. If CO_2 is recirculated through the engine, then the gas index of the working fluid will be lowered, thus reducing system efficiency below that of typical air breathing engines [68].

Furthermore, the CO_2 content in the synthetic atmosphere may lead to poor combustion and misfiring. Because of CO_2's low gas index, when large quantities are present at the engine inlet, the pressure and temperature rise during compression may be insufficient to cause self-ignition. To ensure good combustion under these conditions, the compression ratio of a typical diesel engine would have to be of the order of 50:1, which is technically impractical. However, the same effect on compression pressure and temperature can be achieved by raising the temperature of the initial charge. In practice, this is achieved by recycling a portion of the hot exhaust gases back to the engine inlet, bypassing the exhaust gas cooling stage. This process is shown by the dotted line in Figure 5.1.

Another disadvantage of the recycle diesel engine is associated with discharging surplus exhaust gases (made up of CO_2 and excess O_2) overboard. The power required to compress the exhaust gas mixture to the pressure of the surroundings reduces the net system efficiency. Furthermore, the required compressor power increases with increasing depth. The lack of depth independent operation is a severe limitation of this system, restricting its operation to shallow depths.

5.1.2 Closed Cycle Diesel Engine

The closed cycle diesel engine (CCDE) overcomes problems associated with discharging exhaust gases overboard by storing product CO_2 and H_2O onboard. The nitro-diesel engine, developed at the University of Newcastle, is one such closed cycle diesel engine system [20, 70]. A schematic diagram of this engine is shown in Figure 5.2. Exhaust gas from the engine passes through a cooler/separator unit in which water vapour is condensed and separated. From there, the cooled gas enters a tower scrubber unit in counter flow with potassium hydroxide (KOH) absorbent. Direct contact between gas and liquid absorbent is established over a large surface area, and CO_2 is scrubbed from the exhaust gas by the chemical reactions:

$$CO_2 + 2KOH \rightarrow H_2O + K_2CO_3 \tag{5.2}$$

$$K_2CO_3 + H_2O + CO_2 \rightarrow 2K(HCO_3) \tag{5.3}$$

The exhaust gases, now free of water vapour and largely free of CO_2, are recirculated back to the engine intake where they mix with oxygen to form the simulated air mixture.

This system uses recirculated nitrogen as the oxygen diluent, in place of CO_2. Nitrogen is largely uninvolved in the combustion process. Only a small nitrogen topping-up system is required to replenish nitrogen lost in the formation of nitrous-oxides. The presence of nitrogen in the synthetic atmosphere "fools" the engine into thinking it is operating on air. Test rig operating experience suggests that the performance and efficiency of the nitro-diesel closed cycle engine is comparable to that of typical air breathing engines [20]. Furthermore, this performance is independent of depth.

A similar system has been developed by the German company Bruker Meerestechnik for use in their small experimental submarine, *Seahorse* [71]. This system uses argon instead of nitrogen as the moderating medium in the simulated air mixture. The advantages of argon as an oxygen diluent are: 1) argon

has a higher gas index ($\frac{C_p}{C_v}$) than nitrogen, thereby improving system efficiency (refer to equation 5.1), and 2) argon does not form oxides in the combustion process.

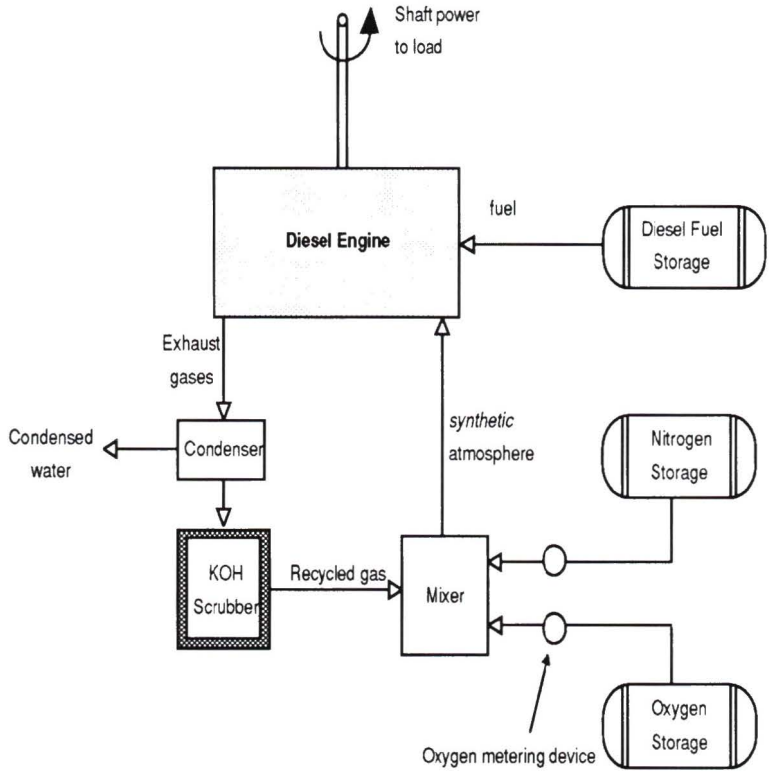

Figure 5.2: Schematic diagram of the nitro-diesel engine system.

The primary disadvantage of the (argon and nitrogen) closed cycle diesel system is the mass and volume required for the KOH scrubbing system. Obara [72] has shown that for the chemical scrubbing process described using 50 wt% KOH solution, approximately four kilograms of liquid absorbent are required per kilogram of CO_2 produced. This may be acceptable for extremely short AUV missions or for stationary seabed applications where mass and volume constraints for neutral buoyancy do not apply. However, for long duration AUV missions, the space required for the KOH scrubbing system represents a major design limitation.

5.1.3 Cryothermal Closed Cycle Diesel Engine

The cryothermal closed cycle diesel engine is presented in [73] and [74]. This system offers the same advantages as the nitro-diesel and argo-diesel concepts previously discussed, namely high system efficiency and depth independent operation. However, it does so with a significant improvement in the mass and volume required for separation and storage of product CO_2. System operation is based on liquefaction of product carbon dioxide using the cooling potential of liquid oxygen storage[1].

A simplified diagram of the cryothermal closed cycle diesel engine system is shown in Figure 5.3. The engine exhausts are cooled by water sprayed in counterflow to allow the separation of solid or liquid particles trapped in the gas stream. Combustion water is condensed and separated and the remaining exhaust gases are compressed. The exhaust gas mixture (consisting of CO_2,

[1] *Exergy* is defined to be the maximum work that a system can provide as it comes into equilibrium with its environment. Liquid oxygen has a large amount of exergy that can be used for the liquefaction of carbon dioxide. As an illustration, consider the stoichiometric combustion of diesel (C_5H_9) with "air" according to the reaction

$$C_5H_9 + 36\frac{1}{4}(.2\,O_2 + .8\,N_2) \rightarrow 5\,CO_2 + \frac{9}{2}\,H_2O + 29\,N_2 \tag{5.4}$$

Product gases are removed of water and compressed before being fed into the heat exchanger. LOX is fed in counterflow to the product gases as shown in the control volume for the heat exchanger. The state properties shown are associated with maximum speed and torque for the cryothermal CCDE [74].

The exergy efficiency can be expressed as the change in flow exergy of the CO_2-N_2 mixture over the change in flow exergy of the O_2 as it is superheated. Entropy and enthalpy values are obtained using GASPAC, a commercially available software package.

$$\eta = \frac{n_{CO_2}(\Delta h - T_o\Delta s)_{CO_2} + n_{N_2}(\Delta h - T_o\Delta s)_{N_2}}{n_{O_2}(\Delta h - T_o\Delta s)_{O_2}} = 0.183 \tag{5.5}$$

where T_o is the environmental temperature, taken to be 298 K. This specific example illustrates the feasibility of this liquefaction scheme.

excess O_2 and either N_2 or Ar) enters a heat exchanger in counterflow with oxygen vapour, which is superheated for delivery to the engine inlet. On the other side, the CO_2 begins to condense. The condensation process is completed in a second, low temperature condenser and storage tank, where liquid oxygen is evaporated. The flow of oxygen in this evaporation loop is controlled by natural convection, thereby eliminating the need for cryogenic pumps. Uncondensed gases (consisting of excess oxygen and an inert moderator such as nitrogen or argon) are rejoined with the pure oxygen flowing from the superheater, thus forming the synthetic atmosphere for combustion.

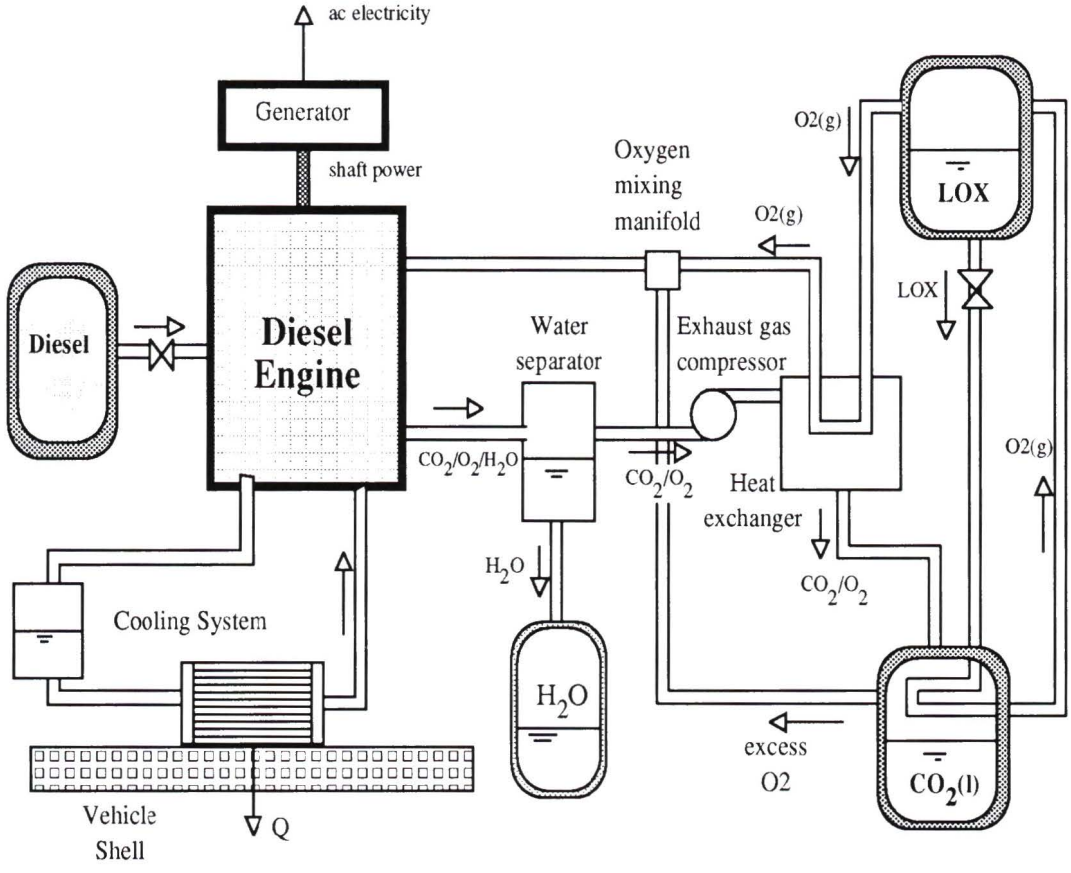

Figure 5.3: Schematic diagram of the cryothermal closed cycle diesel engine system.

This system offers operational advantages over other closed cycle diesel engine systems in terms of mass, volume and parasitic power requirements [74].

This thesis considers the cryothermal system to represent the technical limit of the closed cycle diesel engine. The cryothermal CCDE, using nitrogen as an oxygen diluent, is used in the comparison of Chapter 6.

The following section presents the techno-economic model of the cryothermal CCDE relevant to the simulation and comparison of Chapter 6.

5.2 Techno-Economic Model

The techno-economic model for the cryothermal CCDE is shown in Figure 5.4. The system model is divided into four components: 1) combustion reactants, namely diesel fuel and liquid oxygen, 2) onboard storage of combustion reactants **and** products, 3) the cryothermal CCDE power plant which converts the stored chemical energy into shaft power, and 4) a generator for the conversion of shaft power into ac electricity. The sources and assumptions used in quantifying the model parameters shown in Figure 5.4 are discussed.

Reactants

- Stored energy is expressed in terms of the lower heating value of diesel:

$$lhv_{diesel} = 11.81 kWh/kg_{diesel} \tag{5.6}$$

- Diesel fuel is assumed to be C_5H_9. Stoichiometric combustion is assumed, therefore, 3.4 kg of O_2 are required for each kg of diesel fuel consumed. Also, 3.2 kg of CO_2 and 1.2 kg of H_2O are produced per kg of diesel.

- Diesel fuel delivery cost is assumed to be 0.37 \$/kg$_{diesel}$ [75].

- Liquid oxygen delivery cost is given by Lee [12] to be 0.11 \$/kg$_{O_2}$.

- No cost or value is associated with the liquid carbon dioxide product.

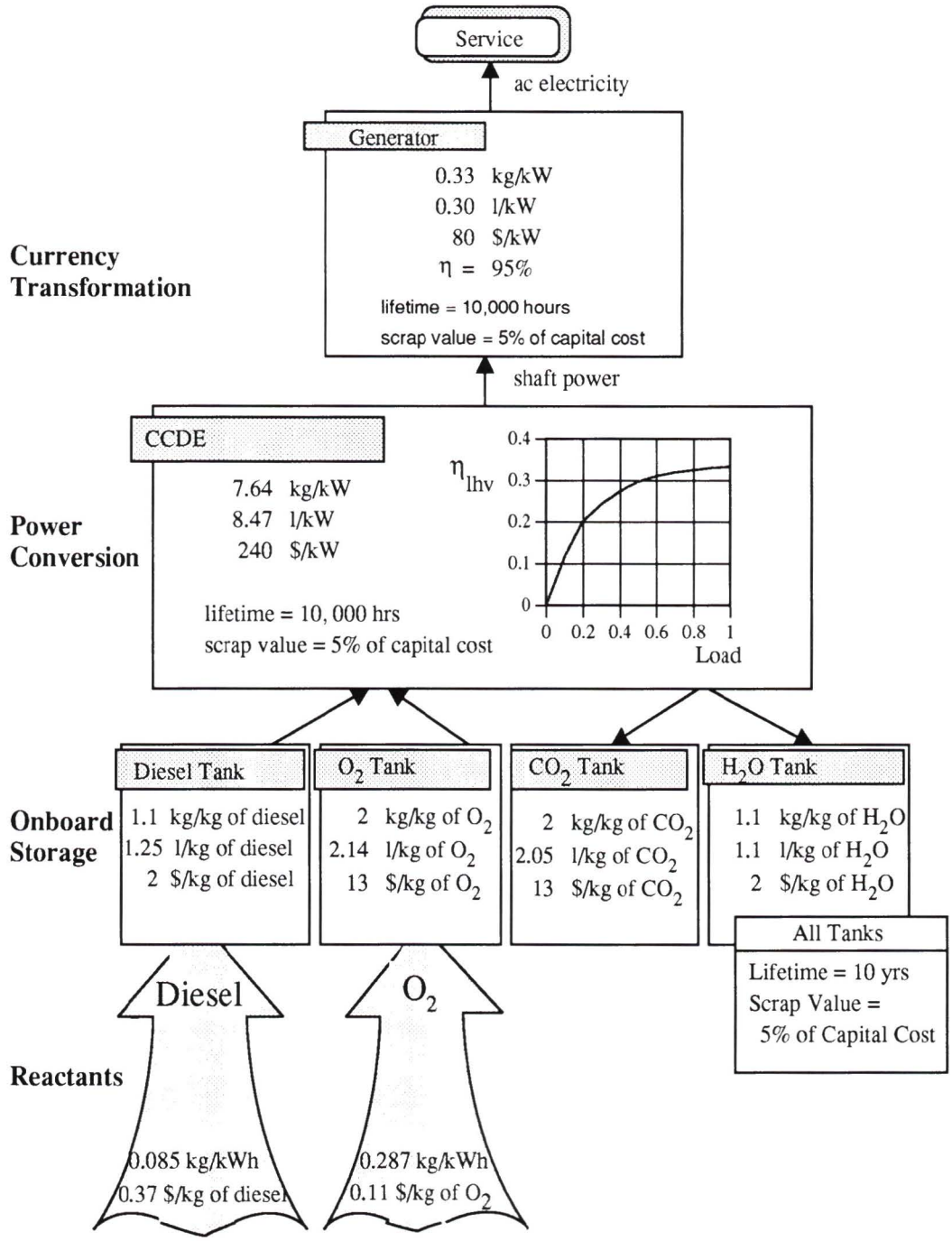

Figure 5.4: Techno-economic model for the cryothermal CCDE.

Onboard Storage

- The diesel storage tank is assumed to contribute an additional 10% to the mass and volume of the diesel fuel stored. Capital cost of the diesel storage tank is assumed to be 2 $\$/kg_{diesel}$.

- Assumptions regarding the storage of product water are the same as those made for diesel.

- Mass, volume and capital cost of liquid O_2 and CO_2 storage dewars are taken from manufacturer's specifications [65]. Manufacturer's prices are divided by two to reflect OEM (original equipment and manufacturing) costs.

- All storage tanks are assigned a lifetime of ten years, corresponding with the service lifetime. At the end of their useful life, storage tanks are salvaged for 5% of their initial capital cost.

Power Conversion

The CCDE power plant converts stored chemical energy into shaft power. It includes the diesel engine, cooling system, reactant/product handling systems, water separator, exhaust gas compressor and liquefaction heat exchangers.

- Specific power and power density for the CCDE are taken to be 7.6 kg/kW and 8.5 l/kW respectively, as reported in [76].

- Engine efficiency assumes data presented by Thomson [70] for a diesel engine operating in closed cycle on a synthetic atmosphere of O_2 and N_2. Further to this, a compression loss factor[2] of 10% is used. The net engine

[2]The compression loss factor (CLF) is defined to be the ratio of power required for the compression of exhaust gases to gross engine power output. Brighenti [73] identifies the CLF to be 8% at minimum load and 12% at maximum load. This thesis assumes a CLF of 10% for all engine loads.

efficiency is shown in Figure 5.4 as a function of load, and is expressed in terms of the lower heating value of diesel fuel.

- The capital cost projection for the CCDE is assumed to be the sum of the component costs for the complete system. Estimates of such costs result in a capital cost of 240 $/kW for the complete CCDE system. This result is consistent with the cost reported in [76].

- The CCDE lifetime is assumed to be 10,000 hours of continuous operation. An upper limit of twenty years is applied to the useful lifetime of the engine. At the end of its useful life, a salvage value of 5% is applied.

Currency Transformation

A generator converts shaft power into ac electricity. A permanent magnet brushless dc motor, as proposed by Unique Mobility Inc. [77], is selected for this purpose.

Chapter 6

Comparison of Power Systems

This chapter compares power systems for application in autonomous underwater vehicles. The objectives are twofold:

- To highlight the characteristics of each power system.
- To evaluate these characteristics for AUV services.

Often, power system comparisons consider only the first of these two objectives. In such cases, the comparison results are not expressed in context with the service. To illustrate this point, consider the techno-economic models for the power systems presented in Chapters 3, 4 and 5. These are summarized in Tables 6.1 and 6.2. Observe the following:

- Battery systems, particularly the lead-acid battery, exhibit low specific energy and energy density, in comparison with the SPFC and CCDE systems.
- Using the CCDE as a benchmark for comparison, the GH_2-SPFC exhibits a very low energy density (Wh/l), and the LH_2-SPFC exhibits a high specific energy (Wh/kg).
- The SPFC has a higher energy conversion efficiency than the CCDE, particularly at part loads.

- The SPFC has a higher initial capital cost than the CCDE.
- The SPFC exhibits a longer lifetime than the CCDE.
- The SPFC, particularly using compressed hydrogen storage, has lower fuel and oxidant costs than the CCDE. This can be attributed to higher system efficiencies and lower oxygen requirements for the SPFC.

These observations illuminate some important features of the power systems. Nevertheless, these characteristics alone are not adequate for a useful comparison. **A useful comparison of power systems must be cast in terms of the service provided.**

The service determines the requirements and constraints of the power system. It dictates which features of the system are relevant to the comparison. For instance, power system lifetime is an important characteristic for commercial AUV applications, but it is certainly of less importance for a torpedo. As a second example, power system mass and volume are important features when considering vehicle applications because of the constraint of neutral buoyancy. However, these characteristics are of less importance for stationary seabed applications for which neutral buoyancy is not necessarily required.

This thesis compares power systems for three categories of AUV missions:

- Survey mission
- Work mission
- Combined mission

The first two mission examples were chosen as *bookends* to the problem. That is to say, they represent two opposite extremes of possible AUV scenarios - low power versus high power. The third mission example combines features of the two extremes.

Table 6.1: Summary of battery modelling parameters.

	Lead-Acid Battery	Na-S Battery
Specific Energy (at 10 W/kg)	35 Wh/kg	85 Wh/kg
Energy Density (at 10 W/kg)	77 Wh/l	111 Wh/l
Peak Power (at 50% DOD)	90 W/kg	90 W/kg
Cycle Life (to 100% DOD)	715	600
Shelf Life (years)	6	10
Capital Cost ($/kWh)	70	110
Recharge Efficiency	70%	90%
Electricity Cost ($/kWh)	0.045	0.045

Table 6.2: Summary of modelling parameters for SPFC and CCDE. Specific energy (kWh/kg) and energy density (kWh/l) of onboard storage includes tanks for reactants and products and does not include energy conversion efficiency. Similarly, fuel and oxidant costs are delivery costs, and do not include energy conversion efficiency.

	GH_2-SPFC	LH_2-SPFC	CCDE
Power Conversion:			
Specific Power (W/kg)	225	225	130
Power Density (W/l)	235	235	120
Full Load Efficiency	46%	46%	31%
Part Load Efficiency	HIGHER	HIGHER	LOWER
Capital Cost ($/kW)	700	700	320
Lifetime (hours)	20,000	20,000	10,000
Onboard Storage:			
Reactants	GH_2-LOX	LH_2-LOX	Diesel-LOX
Products	H_2O	H_2O	H_2O-CO_2(l)
Specific Energy (kWh/kg)	0.77	1.4	1.06
Energy Density (kWh/l)	0.37	0.62	0.72
Capital Cost ($/kWh)	9.7	6.7	7.6
Fuel and Oxidant Costs:			
Hydrogen/Diesel ($/GJ)	7.5	15.7	8.8
Oxygen ($/GJ)	7.3	7.3	8.8

6.1 Example 1: Survey Missions

A survey mission is at one extreme of AUV applications. It is characterized by a low, continuous power requirement for propulsion and hotel loads. Since no on-station task is to be performed, both on-station power and time ratio are set to zero. A constant transit speed of 5 m/s is considered. Depth and duration are treated as mission variables, which when specified, characterize a specific mission. The AUV survey mission is illustrated in Figure 6.1.

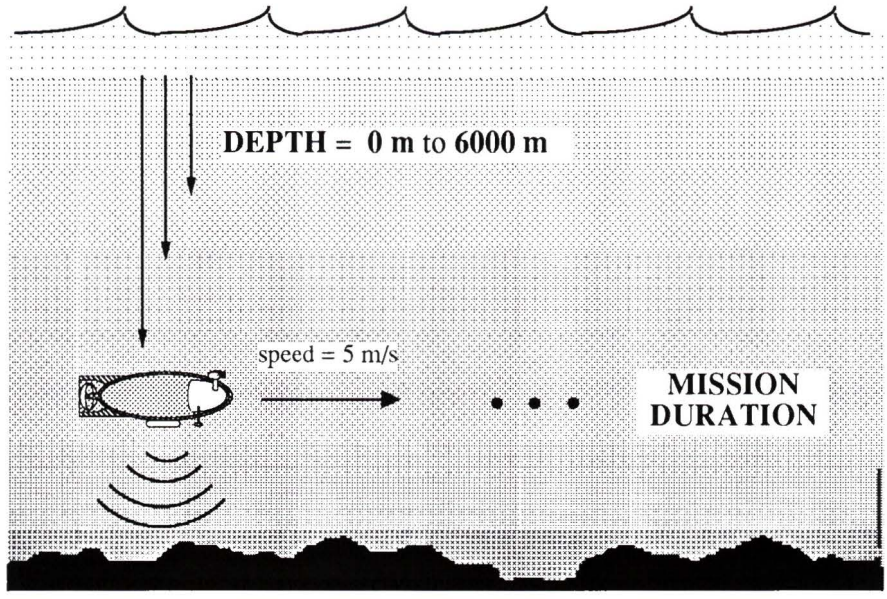

Figure 6.1: Definition of AUV survey mission.

6.1.1 Performance Envelopes

The *Performance Envelope* for a given power system is defined to be the set of AUV missions for which the power system is technically feasible. For the specific example of survey missions, the performance envelope is represented as the feasible combinations of mission depth and duration.

Mapping the Continental Shelf

Figure 6.2 displays the key results for maximum power system endurance for an AUV survey mission at 300 metres depth (typical depth of the Continental Shelf). The calculation procedure is divided into the following steps: 1) Determine the power system requirements and constraints from the service definition, 2) Maximize onboard energy storage while satisfying the requirement for vehicle neutral buoyancy, and 3) Determine the maximum power system endurance by an energy balance.

Maximization of onboard energy is constrained by *either* available power system mass *or* available power system volume, depending on the density of energy storage. The mass and volume balances show that the high density batteries are constrained by available mass, and a vacant buoyancy tank is required to satisfy neutral buoyancy. On the other hand, maximization of onboard energy for the SPFC and CCDE systems is constrained by available power system volume (energy storage includes empty tank(s) for product containment), and a ballast weight is required to ensure vehicle neutral buoyancy.

An energy balance determines the maximum mission endurance for each of the power systems. Note the following:

- The battery systems, particularly the lead-acid battery, are restricted to low duration missions by their low specific energy (Wh/kg).

- At shallow depths, the SPFC system using compressed hydrogen storage is penalized by its low energy density (Wh/l) and cannot match the

Mission Definition

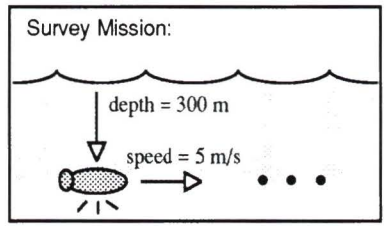

Power Requirement

Propulsion Power = 12.4 kW
Hotel Power = 1.5 kW

Mass and Volume Constraints

	Mass (kg)	Volume (l)	
Vehicle Displacement	4083	4000	
Shell	140	31	Base Vehicle
Power train	100	35	
Pay Load	1000	1000	
Available for power system	**2843**	**2934**	

Mass and Volume Balances

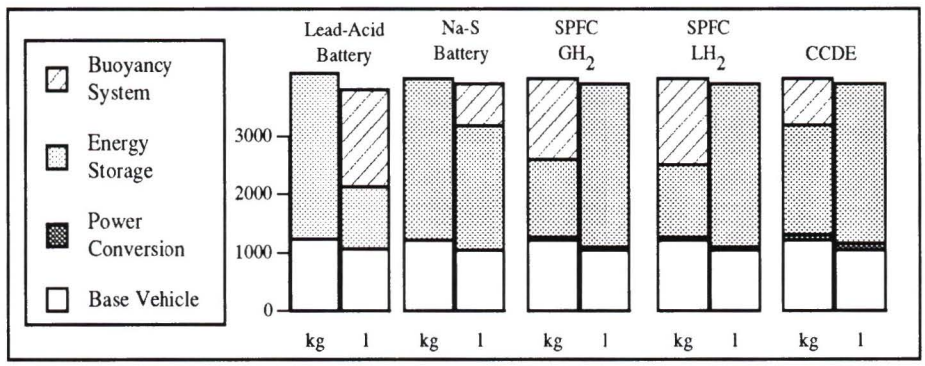

Energy Balances

	Lead Acid	Na-S	SPFC-GH2	SPFC-LH2	CCDE
Fuel mass (kg)			31.4	53.3	173.2
Onboard Energy (kWh)	142	269	1047	1776	2045
Conversion Efficiency	0.66	0.88	0.46	0.46	0.31
Endurance (hrs)	**6.8**	**17.1**	**34.4**	**58.3**	**46.6**

Figure 6.2: Calculation of power system endurance for survey mission at **300** metres depth. This figure highlights the significance of vehicle neutral buoyancy when assessing power system performance.

endurance of the CCDE.

- The energy density of liquid hydrogen storage is significantly better than that for compressed hydrogen storage. Because of its higher energy conversion efficiency, the SPFC using liquid hydrogen storage can provide a greater endurance than the CCDE.

The results shown in Figure 6.2 illustrates the significance of vehicle neutral buoyancy when assessing power system performance. The *simultaneous* satisfaction of mass and volume constraints must be achieved for a meaningful comparison of power system endurance.

Mapping the Mediterranean Sea

Figure 6.3 shows the calculations of maximum power system endurance for a survey mission at **3000** metres depth (typical depth of the Mediterranean Sea). Comparison with Figure 6.2 highlights the significance of mission depth when assessing power system performance.

Increasing the mission depth from 300 to 3000 metres changes the mass and volume constraints imposed on the power system. The increase in mission depth must be accompanied by an increase in vehicle shell thickness to resist the increased ambient pressure. Because of vehicle neutral buoyancy, this increase in shell thickness reduces the available power system mass and, to a lesser degree, reduces the available power system volume.

The mass and volume balances of Figure 6.3 illustrate how each power system responds to this deeper environment when maximizing onboard energy storage.

- The large increase in vehicle shell mass results in a direct decrease in storage battery mass, significantly reducing the maximum possible endurance of these systems.

- The low density of energy storage for the fuel cell systems is compatible with the mass and volume constraints at this increased depth. Despite

Mission Definition

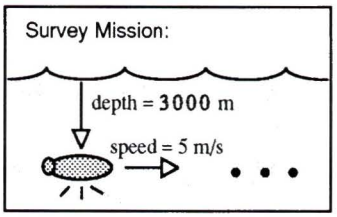

Power Requirement

Propulsion Power = 12.4 kW
Hotel Power = 1.5 kW

Mass and Volume Constraints

	Mass (kg)	Volume (l)	
Vehicle Displacement	4083	4000	
Shell	1400	310	Base Vehicle
Power train	100	35	
Pay Load	1000	1000	
Available for power system	**1586**	**2640**	

Mass and Volume Balances

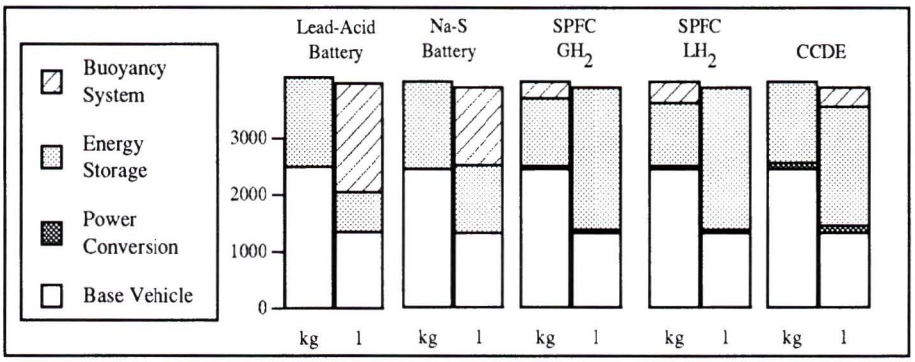

Energy Balances

	Lead-Acid	Na-S	SPFG-CH2	SPFC-LH2	CCDE
Fuel mass (kg)			28.3	48	133.6
Onboard Energy (kWh)	79.3	150	943	1600	1578
Conversion Efficiency	0.63	0.87	0.46	0.46	0.31
Endurance (hrs)	**3.6**	**9.4**	**31**	**52.6**	**36**

Figure 6.3: Calculation of power system endurance for survey mission at **3000** metres depth. This figure illustrates the significance of increased depth and the resulting increase in shell mass on power system performance.

the large increase in vehicle shell mass, the SPFC systems remain to be constrained by available volume. Consequently, increasing mission depth from 300 to 3000 metres has only a small effect on the maximum endurance of the fuel cell systems.

- The density of energy storage for the CCDE system is greater than that for the fuel cell systems. Consequently, at a depth of 3000 metres, the maximization of onboard energy for the CCDE is constrained by available power system *mass*. The transition from a volume constraint to a mass constraint occurs at a depth of 2300 metres. Increases in depth beyond this transition point result in substantial losses in energy storage mass. For this reason, the CCDE exhibits a more dramatic decrease in maximum mission endurance than do the SPFC systems for the examined increase in mission depth.

The results of Figure 6.3 indicate that the performance advantage shown by the liquid hydrogen fuel cell at 300 metres depth grows substantially at 3000 metres depth. This is directly related to issue of neutral buoyancy and the mass and volume constraints imposed by the vehicle configuration. The results show that the low density of reactant/product storage for the solid polymer fuel cell system (using compressed gas or cryogenic liquid) is advantageous for missions at great depths where available power system mass is limited.

Performance Envelopes

Figure 6.4 compares power system performance envelopes for AUV survey missions. It shows for each power system, the maximum mission duration obtainable for a given depth. The area to the left of the curve represents the domain of possible AUV survey missions for which the power system is feasible.

From Figure 6.4, we can conclude the following:

- Lead-acid batteries are constrained to extremely short duration missions.

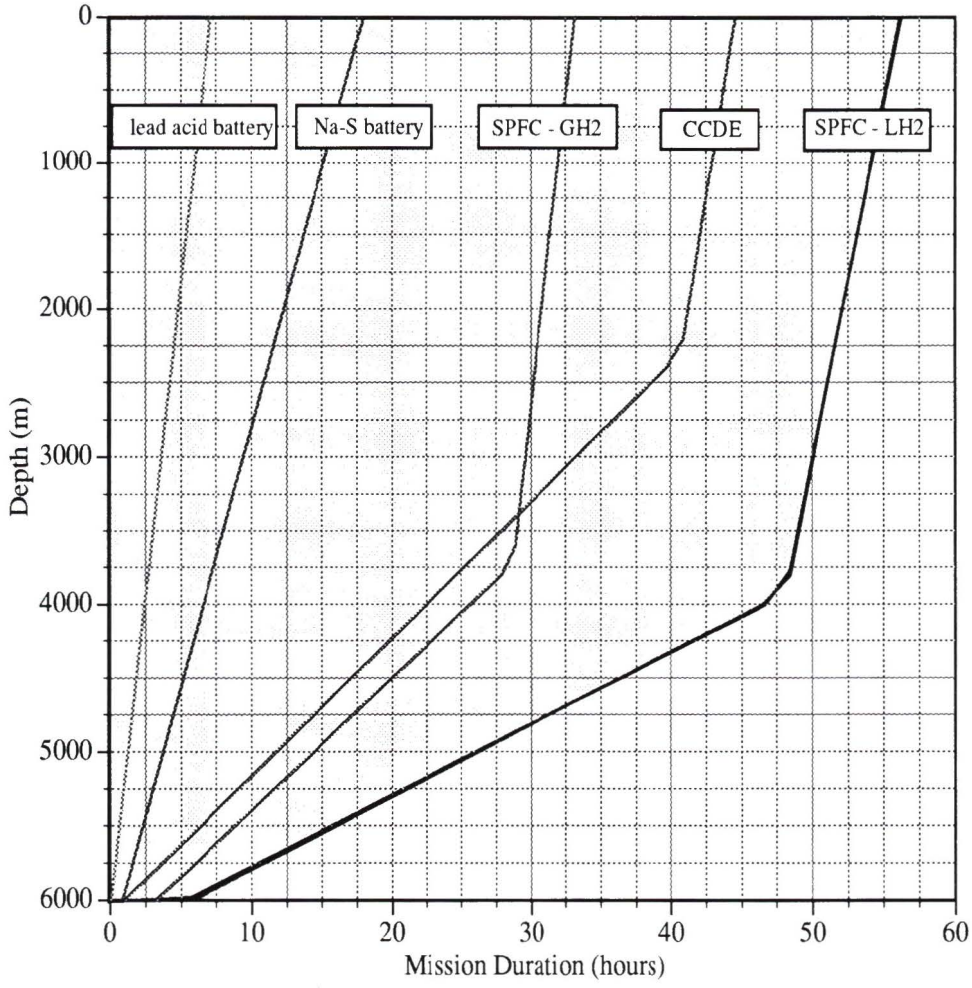

Figure 6.4: Performance envelopes for survey mission. The area to the left of each curve represents the set of feasible survey missions for each power system.

- The sodium-sulfur battery system can provide roughly 2.5 times the endurance of the lead-acid battery.

- The GH_2-SPFC and the CCDE provide comparable envelopes of performance. Choosing the winner involves specifying the design depth for the vehicle. For low depths, where the onboard energy storage is limited by the available volume, the engine can provide the greater endurance. This is because of the low energy density (Wh/l) of compressed hydrogen storage. However, for increased depth, where onboard storage mass is the limitation, the GH_2-SPFC surpasses the CCDE in terms of maximum mission endurance.

- The solid polymer fuel cell, using liquid hydrogen, can provide the greatest endurance for all depths. The performance advantage of the LH_2-SPFC increases with increasing depth. For great depths where the available energy storage mass is severely limited, the high specific energy (Wh/kg) of liquid hydrogen storage is advantageous in maximizing onboard energy.

It is important to note that there is no system to take over from the LH_2-SPFC after its domain of feasibility expires. Nuclear power plants are not a realistic alternative for small displacement, commercial AUV's because of their prohibitive size (for shielding) and cost. Therefore, the performance envelope for the solid polymer fuel cell represents the current technology limit to feasible AUV survey applications. The further significance of this is that the SPFC allows an expanded set of AUV survey missions, and consequently increases market opportunities for AUV's.

6.1.2 Domains of Least Cost

One can conclude from the performance envelope comparison of the previous section that the LH_2-SPFC has a secured market niche for extended duration AUV survey missions, where it is the only feasible power system. But for most missions, for which more than one power system is feasible, how does one choose among candidates? Some criterion for comparison is required. This thesis considers life cycle cost to be such a metric for evaluation.

The life cycle cost (LCC) of each power system is calculated over all survey missions within its performance envelope. Comparing, we obtain the set of missions for which each power system is the least cost alternative. These are referred to as *Domains of Least Cost.*

Influence of Mission Depth

In this analysis, increases in mission depth have no effect on the power system life cycle cost. It is recognized that increases in required shell thickness would have an effect on the total vehicle costs. But this effect is common to all power systems and not included within the comparison. (Nevertheless, increasing depth does reduce the maximum endurance of each power system, as previously shown.)

Influence of Mission Duration

The influence of mission duration on power system life cycle cost is an important result of this thesis. Life cycle cost is expressed per hour of service provided. For a given mission frequency, variations in mission duration will influence the relative contribution of capital cost and operating cost to the total system cost.

Figure 6.5 compares the components of LCC for the CCDE and the SPFC using compressed hydrogen storage. A mission depth of 300 metres is chosen, and a mission frequency of 50 missions per year is considered. Note that all life cycle cost calculations are performed over a service lifetime of ten years.

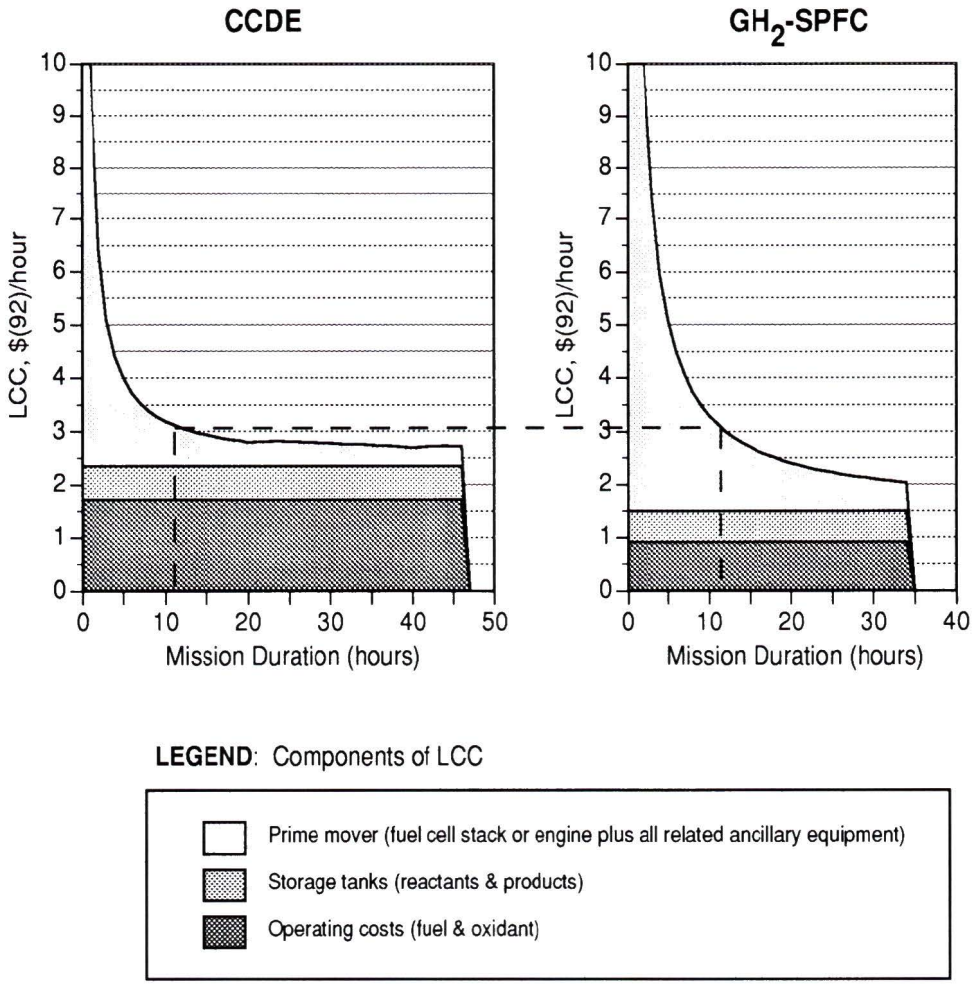

Figure 6.5: influence of mission duration on the life cycle cost of the CCDE and GH_2-SPFC. Mission depth is 300 metres. AUV life cycle is 50 missions per year for 10 years.

The contributions of operating costs (for fuel and oxidant) and storage tank costs (for onboard containment of reactants and products) is independent of mission duration. This would be expected since life cycle cost is expressed per hour of service provided. Underlying this observation is the assumption that tank lifetime and salvage value are 10 years and 5% of initial capital cost, respectively, independent of the utilization over that period.

For short mission durations (say 5 hours), the total LCC of both power systems is dominated by the cost contribution of the prime mover (fuel cell or engine plus all related ancillary equipment). For these low levels of utilization, the full lifetime of the power conversion technology is not being used, and a large portion of the initial capital cost is lost through depreciation. Because of the high initial cost of the solid polymer fuel cell stack, the SPFC system is relatively expensive for short mission durations.

The LCC of both prime movers decreases with increasing mission duration, as the initial capital cost is amortized over more service hours. This effect continues until a point where the engine or fuel cell stack must be replaced within the AUV's 10 year life cycle. For the CCDE, this occurs at a mission duration of 20 hours. Further significant reductions in life cycle cost of the CCDE cannot be obtained by increasing utilization beyond this point.

Because of the longer lifetime of the SPFC (assumed to be 20,000 hours), its life cycle cost continues to decline with increasing mission duration beyond 20 hours. Consequently, despite its significantly higher initial capital cost, the *life cycle* cost of the fuel cell stack can approach that of the engine for scenarios of high utilization.

For long mission durations (say 30 hours), the total LCC of both system is dominated by operating (fuel and oxidant) costs. The SPFC system exhibits lower operating costs than does the CCDE. This is largely due to the higher oxygen requirements and lower energy conversion efficiency associated with the engine. (We must also acknowledge the high production rates assumed for

hydrogen.) Consequently, the SPFC demonstrates a LCC advantage over the CCDE for long duration missions.

In short, the CCDE is preferred for short mission durations because of its lower initial capital cost, and the GH_2-SPFC is preferred for long mission durations because of its longer lifetime and lower operating costs.

Figure 6.6 shows the variation of life cycle cost with mission duration for all power systems considered in this analysis. Once again, a mission depth of 300 metres and a mission frequency of 50 missions per year are chosen. Using Figure 6.6, domains of least cost are constructed as shown in Figure 6.7. Note that Figure 6.7 shows the set of missions for which each power systems is least cost, but it does not show by how much one system is preferred to another. For this information, one must refer to Figure 6.6.

From Figures 6.6 and 6.7 we may conclude the following:

- The lead-acid battery is the least cost power system for all survey mission for which it is technically feasible. However, it is restricted to extremely short duration missions. For the lead-acid battery to satisfy mission durations beyond its presented performance envelope, a larger AUV and increased support vessel requirements would be needed. Both add considerable cost to the total project cost. In order to eliminate AUV and support vessel costs from the power system comparison, the possibility of varying vehicle size is not pursued in this thesis.

- The sodium-sulfur (Na-S) battery never occupies a domain of least cost for the low power survey missions considered in this section.

- The CCDE occupies a small domain of least cost for mission durations less than 11 hours for which: 1) the lead acid-battery is not technically feasible

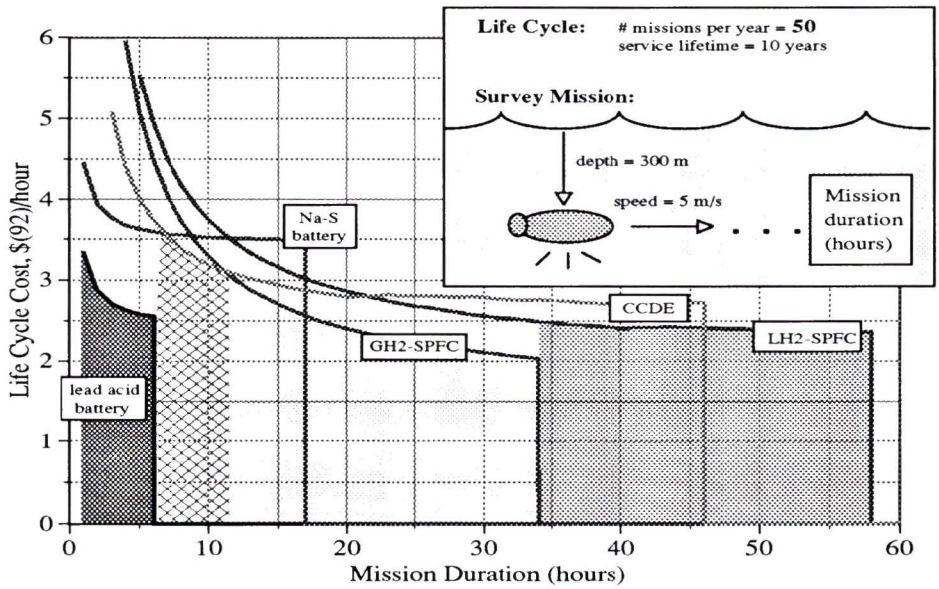

Figure 6.6: Power system LCC vs mission duration for survey mission. Mission depth is 300 metres. AUV life cycle is 50 missions per year over 10 years.

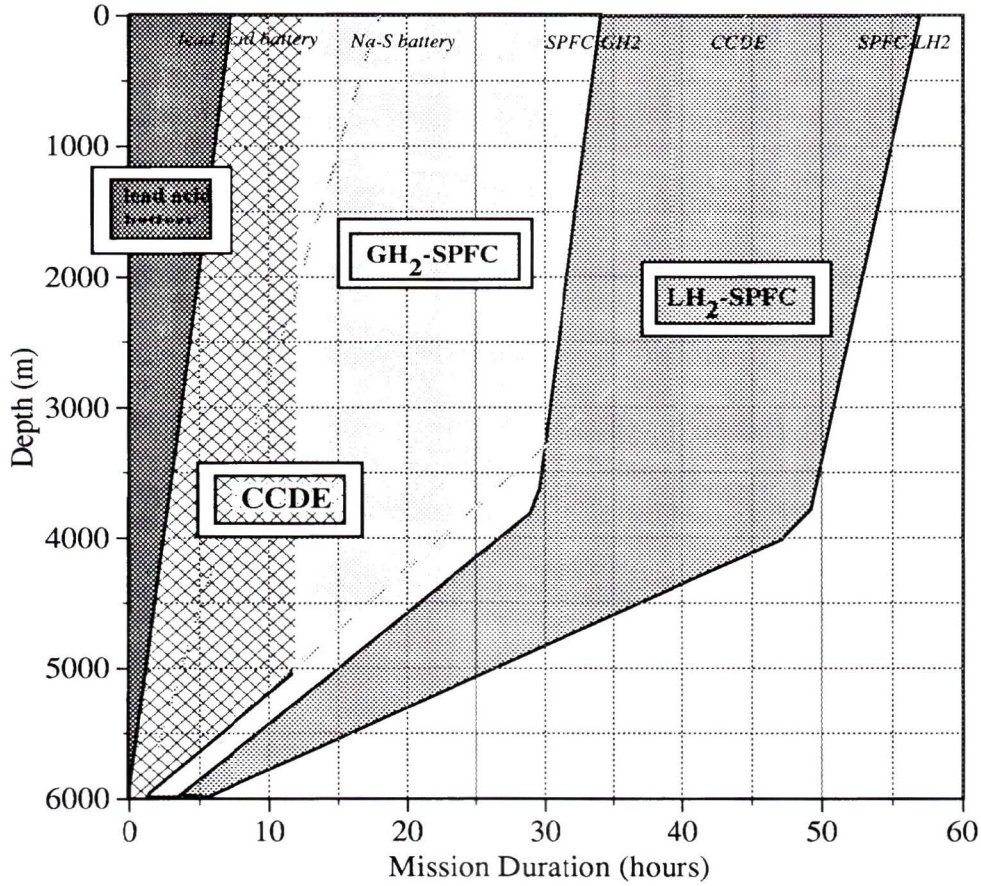

Figure 6.7: Domains of Least Cost for survey mission. AUV life cycle is 50 missions per year over 10 years.

and 2) the relatively low initial capital cost of the engine (compared with the fuel cell stack) is advantageous.

- The SPFC is the least cost power system for the majority of AUV survey missions. For missions of duration greater than 11 hours, the SPFC exhibits a cost advantage over the CCDE because of lower operating costs and longer system lifetime.

Influence of Mission Frequency

The domains of least cost developed in the previous section assume a mission frequency of 50 missions per year. This section addresses how the results vary for different values of mission frequency.

Figure 6.8 compares the components of life cycle cost for the CCDE and GH_2-SPFC. A mission duration of 5 hours and a mission depth of 300 metres are assumed. (An example might be the surveillance of Victoria Harbour.) Mission frequency is varied from 10 to 300 missions per year to examine its influence on power system LCC.

For low values of mission frequency, the total life cycle cost for both systems is dominated by the capital cost of the prime mover and the storage tanks. This condition favours the CCDE in a life cycle cost comparison. For high values of mission frequency, the total life cycle cost of both systems is dominated by operating (fuel and oxidant) costs. This condition favours the SPFC. For mission frequencies greater than 120 missions per year, the GH_2-SPFC exhibits a LCC advantage over the CCDE.

Shown in the heavy dotted line is the LCC of the lead-acid battery as a function of mission frequency. Notice that for extremely high utilization rates (say 300 missions per year), the LCC of the SPFC for this extremely low duration survey mission approaches that of the lead-acid battery. In such cases, the marginal cost-advantage shown by the lead-acid battery may be outweighed by the ability of the fuel cell to *go farther*.

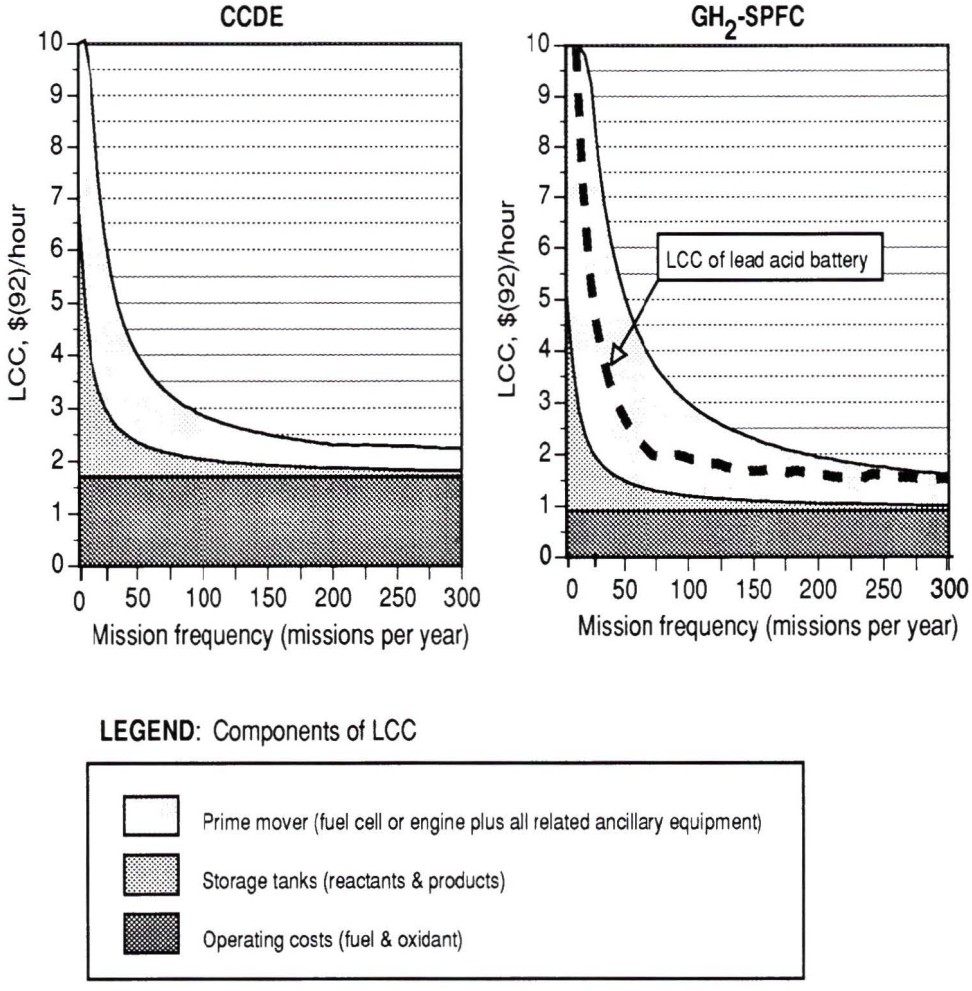

Figure 6.8: influence of mission frequency on the life cycle cost of CCDE and GH_2-SPFC. Mission depth is 300 metres and mission duration is 5 hours (eg. Survey Victoria Harbour).

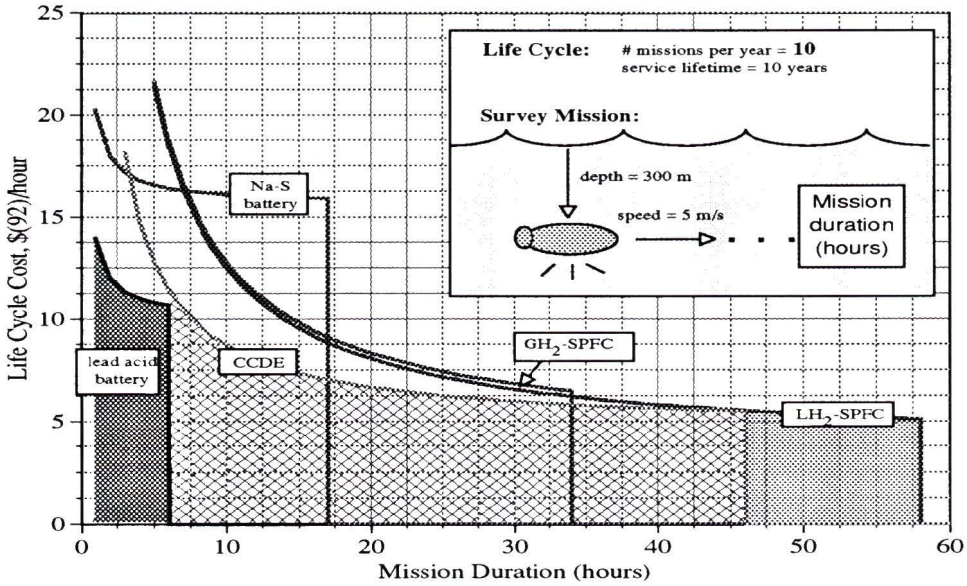

Figure 6.9: Power system LCC vs mission duration for survey mission. Mission depth is 300 metres. AUV life cycle is **10** missions per year over 10 years.

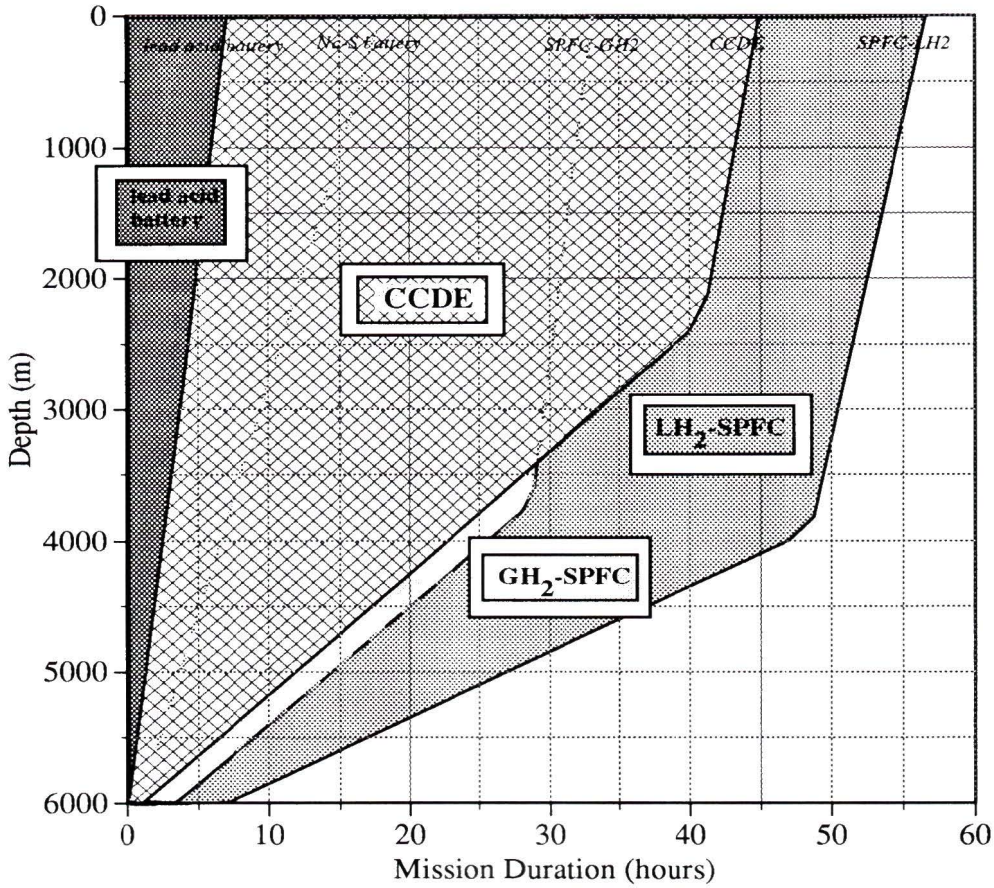

Figure 6.10: Domains of least cost for survey mission. AUV life cycle is **10** missions per year for 10 years.

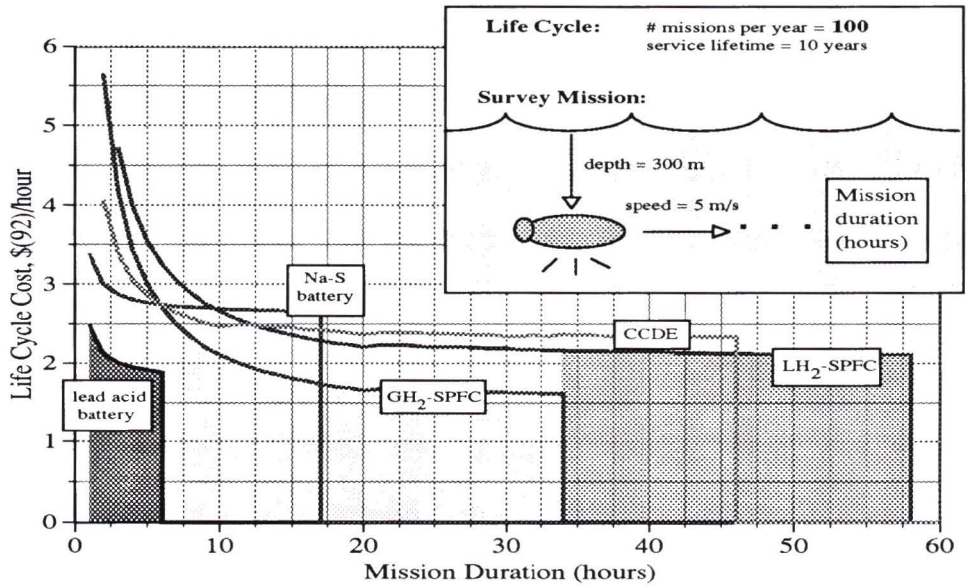

Figure 6.11: Power system LCC vs mission duration for survey mission. Mission depth is 300 metres. AUV life cycle is **100** missions per year over 10 years.

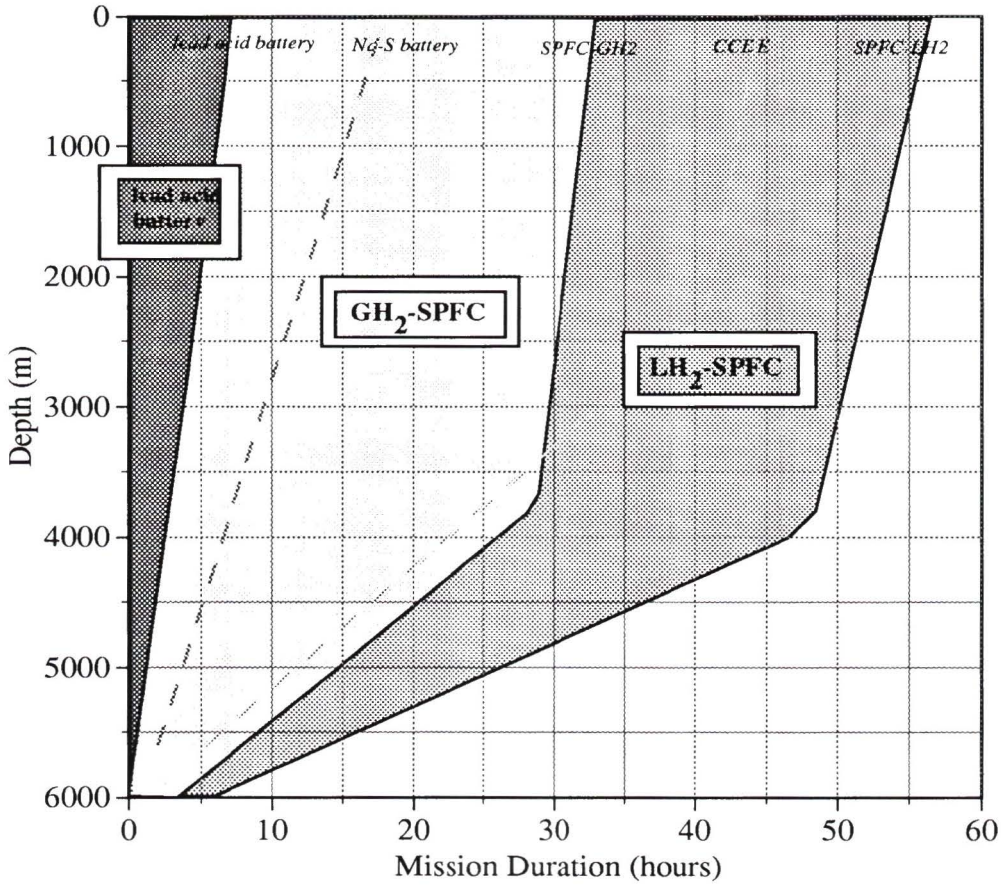

Figure 6.12: Domains of least cost for survey mission. AUV life cycle is **100** missions per year for 10 years.

Figures 6.10 and 6.12 show the resulting domains of least cost for mission frequencies of 10 and 100 missions per year respectively. These figures show the subset of AUV survey missions for which each power system is preferred by the criterion of life cycle cost. But they do not show by how much one system is preferred to another. For such information, refer to Figures 6.9 and 6.11. These are cross-sections of the domain pictures taken at 300 metres depth, illustrating LCC versus mission duration for each power system. From these figures, we can make some general conclusions about power systems for AUV survey missions:

- The lead-acid battery is the preferred power system for all missions where it is technically feasible. However, it is restricted to extremely short duration missions.

- The LH_2-SPFC has an assured market niche for extended duration AUV survey missions, where it is the only technically feasible system.

- The *middle ground* between these two extremes is shared by the GH_2-SPFC and the CCDE. For low mission frequency (such as 10 missions per year), the CCDE dominates as the preferred system in this market domain. But for high mission frequency (such as 100 missions per year), the SPFC is the least cost power system for all survey missions within this middle ground.

6.2 Example 2: Work Missions

Work missions represent a second extreme of possible AUV mission scenarios. For these missions, a time ratio of 1 is assumed. That is to say, the entire mission is spent on-station. No transit operations are performed, aside from the vertical transit to and from the surface. Ascent and descent is controlled by the buoyancy system, as described in Chapter 2. No propulsion power is required for these periods of transit. Mission depth is assumed to be 300 metres (typical depth for the Continental Shelf). The on-station working task to be performed may vary from light robotics, to diver support, to high power welding. Consequently, on-station power is treated as a mission variable, along with mission duration. The definition of the AUV work mission is shown in Figure 6.13.

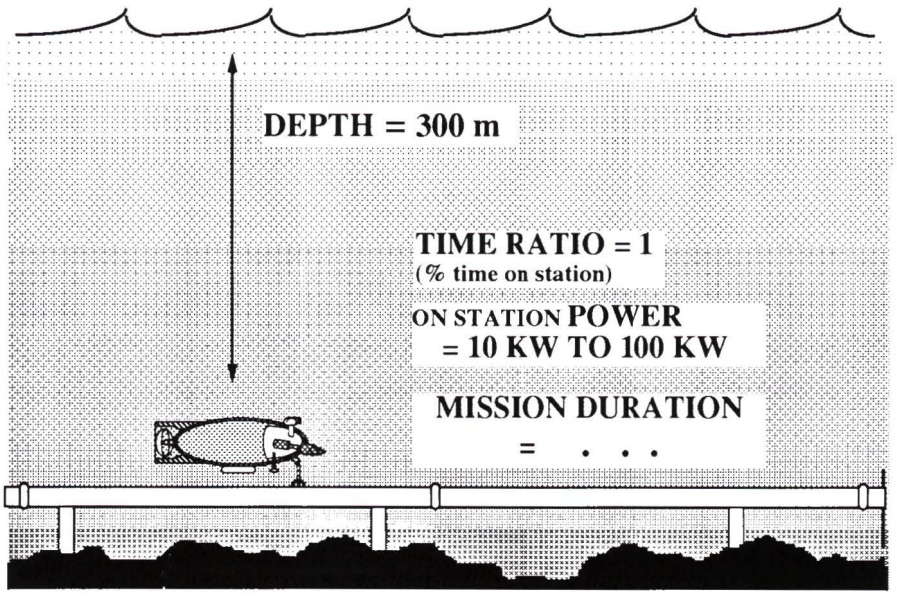

Figure 6.13: Definition of AUV work mission.

6.2.1 Performance Envelopes

A power system's performance envelope is defined to be the set of AUV missions for which it is technically feasible. For the specific example of a work mission, this is represented as the feasible combinations of on-station power and mission duration. Performance envelopes for the power systems considered in this study are presented in Figure 6.14. The plotted curves indicate the maximum power system endurance as a function of on-station power. The area below the curve represents the set of feasible missions, or the performance envelope, for the power system.

Figure 6.14 shows that the maximum endurance for each power system decreases with increasing on-station power, as would be expected. But the *relative* endurance among power systems changes very little, with on-station power varying from 10 kW to 100 kW. This suggests that specific power (W/kg) and power density (W/l) are of small significance when assessing *relative* system performance for high power work missions. This result may be surprising to those who still perceive the solid polymer fuel cell as a low specific power conversion technology. This is a myth based on old technology. Recent advances in membrane technology and stack hardware have increased the specific power of the SPFC dramatically. In fact, using operating data for today's technology, this thesis reports the SPFC to have a higher specific power and power density than the CCDE.

The LH_2-SPFC can provide the greatest mission duration for any on-station power required. That is to say, it expands the set of possible AUV work mission and in doing so, creates market opportunities for AUVs.

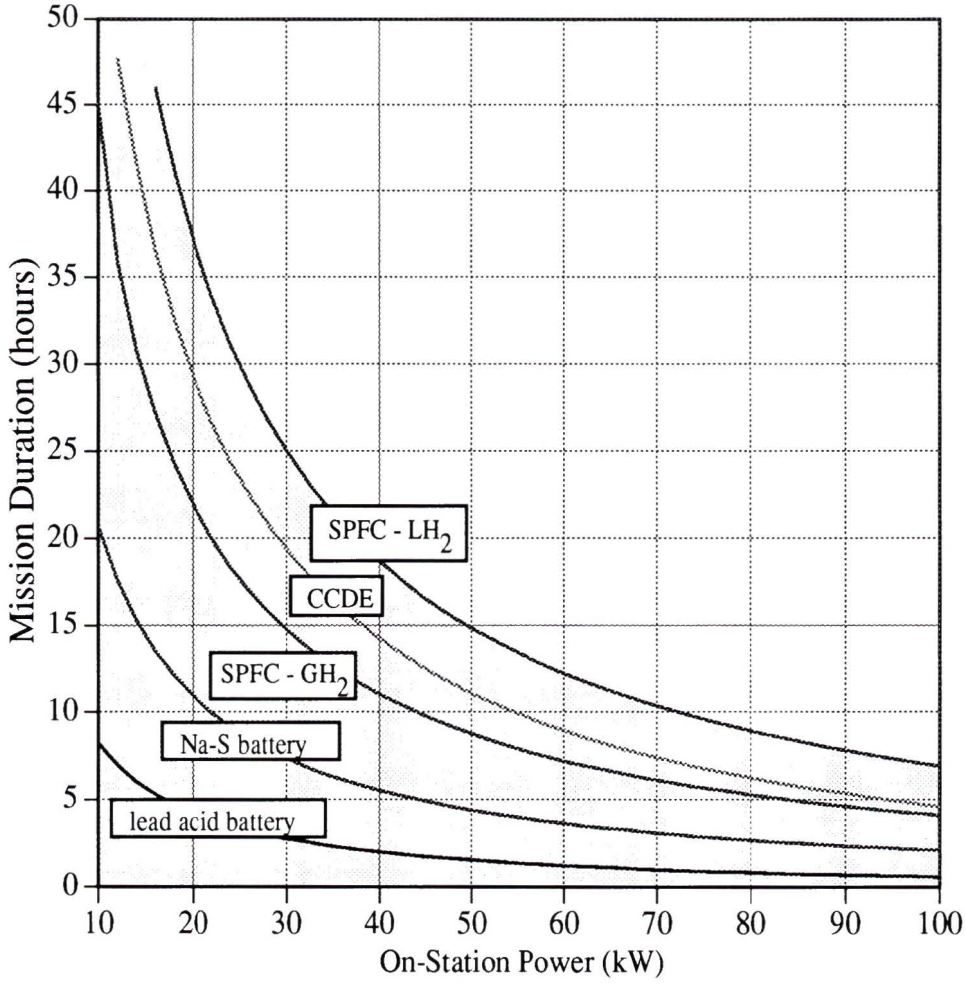

Figure 6.14: Performance envelopes for AUV work mission. The area below each curve represents the set of feasible AUV work missions for each power system.

6.2.2 Domains of Least Cost

The life cycle cost of each power system is calculated over its performance envelope. An AUV life cycle of 50 missions per year over 10 years is considered. Domains of least cost are shown in Figure 6.16. Figure 6.15 illustrates a cross-section of these domains, taken at an on-station power requirement of 50 kW. From Figures 6.15 and 6.16, we may note the following:

- The lead-acid battery is the least cost power system for all AUV work missions for which it is technically feasible. But is restricted to extremely short mission durations.

- The Na-S battery occupies a domain of least cost for work missions characterized by high on-station power and low mission duration. Because of the high initial capital cost associated with the SPFC and CCDE for high power work missions, the Na-S battery exhibits a life cycle cost advantage for such AUV scenarios.

- At the opposite extreme to battery performance, the LH_2-SPFC occupies market niche for extended duration work missions, for which it is the only feasible system.

- The *middle ground* between these two extremes is shared by the GH_2-SPFC and the CCDE. For low on-station power, this market is dominated by the GH_2-SPFC, where it can benefit from lower fuel costs and longer system lifetimes. For high power missions, the CCDE benefits from its lower initial capital cost and occupies the entire middle domain as the least cost power system.

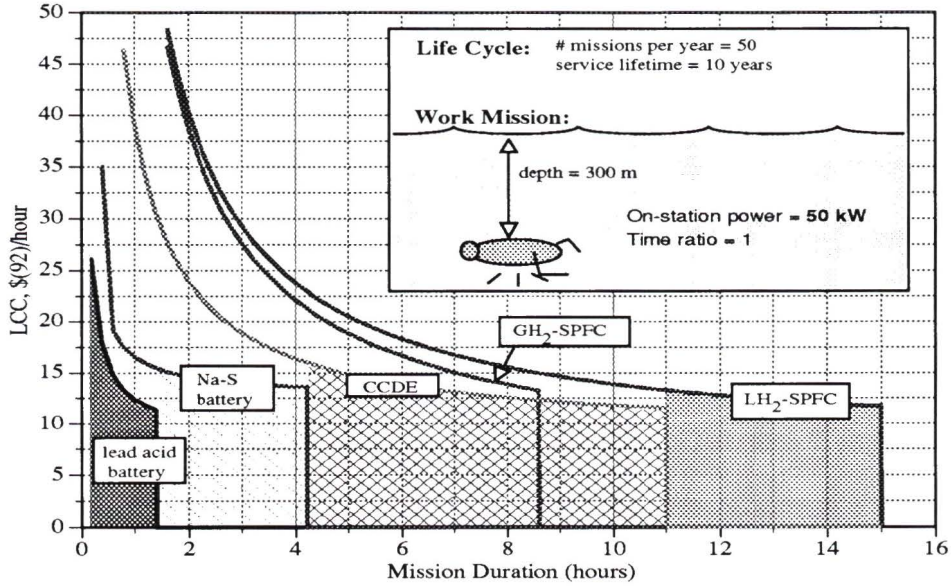

Figure 6.15: Power system LCC vs mission duration for AUV work mission. On-station power is **50 kW** (eg.welding). Mission depth is 300 metres. AUV life cycle is 50 missions per year over 10 years.

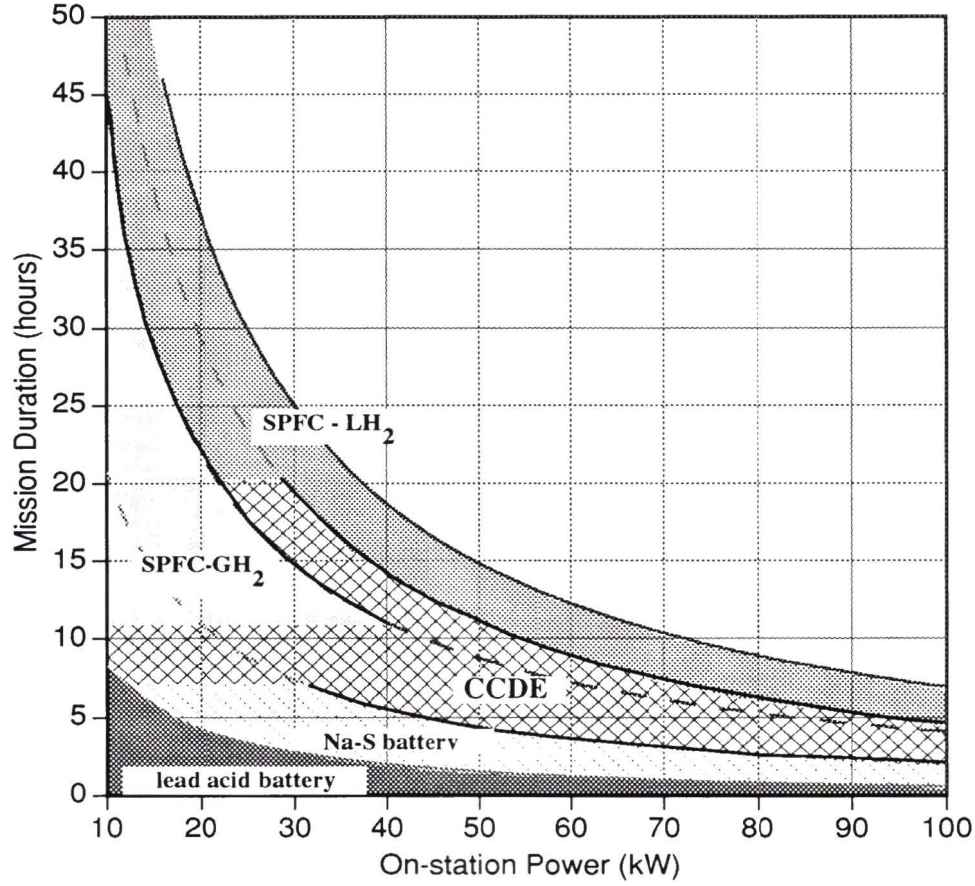

Figure 6.16: Domains of least cost for AUV work mission. Mission depth is 300 metres. AUV life cycle is 50 missions per year over 10 years.

6.3 Example 3: Combined Missions

This AUV mission combines the extremes of two previous examples. The mission consists of both transit and on-station work operations. The vehicle swims at a constant speed of 5 m/s. On-station, the vehicle performs a welding operation, requiring constant power of 50 kW. The time ratio is varied from 0 to 1, to allow examination of different combinations of these two operations. A depth of 300 metres is considered. The mission definition is illustrated in Figure 6.17.

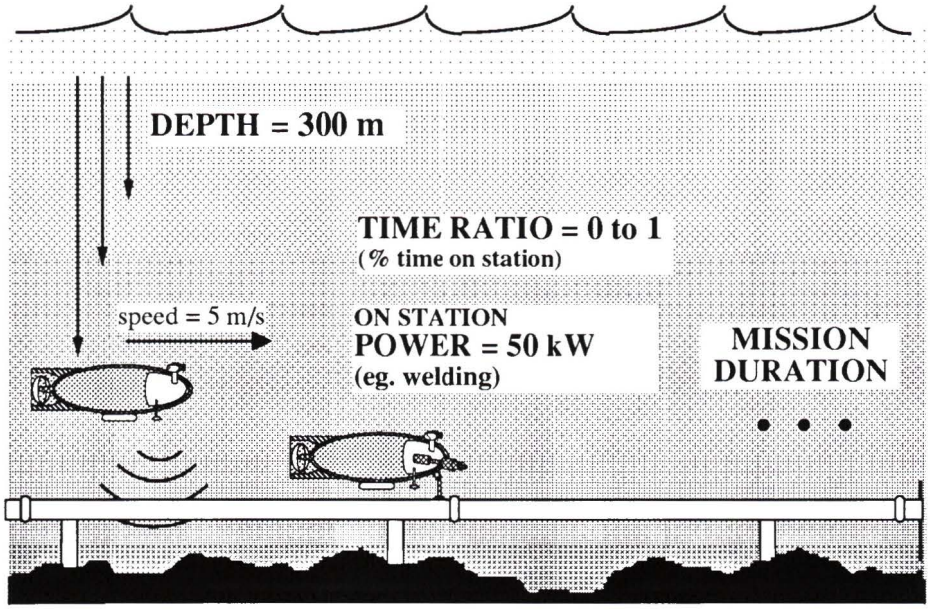

Figure 6.17: Definition of combined AUV mission.

6.3.1 Performance Envelopes

The significance of this mission is that it considers **two** steady state operating points, rather than one. This forces the examination of part load efficiency of the power systems during transit. This point is well illustrated in Figure 6.18, which shows the calculations of maximum power system endurance for two extreme values of time ratio.

For purpose of discussion, refer to the energy balances of Figure 6.18. Note the high transit efficiency of the fuel cell, as compared to the low transit efficiency of the engine. As can be seen from the results, the high part load efficiency of the SPFC gives it a large performance advantage over the CCDE for combined missions characterized by a low time ratio.

Performance envelopes for the combined AUV mission are represented as feasible combinations of time ratio and mission duration, as illustrated in Figure 6.19. Once again, the LH_2-SPFC can satisfy AUV missions for which no other power system is feasible. This is particularly strong for combined missions characterized by a low time ratio (or high percentage of total time spent at part load), where the fuel cell benefits from its high part load efficiency.

Mission Definition

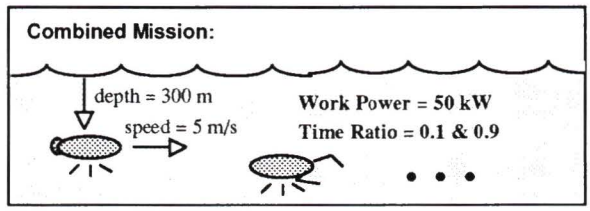

Power Requirement

Propulsion Power = 12.4 kW
Hotel Power = 1.5 kW
Work Power = 50 kW

Mass and Volume Constraints

	Mass (kg)	Volume (l)	
Vehicle Displacement	4083	4000	
Shell	140	31	Base Vehicle
Power train	100	35	
Pay Load	1000	1000	
Available for power system	**2843**	**2934**	

Mass and Volume Balances

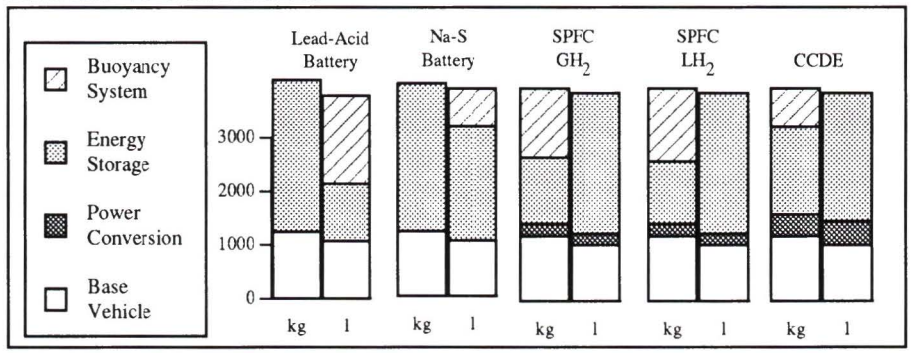

Energy Balances

	Lead-Acid	Na-S	SPFC-GH2	SPFC-LH2	CCDE
Fuel mass (kg)			29.7	50.3	152.7
Onboard Energy (kWh)	142	269	990	1676	1803
transit efficiency	**0.66**	**0.88**	**0.58**	**0.58**	**0.22**
station efficiency	**0.56**	**0.84**	**0.46**	**0.46**	**0.31**
	Endurance (hours)				
time ratio = 0.9	**1.5**	**4.7**	**9.5**	**16.1**	**11.8**
time ratio = 0.1	**4.2**	**12.6**	**30.3**	**51.3**	**24.7**

Figure 6.18: Calculation of power system endurance for combined mission at 300 metres depth. This figure illustrates the significance of part load efficiency during transit.

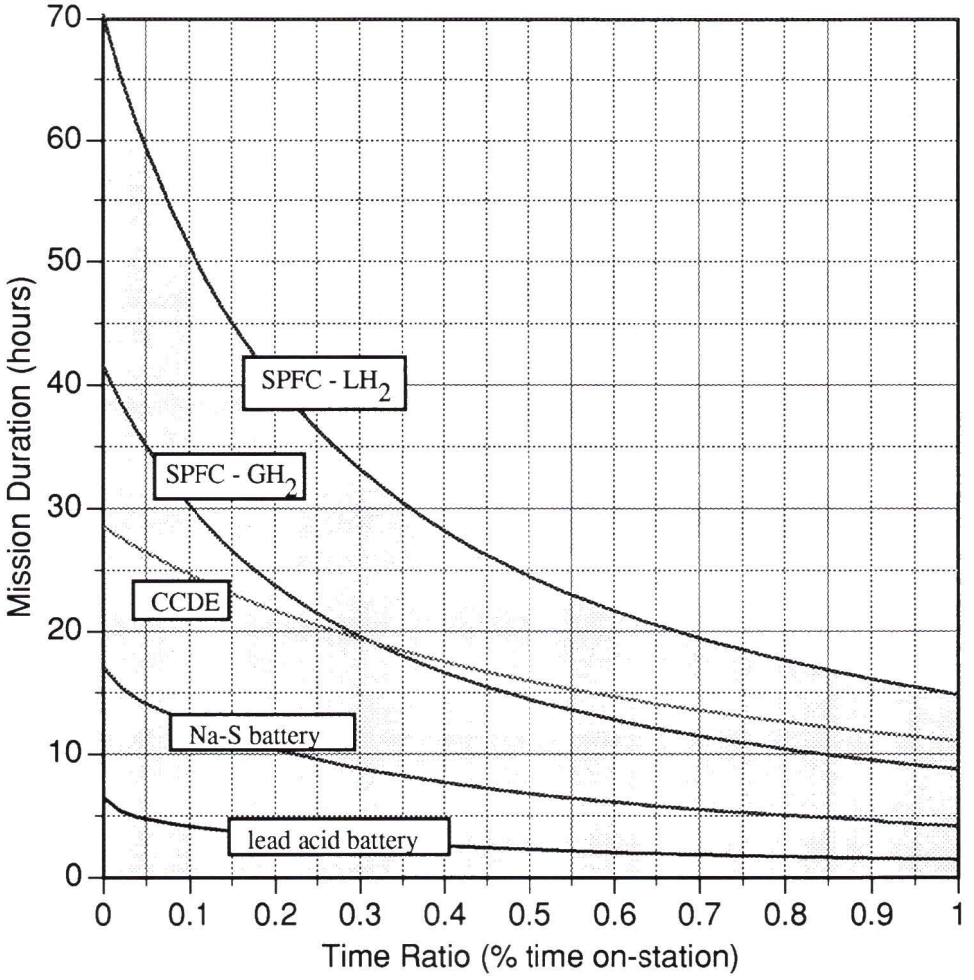

Figure 6.19: Performance envelopes for combined AUV mission. The area below each curve represents the set of feasible combined AUV missions for each power system.

6.3.2 Domains of Least Cost

As was done for the previous two examples, the life cycle cost of each power system is calculated for all feasible AUV missions. Again, the AUV life cycle is taken to be 50 missions per year over 10 years. Figure 6.20 illustrates the variation of power system life cycle cost with mission duration for a time ratio of 0.1. Domains of least cost are shown in Figure 6.21. From these two figures, we may conclude the following:

- The lead-acid battery is the least cost power system for all missions for which it is technically feasible. But it is restricted to extremely short mission durations.

- The Na-S battery occupies a domain of least cost for short duration missions characterized by high on-station power, regardless of the time ratio. In fact, the cost advantage of the Na-S battery over the SPFC and CCDE grows with decreasing time ratio. Note that in this thesis, the capital cost of the battery is expressed in dollars per unit energy, whereas the capital cost of the fuel cell stack and engine is expressed in dollars per unit power.

- The LH_2-SPFC expands the set of feasible AUV services. This is particularly true for missions characterized by a high percentage of part load operation, where the SPFC benefits from its high part load efficiency. Consequently, the LH_2-SPFC is the assured system of choice for extremely long endurance missions, for which it is the only technically feasible system.

- The mission domain which lies between the Na-S battery and the LH_2-SPFC is shared by the GH_2-SPFC and the CCDE. In this domain, the SPFC is preferred for missions characterized by a low time ratio. On the other hand, the CCDE is preferred for missions characterized by a high time ratio.

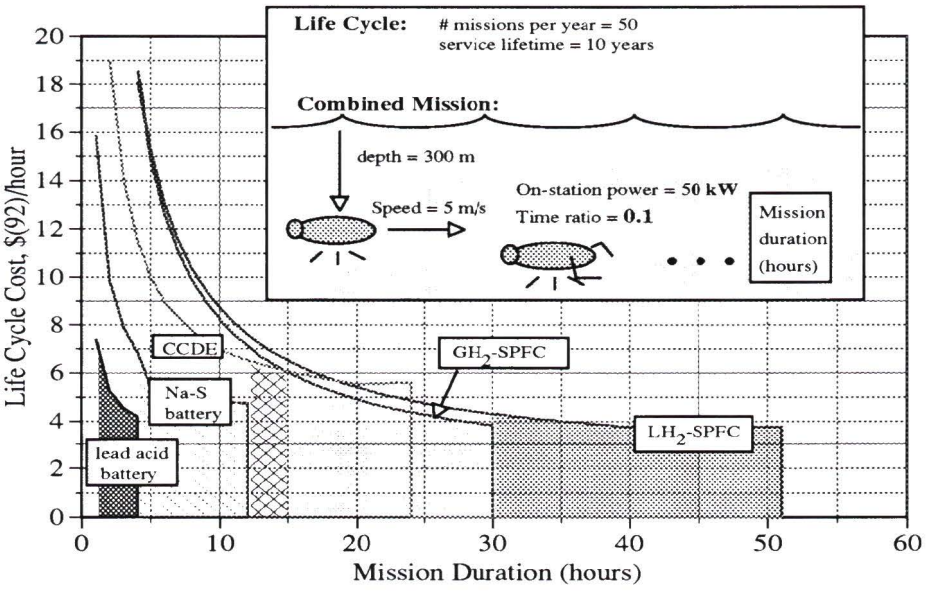

Figure 6.20: Power system LCC vs mission duration for combined AUV mission. A time ratio of 0.1 and a mission depth of 300 metres are considered. AUV life cycle is 50 missions per year over 10 years.

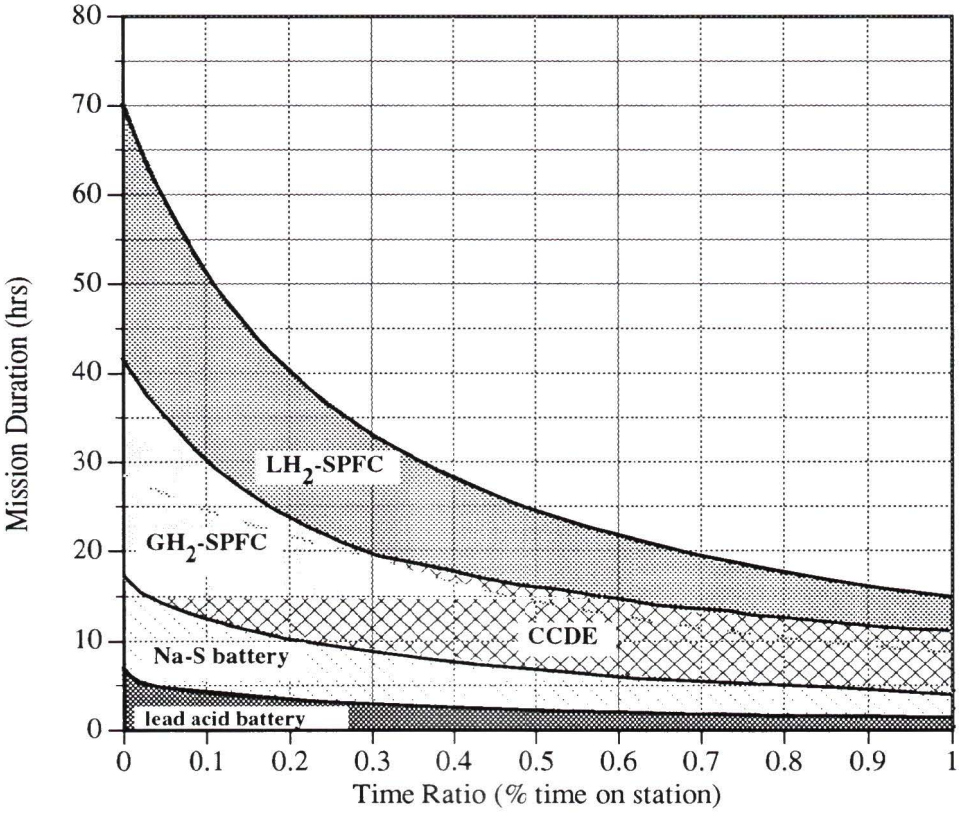

Figure 6.21: Domains of least cost for combined AUV mission. A mission depth of 300 metres is considered. AUV life cycle is 50 missions per year over 10 years.

Chapter 7

Concluding Comments

7.1 Conclusions

The lead-acid battery has dominated subsea power for decades. But its inherent low energy density and consequent limited submerged endurance capability has been a long-standing barrier to the market development of autonomous submersibles. This point is well illustrated by the performance envelope comparison of Chapter 6.

Currently, many underwater vehicle development projects (eg. *Seahorse* by Bruker Meerestechnik) are focussing on the CCDE as a subsea power plant. As the results of this comparison illustrate, the CCDE can provide submerged endurance capability far in excess of the lead-acid battery. Furthermore, the CCDE system benefits by being comprised of components which are readily available and relatively inexpensive in comparison with other advanced power systems for subsea applications.

Other current AUV development projects (eg. DARPA) are considering the SPFC as the principal power plant. The characteristics of H_2-O_2 as a fuel-oxidant pair, and high energy conversion efficiency of the fuel cell stack make the SPFC system particularly attractive for AUV applications. The results of this thesis show that the SPFC can provide submerged endurance greater than all other power systems examined. This performance advantage is particularly

strong for AUV missions characterized by:

- great depth, for which the high specific energy of liquid hydrogen storage is beneficial, and
- low time ratio, for which the high part load efficiency of the SPFC stack is advantageous.

Consequently, despite its high present cost (currently, the capital cost of the SPFC stack is in the order of 6,000 $/kW), the SPFC system has a market niche for long duration AUV missions for which no other power system is technically feasible.

This thesis considers *cost projections* for the power system technologies, allowing each to benefit from the economies of scale. Keeping in mind the modelling assumptions made in Chapters 3, 4 and 5, this thesis shows that the SPFC exhibits a lower life cycle cost than the CCDE for AUV services characterized by long mission duration and high mission frequency. This is mainly due to the lower operating costs and longer lifetime associated with the fuel cell. When interpreting these results, one must consider the optimized production cost assumed for the fuel cell stack and the large production rates assumed for compressed and liquid hydrogen. The time horizon for these cost projections in unclear and depends largely on the success of the SPFC to compete for land-based transportation markets. Nevertheless, this thesis shows that the SPFC has the potential to become cost-competitive with the CCDE for providing equivalent AUV services.

The performance envelope comparison shows that the submerged endurance capability of the Na-S battery is roughly $2\frac{1}{2}$ time greater than the lead-acid battery, but still not comparable with the SPFC and CCDE systems. Nevertheless, with the assumption of large-scale production, the LCC comparison illustrates a domain of preference for the Na-S battery which is characterized by low mission duration and high on-station power. For such scenarios, the high initial cost

of the fuel cell and engine result in a high life cycle cost per hour of service provided.

Finally, this thesis has clearly shown the lead-acid battery to be preferred in terms of LCC for those AUV services for which it is technically feasible. And despite its limited submerged endurance capability, the low cost associated with the lead-acid battery will likely ensure that it remains a prominent subsea power system in the foreseeable future.

7.2 Opportunities for Future Work

The results show that the solid polymer fuel cell exhibits characteristics which are favourable for low power missions coupled with long mission duration. Opposite to this, battery systems are preferred for missions requiring high on-station power, but are restricted to short mission durations by their characteristic low energy density. One possibility for future work may be to examine fuel cell/battery *hybrid* configurations. It is anticipated that such a power system configuration could offer advantages for missions requiring short bursts of high power.

Another opportunity for future work may be to include the ROV in such a comparison, to determine the services for which remote power is cost effective. For such a study, differences in vehicle configurations and surface support vessel requirements would have to be included in the analysis. One would expect that the cost-effectiveness of the ROV would decline with increasing mission depth, as the length of the expensive tether increases, along with the likelihood of tether damage and mission interruption.

Bibliography

[1] M. B. Moncaster, "An Oil Company View of Remotely Operated Underwater Vehicle Operations", *Subtech '83, The Design and Operation of Underwater Vehicles*, London, England, November 1983, pp. 139-147.

[2] G. T. Reader, et. al., "Energy Conversion for Commercial Underwater Vehicles", *25th Intersociety Energy Conversion Engineering Conference*, Vol. 5, Reno, Nevada, 1990, pp. 534-539.

[3] Julio E. Melegari, "The Evolving Role and Expanding Array of Submersibles and Underwater Vehicles", *Subtech '83, The Design and Operation of Underwater Vehicles*, London, England, November 1983, pp. 11-42.

[4] Shinichi Takagawa et. al., "6,500 Deep Manned Research Submersible Shinkai 6500 System", *Oceans '89*, Seattle, Washington, 1989, Vol. 3, pp. 741-746.

[5] A. B. Billet, "New Technology in Small Remotely Controlled Underwater Vehicles", *5th International Offshore Mechanics and Arctic Engineering (OMAE) Symposium*, Tokyo, Japan, 1986, Vol. 3, pp. 252-259.

[6] Mustuo Hattori, "Scientific Applications of the Deep ROV Dolphin-3K", *Oceans '89*, Seattle, Washington, 1989, Vol.3, pp. 771-776.

[7] Lance L. Stewart and Peter J. Auster, "Low Cost ROV's for Science", *Oceans '89*, Seattle, Washington, 1989, Vol. 3, pp. 771-776.

[8] Gerald L. Guerrier, "Autonomous Manned Craft", *Subtech '83, The Design and Operation of Underwater Vehicles*, London, England, November 1983, pp. 81-87.

[9] David S. Scott, "Hydrogen in the Evolving Energy System", *9th World Hydrogen Energy Conference*, Paris, France, June 1992.

[10] Gerald Sedor, "An Evaluation of Energy Systems for an Unmanned Underwater Vehicle", *15th Annual Technical Symposium and Exhibition of the Association for Unmanned Vehicle Systems*, San Diego, California, June 1988.

[11] William H. Kumm, "Evaluation Methodology for AUV Energy Systems Analysis", *6th International Symposium on Unmanned Untethered Submersible Technology*, June 1989, pp. 113-120.

[12] Arthur Lee et. al., "Power Sources for Unmanned Underwater Vehicles", *Sea Technology*, October, 1989, pp. 25-32.

[13] Attilio Brighenti, "Parametric Analysis of the Configuration of Autonomous Underwater Vehicles", *IEEE Journal of Oceanic Engineering*, Vol. 15, No. 3, 1990, pp. 179-188.

[14] Robert J. Brown and Rudolph R. Yanuck, *Introduction to Life Cycle Costing*, Prentice-Hall Inc., 1985.

[15] Robert D. Cook and Warren C. Young, *Advanced Mechanics of Materials*, Macmillan Publishing Company, New York, 1985.

[16] *Principles of Naval Architecture*, Society of Naval Architects and Marine Engineers, 1967.

[17] H. Kuno and Y. Kimura, "Development of the IGBT Inverter for Electric Vehicle", 10th International Electric Vehicle Symposium, Hong Kong,

December 1990, pp. 235-242.

[18] T. Ishikawa and M. Furutani, "AC Motor Propulsion System for Electric Vehicle", 10^{th} International Electric Vehicle Symposium, Hong Kong, December 1990, pp. 228-234.

[19] H. Mindy et. al., "Syntactic Foam Buoyancy Systems for Manned and Unmanned Submersibles", *Oceans '85*, Vol. 2, San Diego, California, November 1985, pp. 1253-1259.

[20] Alan Fowler, "Underwater Power Systems", *Subtech '83, The Design and Operation of Underwater Vehicles*, London, England, November 1983, pp. 389-404.

[21] Tsutomu Kawahawa et. al., "Silver-Zinc Battery Power System for 2,000m Deep Submergence Research Vehicle Shinkai 2000", *Oceans '82*, Washington D.C., 1982, pp. 50-56.

[22] David Harma, "Suitability of Silver-Zinc and Silver-Cadmium Electrochemistries to Provide Electric Power for Undersea Systems", *15^{th} Annual Technical Symposium and Exhibition of the Association for Unmanned Vehicle Systems*, San Diego, California, June 1988.

[23] C. David Flickinger and Edward S. Buzzelli, "Silver-Iron Battery System for ROV and Submersible Applications", *15^{th} Annual Technical Symposium and Exhibition of the Association for Unmanned Vehicle Systems*, San Diego, California, June 1988.

[24] Joseph F. McCartney and Thomas J. Lund, "Application of Lithium Thionyl Chloride Batteries to Marine Requirements", *Oceans '79*, San Diego, California, September 1979, pp. 177-185.

[25] John Leonard Braun, *Propulsion Alternatives for an Undersea Autonomous Vehicle*, M.S. Thesis, Massachusetts Institute of Technology, 1987.

[26] Nikola Marincic, "Design Features of Large High Rate Lithium Batteries for Torpedo-Like Applications", *30th Power Sources Symposium*, Atlantic City, NJ, 1982, pp. 208-210.

[27] P. B. Patil and R. I. Davis, "ETX-II Propulsion System Design", *9th International Electric Vehicle Symposium*, Toronto, November 1988.

[28] M. Altmejd and M. Dzieciuch, "A Sodium-Sulfur Battery for the ETX-II Propulsion System", *9th International Electric Vehicle Symposium*, Toronto, November 1988.

[29] W. Fischer and T. Shiota, "State of Development of Sodium Sulphur Batteries at ABB and Powerplex", *9th International Electric Vehicle Symposium*, Toronto, November 1988.

[30] Keld Fenwick, "NaS Batteries Charge into Battle", *Professional Engineering*, February 1991, pp. 24-26.

[31] M. F. Mangan, "Sodium Sulphur Batteries for Electric Road Vehicles", *9th International Electric Vehicle Symposium*, Toronto, November 1988.

[32] David Linden, *Handbook of Batteries and Fuel Cells*, McGraw-Hill Book Company, 1984.

[33] Robert Weaver et. al., "Some Reliability Considerations of Various Networks of Sodium Sulfur Batteries", *24th Intersociety Energy Conversion Engineering Conference*, Vol. 3, Washington D.C., 1989, pp. 1355-1361.

[34] W.H. DeLuca et. al., "Performance Evaluation of Advanced Battery Technologies for Electric Vehicle Applications", *25th Intersociety Energy Conversion Engineering Conference*, Vol. 3, Reno, Nevada, 1990, pp. 314-319.

[35] A. F. Burke and G. H. Cole, "Applications of the GSFUDS to Advanced Batteries and Vehicles", *10th International Electric Vehicle Symposium*, Hong Kong, December 1990, pp. 411-420.

[36] James E. Quinn et. al., "Projected Costs for Sodium-Sulfur Electric Vehicle Batteries", *24th Intersociety Energy Conversion Engineering Conference*, Vol. 3, Washington D.C., 1989, pp. 1335-1340.

[37] K. S. Hardy and M. A. Gyamil, *Advanced Vehicle Systems Assessment: Vol. 3*, Technical Report DOE/CS-54209-22, Jet Propulsion Laboratory, California Institute of Technology, Pasadena, California, March 1985.

[38] Thomas J. Lund and Joseph F. McCartney, "Survey of Power Systems for Small Undersea Vehicles", *Society of Automotive Engineers Transactions*, Vol. 87, 1979, pp. 2737-2747.

[39] Keith Prater, "The Renaissance of the Solid Polymer Fuel Cell", *Proceedings of the Grove Anniversary Fuel Cell Symposium*, London, England, 1989, pp. 239-250.

[40] Personal communications with Ballard Power Systems, North Vancouver, Canada, May 1991 - May 1992.

[41] R. Ewald and M. Kesten, "Cryogenic Equipment of Liquid Hydrogen Powered Automobiles", *Advances in Cryogenic Engineering*, Vol. 35, 1990, pp. 1777-1781.

[42] Ross A. Lemons "Fuel Cells for Transportation", *Proceedings of the Grove Anniversary Fuel Cell Symposium*, London, England, 1989, pp. 251-264.

[43] D. S. Cameron, "World Development of fuel Cells", *International Journal of Hydrogen Energy*, Vol. 15, No. 9, 1990, pp. 669-675.

[44] D. Watkins et. al., "Canadian Solid Polymer Fuel Cell Development", *5th Annual Battery Conference*, Long Beach, California, 1990.

[45] K. Strasser, "PEM Fuel Cells for Energy Storage Systems", *Proceedings of the 26th Intersociety Energy Conversion Engineering Conference*, Vol. 3, Boston, Massachusetts, 1991, pp. 630-635.

[46] V. W. Adams, "Possible Fuel Cell Applications for Ships and Submarines", *Proceedings of the Grove Anniversary Fuel Cell Symposium*, London, England, 1989, pp. 181-192.

[47] J. F. McElroy et. al., "SPE Hydrogen/Oxygen Fuel Cells for Rigorous Naval Applications", *Proceedings of the 34th International Power Sources Symposium*, Cherry Hill, N.J., 1990, pp. 403-407.

[48] A. J. Appleby and F. R. Foulkes, *Fuel Cell Handbook*, Van Nostrand Reinhold, New York, 1989.

[49] Earl Carey et. al., "Enhanced Mission Duration for an Underwater Vehicle Using a PEM Fuel Cell Power Source", *Proceedings of the Symposium on Autonomous Underwater Vehicle Technology, AUV '90*, Washington D.C., June 1990, pp. 105-108.

[50] R. J. Lawrance and V. A. Margiott, "Proton Exchange Membrane Fuel Cell Development", *24th Intersociety Energy Conversion Engineering Conference*, Vol. 3, Washington D. C., 1989, pp. 1587-1591.

[51] *The Ballard Fuel Cell*, Technical Report 700.306.008, Ballard Power Systems, North Vancouver, Canada, 1990.

[52] Robert Gordon, "Composite Pressure Vessels for Gaseous Hydrogen Power Vehicles", *5th World Hydrogen Energy Conference*, Toronto, 1984, pp. 1225-1236.

[53] W. Preschka, "The Status of Handling and Storage Techniques for Liquid Hydrogen in Motor Vehicles", *International Journal of Hydrogen Energy*, Vol. 12, No. 11, 1987, pp. 753-764.

[54] Paul M. Dunn et. al., "Dense Hydrogen and Oxygen Sources for Fuel Cells", *26th Intersociety Energy Conversion Conference*, Vol. 3, Boston, Massachusetts, 1991, pp. 527-532.

[55] Roger P. Hollandsworth et. al., "A Comparison of PEM Fuel Cell Systems for Both Open and Closed Loop Applications", *26th Intersociety Energy Conversion Engineering Conference*, Vol. 3, Boston, Massachusetts, 1991, pp. 492-497.

[56] Richard Gorman, "Aluminum-Hydrogen Peroxide Fuel Cell Power System for Ocean Bottom Electrical Power", *Oceans '89*, Seattle, Washington, 1989, Vol. 3, pp. 843-848.

[57] J. G. Hawley et. al., "Cryogenic Oxygen Storage for Underwater Vehicles", *26th Intersociety Energy Conversion Engineering Conference*, Vol. 5, Boston, Massachusetts, 1991, pp. 533-538.

[58] D. Nahmias, "Large-Scale Commercial Liquid Hydrogen Plants", *18th International Congress of Refrigeration*, Montreal, August 1991, pp. 322-330.

[59] John A. Barclay, "Prospects for Magnetic Liquefaction of Hydrogen", *18th International Congress of Refrigeration*, Montreal, August 1991, pp. 297-305.

[60] Paul E. Scheihing, "Industrial Magnetic Refrigeration for Hydrogen Liquefaction", *18th International Congress of Refrigeration*, Montreal, August 1991, pp. 363-369.

[61] H. J. Plass et. al.,"Economics of Hydrogen as a Fuel for Surface Transportation", *International Journal of Hydrogen Energy*, Vol. 15, No. 9, 1990, pp. 663-668.

[62] M. T. Syed et. al., "Economics of Hydrogen Liquefaction", *Proceedings of the Winter Annual Meeting of the American Society of Mechanical Engineers, Solar Energy Division, v. 10*, Dallas, Texas, November 1990, pp. 77-87.

[63] Personal communications with Structural Composites Industries, Pomona, California, June 1991.

[64] M. A. DeLuchi, "Hydrogen Vehicles: An Evaluation of Fuel Storage, Performance, Safety, Environmental Impacts, and Cost", *International Journal of Hydrogen Energy*, Vol. 14, No. 2, 1989, pp. 81-130.

[65] Personal communications with Minnesota Valley Engineering Inc., New Prague, Minnesota, April 1992.

[66] Alfred P. Meyer, "Status of Solid Polymer Fuel Cell Power Plant Development at International Fuel Cells Corporation", *24th Intersociety Energy Conversion Engineering Conference*, Vol. 3, Washington D. C., 1989, pp. 1619-1622.

[67] Supramaniam Srinivasan et. al., "Recent Advances in Solid Polymer Electrolyte Fuel Cell Technology With Low Platinum Loading Electrodes", *24th Intersociety Energy Conversion Engineering Conference*, Vol. 3, Washington D. C., 1989, pp. 1623-1629.

[68] G. T. Reader and J. G. Hawley, "Problems Associated With the Use of Synthetic Atmosphere Diesels in Naval Submarines", *24th Intersociety Energy Conversion Engineering Conference*, Vol. 5, Washington D. C., 1989, pp. 2457-2465.

[69] G. T. Reader and J. G. Hawley, "Closed and Recycled Engine Development for Submersible Power Plants", *24th Intersociety Energy Conversion Engineering Conference*, Vol. 5, Washington D. C., 1989, pp. 2449-2456.

[70] Raymond V. Thompson and Alan Fowler, "Development of a Depth Independent Closed Cycle Diesel Engine", *13th Annual Offshore Technology Conference*, Houston, Texas, 1981.

[71] J. Haas, "Air Independent Power Sources of High Energy Storage Density: The Bruker-Man Argon Diesel and the Bruker CO_2-Diesel", *3rd Hydrocarbon Symposium*, Luxembourgh, 1988, pp. 779-783.

[72] Takashi Obara et. al., "A New Closed Circuit Diesel Engine for Underwater Power", *ROV '89*, San Diego, California, 1989, pp. 276-282.

[73] Attilio Brighenti, "The 'Cryo-thermal' Closed Cycle Diesel Engine: Detailed Analysis of Stationary Working Conditions", *Defence Oceanology International '91 Exhibition & Conference*, Brighton, U. K., 1991.

[74] Attilio Brighenti et. al., "The Cryo-thermal Engine Underwater Power System: Performances, Dynamics and Control", *Oceans '89*, Vol. 3, Seattle, Washington, 1989, pp. 832-842.

[75] *Energy Prices and Taxes, First Quarter 1990*, International Energy Agency, Paris, France, 1990.

[76] *Marine Uses of Hydrogen*, Technical report prepared for Chemetics International Ltd. by Canocean, New Westminster and Highquest Engineering Inc., Vancouver, January 1985.

[77] W. M. Anderson and C. Cambier, "An Advanced Electric Drivetrain for EVs", *Proceedings of the 10th International Electric Vehicle Symposium*, Hong Kong, December 1990, pp. 209-221.

VITA

Surname: Schubak Given Names: Gary Edward
Place of Birth: Winnipeg, Manitoba Date of Birth: 66/05/13

Educational Institutions Attended:

University of Victoria	1990 to 1992
University of British Columbia	1985 to 1989
University of Victoria	1984 to 1985

Degrees Awarded:

M.A.Sc.	University of Victoria	1992
B.A.Sc.	University of British Columbia	1989

Publications:

1. *H_2-O_2 Fuel Cells vs. Advanced Battery Power Systems for Autonomous Underwater Vehicles: A Performance Envelope Comparison.* G. E. Schubak, D. S. Scott. Hydrogen Energy Progress VIII, Proceedings of the 9th World Hydrogen Energy Conference, Pergamon Press, June, 1992.

PARTIAL COPYRIGHT LICENSE

I hereby grant the right to lend my thesis to users of the University of Victoria Library, and to make single copies only for such users or in response to a request from the Library of any other university, or similar institution, on its behalf or for one of its users. I further agree that permission for extensive copying of this thesis for scholarly purposes may be granted by me or a member of the University designated by me. It is understood that copying or publication of this thesis for financial gain shall not be allowed without my written permission.

Title of Thesis: A Comparison of Power Systems for Autonomous Underwater Vehicles

Author [redacted]
(Signature)

GARY SCHUBAK
(Name in Block Letters)

SEPTEMBER 28, 1992
(Date)